# ADENO-ASSOCIATED VIRUS (AAV)-MEDIATED JOINT RESTORATION APPROACHES: CHARACTERIZATION AND APPLICATION

by

**Hannah Hoeun Lee**

BS, Cornell University, 2006

Submitted to the Graduate Faculty of

Swanson School of Engineering in partial fulfillment

of the requirements for the degree of

Doctor of Philosophy

University of Pittsburgh

2012

UNIVERSITY OF PITTSBURGH

SWANSON SCHOOL OF ENGINEERING

This dissertation was presented

by

Hannah Hoeun Lee

It was defended on

May 22, 2012

and approved by

Partha Roy, PhD, Associate Professor, Departments of Bioengineering and Pathology

Yadong Wang, PhD, Associate Professor, Department of Bioengineering

Xiao Xiao, PhD, Professor, Division of Molecular Pharmaceutics, University of North Carolina

Dissertation Director: Constance Chu, MD, Professor, Departments of Orthopaedic Surgery and Bioengineering

**ADENO-ASSOCIATED VIRUS (AAV)-MEDIATED JOINT RESTORATION APPROACHES: CHARACTERIZATION AND APPLICATION**

Hannah Hoeun Lee, PhD

University of Pittsburgh, 2012

Osteoarthritis is the leading cause of morbidity world-wide. Articular cartilage has limited regenerative potential and effective disease-modifying treatments for osteoarthritis are lacking. Hence, tissue engineering strategies to enhance cartilage repair potential are widely investigated. Adeno-associated virus (AAV) is a promising gene vector for articular cartilage and has already been used in clinical trials. We hypothesized that gene delivery of bioactive molecules to articular joints using AAV is efficacious to promote joint restoration. In the first two parts of the study, we showed persistent, localized, and controllable transgene expression within intact and injured joints following a single intra-articular injection of AAV. Most of the transduction occurred in the intra-articular soft tissues for intact joints and when the AAV was injected prior to joint injury, whereas some cartilage transduction but limited soft tissue transduction was seen when the AAV was injected following joint injury. Doxycycline was used as an induction agent of the AAV-mediated transgene expression. In the third part of the study, doxycycline was shown to have matrix-metalloproteinase-13 suppressing function during mesenchymal stem cell (MSC) chondrogenesis as well as *in vivo* cartilage repair. This supports potential use of doxycycline either alone or in gene therapy applications to improve cartilage repair. In the fourth part of the study, we optimized native biomaterial fibrin glue (FG) for its function as an AAV-releasing scaffold for tissue engineering applications. Bioactive AAV from diluted FG showed

improved release, transduction efficiency, and chondrogenic effect on MSC. Lastly, AAVs encoding for anabolic and/or anti-inflammatory factors were explored to enhance MSC chondrogenesis in an inflammatory milieu. The MSCs transduced with AAV-interleukin-1 receptor antagonist (IRAP), but not AAV-transforming growth factor (TGF)-$\beta_1$, resulted in improved chondrogenic potential. In conclusion, various aspects of AAV-mediated joint restoration approaches were investigated, from characterization of AAV delivery by direct injection or with the use of FG, to therapeutic applications with doxycycline, AAV-IRAP, and AAV-TGF-$\beta_1$. These results support continued investigations of therapeutic potential of AAV for safe, localized, and controlled delivery of bioactive substances to promote joint restoration, which may delay/prevent the onset of debilitating osteoarthritis.

## TABLE OF CONTENTS

## LIST OF TABLES

## LIST OF FIGURES

## NOMENCLATURE

AAV, adeno-associated virus

ADAMTS, a disintegrin-like and metalloproteinase with thrombospondin motif

BM, bone marrow

Col-I, collagen type I

Col-II, collagen type II

Col-X, collagen type X

CMV, cytomegalovirus

DMEM, Dulbecco's Modified Eagle Medium

DMMB, dimethylmethylene blue

Dox, doxycycline

ECM, extracellular matrix

EDTA, ethylenediaminetetraacetic acid

FBS, fetal bovine serum

FG, fibrin glue

GAG, glycosaminoglycan

GFP, green fluorescent protein

IL-1, interleukin-1

IL-1Ra, interleukin-1 receptor antagonist

IRAP. Interleukin-1 receptor antagonist protein

Luc, luciferase

MMP-13, matrix metalloproteinase-13

MSC, mesenchymal stem cell

OA, osteoarthritis

OCT, optical coherence tomography

PBS, phosphate buffered saline

Pen/strep, penicillin-streptomycin

rtTA, reverse tetracycline-controlled transactivator

SD, Sprague Dawley

SEM, scanning electron microscopy

tgf-$\beta_1$, transforming growth factor-$\beta_1$

tgf-βrII, tgf-beta-receptor type II

TNF, tumor necrosis factor

TRE, tetracycline response element

vg, vector genomes

# PREFACE

First and foremost, I thank God for the incredible opportunities he has presented for me. It is by your grace that I am here today, and I dedicate this to you.

I would like to express my deepest appreciation to my dissertation advisor, Dr. Constance Chu. Thank you for providing me with the opportunity to be a member of your wonderful team. It has been a very rewarding experience and I truly appreciate the constant support and guidance you have provided. It was very helpful to have a clinician-scientist mentor that has such a great enthusiasm for research, and thus is a great role-model for my MD/PhD training.

To Drs. Roy, Wang, and Xiao: thank you for serving on my dissertation committee. I truly appreciate your time, advice, and guidance. To Drs. Clayton Wiley, Richard Steinman, and George Stetten; thank you for your endless support from the Medical Scientist Training Program (MSTP) side. A special thank you to Dr. Harvey Borovetz. You have challenged and encouraged me about my career path from the interview day and throughout all these years, and I appreciate all your help. Thank you also to CATER (Cellular Approaches in Tissue Engineering and Regeneration) faculty members: Drs. Alan Russell, Paul Monga, and Kacey Marra.

I would like to thank all the members, present and past, of the Cartilage Restoration Center for their help and kindness. To Karin Payne, who is a mentor and a friend, you have truly guided my development as a scientist and I appreciate all your help. Thank you to Christian

Coyle, Amgad Haleem, Veronica Yao, and Jean Zamzow, who have been incredibly helpful. I would also like to thank Kimberly Suter, Michele Mulkeen, and Cecilia Huang, who has provided me with technical assistance on my projects. Thank you to all the Orthopaedic Surgery Residents who spent their research years in Cartilage Restoration Center, doing projects that are/are not related my work and have provided guidance in clinical realms: Venkat Seshadri, David Bear, Sarah Henry, Michael O'Malley, and Nicole Friel. In addition, I would like to acknowledge other members of the Chu lab: Ashley Williams, Megan Bowers, Kimberly Diamond, Steve Bruno, Patricia Stepp, and Andrew Lynch.

Endless thank you to all the students in the MSTP for their friendship and scientific camaraderie. Special call out to Jeffrey Wong, Lolita Nidadavolu, and John Kang, who started the MSTP training with me. As well, thank you to Ken Urish and Joe Vella for their guidance through Bioengineering program as an MD/PhD student. Thank you for my fellow School of Medicine and Bioengineering students. I learned everyday from you and it was a pleasure working with all of you.

Deep gratitude to my KCCP family, for their prayers and support. I would especially like to note Judong Lee and Junchol Park for their help in technical areas. I really appreciate it!

Most of all, thank you to my parents and Debbie. I love you all so much and you are the reason that I am who I am today. I can't possibly express enough gratitude!

Lastly, I would like to thank the National Institutes of Health (NIH) and the National Institute of Biomedical Imaging and Bioengineering for providing me with the T32 Institutional National Research Service Award through the CATER program for generously providing me with funding for the last two years of graduate school. This work was also supported by funding to Dr. Constance Chu from the NIH, Chondrogenesis in situ (R01 AR051963), Multicenter

cartilage repair preclinical trial in horses (RC2 AR058929), and AOSSM Post-joint injury conference II (U13 AR060692), and from the Albert B. Ferguson, Jr. MD Endowed Chair in Orthopaedic Surgery at the University of Pittsburgh.

# 1.0 INTRODUCTION: OSTEOARTHRITIS

Osteoarthritis (OA) is the most common type of arthritis in the world and the single largest cause of disability (1, 2). According to the World Health Organization (WHO), OA is among the top 10 conditions representing a global disease burden (3). It affects nearly 27 million people and costs almost $128 billion per year in medical care and indirect expenses in the US alone (4, 5). OA is symptomatically characterized by joint pain, tenderness, occasional effusions, deformity, and eventually loss of joint function with restrictions of motion (6). Clinical signs of OA include progressive degeneration of articular cartilage, which leads to fibrillation, ulceration, and joint space narrowing. Pathophysiology of OA is multi-factorial, but believed to be a combination of genetic, mechanical, and biochemical factors (7). It is traditionally regarded to result from "wear and tear" of the joint and hence associated with aging and obesity (8, 9). However, concerns with subjects with high physical activity, such as high impact sports athletes, and their risk of developing OA are also high (10, 11). Many studies have found a link between the development of OA and a history of participation in sports at an elite or professional level, especially for soccer, hockey, American football, and tennis (12).

## 1.1 ARTICULAR CARTILAGE JOINT

### 1.1.1 Articular cartilage joint in physiology

The articular surface plays an essential role of allowing smooth transmission of force between two bones, thereby permitting painless movements of the joint (13). Articular cartilage is an avascular, aneural, and alymphatic tissue with a sparse population of chondrocytes embedded within a highly organized, dense extracellular matrix (ECM) (14). The mesenchymal cell-derived chondrocytes are the single cell type within the cartilage, and they maintain the homeostasis of the extensive framework of ECM via the synthesis of various anabolic and catabolic factors. The ECM is primarily composed of water, collagen type II (col-II), and aggrecan, which is a large aggregating proteoglycan that is highly hydrated due to the negative charge density of its sulfated glycosaminoglycan (GAG) (15). The col-II provides tensile strength while aggrecan allows the cartilage to resist compressive load and provides a friction-free articulating surface. The catabolic factors involved in cartilage homeostasis include matrix metalloproteinases (MMPs) that degrade collagens, and aggrecanases, such as a disintegrin-like and metalloproteinase with thrombospondin motif (ADAMTSs), which degrade aggrecans (14). With these compositions, the articular cartilage is a fluid-rich structure that functions in load-bearing via controlling the fluid movement in order to disperse the load/weight throughout the cartilage and to the underlying bone. As well, joint movement facilitates synovial fluid circulation and nutrient delivery to cartilage. However, due to the limited intrinsic capacity for self-repair, articular cartilage injuries due to trauma or degenerative inevitably progress to OA (16).

In addition to articular cartilage, there are number of soft-tissue structures that are integral components of the joint. The anterior cruciate ligament (ACL) and menisci are the two

most relevant structures for the knee joint, as they are essential for joint stability and are commonly injured in the general population as well as in athletes (17). ACL connects the femur to tibia and is essential for the normal motion and stability of knee joints (18). It mainly consists of fibroblasts and ECM composed of non-parallel collagen types I and III fibers with multiple fascicles and is surrounded by synovium (18-20). ACL also contains small amounts of proteoglycans and glycoproteins (20). There are two bundles to the ACL, anteromedial and posterolateral, respective of their position on the tibia, and limits the forward motion of the tibia (21). ACL, alike articular cartilage, has a limited capacity to heal and regenerate after injury due to poor vascularity (22). Menisci are a pair of wedge-shaped semilunar fibrocartilages that are interposed between the femoral condyles and tibial plateaus of the knee joint (23). They function to correct the incongruency between these two articular cartilage surfaces, increasing the contact area in the femorotibial joint and reducing the stresses on tibial cartilage. Additional roles serves by menisci are shock absorption, stability enhancement, and lubrication (24). Molecular compositions of the menisci are mainly collagen type I (col-I), and small portions of collagens type II, III, V, and VI (25). Menisci also contain proteoglycan at a lesser degree than hyaline cartilage.

### 1.1.2 Articular cartilage joint in pathology

OA involves all joint components: cartilage, synovial membrane/synovium, and subchondral bone. During the OA pathogenesis, slow focal destruction of articular cartilage leads to a roughening and thinning of the weight-bearing regions of the articular surface, resulting in progressive immobility and pain (26). The process begins with the disruption of the cartilage cell-matrix interactions, with the alteration of matrix molecular structure and composition and

the loss of aggrecans. Inflammatory cytokines, such as interleukin-1 (IL-1) and tumor necrosis factor (TNF), and synovial inflammation have also been implicated as important mediators of the OA progression. These inflammatory cytokines upregulate expressions of MMPs and ADAMTSs (14). They also stimulate the chondrocytes to proliferate and synthesis more matrix components in an attempt to heal the articular cartilage. However, the chondrocytes' proliferative potential and ECM synthesis capacity declines with time and age (27). The synovium is also capable of accelerating the articular cartilage degradation by degenerating soluble aggrecanases and inflammatory cytokines (15, 28). The col-II and aggrecan breakdown products have been shown to accumulate in the cartilage ECM as well as the synovial fluid during the OA process. Therefore, with progressive joint degeneration, the anabolic response eventually becomes overwhelmed by the catabolic activities, leading to progressive thinning of articular cartilage and to OA (14).

Indirect cartilage injury and subsequent arthritis development due to joint instability induced by damaging the extra-cartilage soft tissue structure is also a common pathological process for the knee joint. Both ACL and menisci injuries have been shown to be followed by arthritic changes of the knees (29). In addition to the initial high force that damages intra-articular structures involved in the trauma, the ACL and menisci ruptures initiate a cascade of pathogenic processes in the acute phase that can lead to the development of OA in itself (17, 30). In addition to acute effects, the lack of a functionally normal ACL or menisci leads to chronic changes in the static and dynamic loading of the knee and increase forces on the cartilage and other joint structures. Consequently, additional damages commonly occur in the ACL and/or menisci-injured knees, further contributing to initiation and progression of OA development (31, 32).

## 1.2 CURRENT TREATMENTS AND LIMITATIONS

Clinical strategies for management of cartilage pathology have evolved from primarily palliative methods to treat early disease until joint replacement for end-stage disease, toward more biologic, joint-conserving measures. These include cartilage reconstruction as in osteochondral graft transplantation (33), and cartilage repair as in bone marrow (BM) stimulation (34, 35), autologous chondrocyte implantation (36), or stem cell implantation (37). However, results of cartilage repair procedures have been equivocal, and no single approach has been shown to be superior (38, 39). Therefore, an important strategy for cartilage repair and tissue engineering is on investigating utilization of bioactive factors and biodegradable scaffolds to promote local, recruited, or transplanted cell proliferation and differentiation within cartilage wounds. Despite the promising results of *in vitro* growth factor application, *in vivo* application has not been as successful due to the short half-life of these growth factors and the need for high repetitive dosing as well as a costly purification process.

## 1.3 TISSUE ENGINEERING AND GENE THERAPY FOR ARTICULAR CARTILAGE RESTORATION

### 1.3.1 Adeno-associated virus and gene therapy

Gene therapy can overcome the obstacles of short half-life, need for high repetitive dosing, and costly purification process associated with growth factor applications by delivery genes that encode chondrogenic growth factors or inhibitors of cartilage catabolites in various vector

constructs. This also provides for a local delivery system that drives the expression of therapeutic molecules over an extended period and overcome the need for repeated administrations or interventions. Gene carriers include plasmids, non-viral vectors, and viral vectors. Although plasmids and non-viral vectors are less toxic, less immunogenic, and easier to prepare, their gene delivery efficiencies are significantly lower compared to viral vectors (40). Hence, viral vectors are currently considered the most effective agents for *in vivo* gene transfer (41).

Viral vectors that have been used in the pre-clinical setting include adenovirus, adeno-associated virus (AAV) (42), and lentivirus (43). Many delivery vehicles can successfully target synovium and other soft tissues surrounding the articular cartilage (44-46). However, cartilage is particularly challenging for any type of transportation due to its highly impermeable and negatively charged ECM.

AAV is derived from an endemic, non-pathogenic parvovirus. It has the following advantages over other viruses: sustained transgene expression over longer period, reduced potential for host immune response, and the capacity to transduce both dividing and non-dividing cells (47). After transduction, the viral genome translocates into the target cell nucleus, and the DNA polymerase generates the transducing episome. Numerous serotypes of AAV have been identified, each having different preferential targets. Among the different serotypes, AAV serotype 2 (AAV2) is considered to have the best defined safety profile as it has already been used in clinical trials (48).

There are three general approaches for cartilage viral gene therapy applications: direct, indirect, and hybrid. The direct method involves the injection of viral vectors directly into the articular joint space to transducer local cells (47). The indirect approach involves the use of genetically modified cells (42), and/or biodegradable scaffolds that release genetically modified

cells (49, 50). This leads to the site-specific release of bioactive molecules important in tissue regeneration, though temporary. In addition, this approach requires *ex vivo* manipulation of cultured cells, which faces high barriers with respect to clinical translation. The third hybrid approach involves implantation of biodegradable scaffolds embedded with genetic materials (51, 52), leading to direct and localized *in situ* delivery of bioactive vectors to the host cells in proximity to the scaffold, as well as the sustained expression of the transgene.

### 1.3.2 Scaffold Biomaterial: Fibrin Glue

Fibrin glue (FG) is a natural substance available for human use clinically as a commercial product or readily prepared from plasma for autologous applications (53). These properties mean that laboratory findings may be more readily translated into potential human clinical applications than similar findings with synthetic polymers. Despite being widely used in clinical surgical practice as an adhesive and sealant for hemostasis (54), only in recent years has the ability of FG to act as a delivery scaffold received attention (55). Besides being commercially available for sterile applications, it is non-immunogenic, biodegradable, and malleable so that it can be molded into irregular tissue defects. All of these advantages make FG an appealing scaffold for pre-clinical translational cartilage tissue engineering applications.

### 1.3.3 Cell types used in joint restoration

Tissue engineering strategies for cartilage repair with autologous cell sources mostly involves use of chondrocytes isolate from cartilage (56), or mesenchymal stem cells (MSCs) from bone marrow (57), fat (58), and muscle (59). While autologous chondrocytes has good

biocompatibility and better suited to produce cartilage tissue compared to other cell types, donor-site morbidity and need for initial arthroscopic surgery is severely limiting. New clinical approaches in tissue engineering or regenerative medicine heavily utilize stem cells. Since chondrocytes are of mesodermal lineage, MSCs are more appropriate than epidermal or endodermal stem cells. Extraction of MSCs is also associated with less donor-site morbidity and does not disrupt normal healthy cartilage tissue.

Clinically, some level of variability has been observed from outcomes of microfracture, that involves MSC chondrogenesis (57). As well, most of the repair tissues have been characteristics of fibrocartilage versus hyaline cartilage. A potential approach to overcome the decreased differentiation ability of certain MSC populations and enhance hyaline cartilage formation is the addition of growth factors. Hence, supplementation of additional bioactive factors, such as anabolic or anti-catabolic factors, may enhance the results of these MSC-based cell therapies for cartilage restoration

### 1.3.4 Bioactive factors in joint restoration

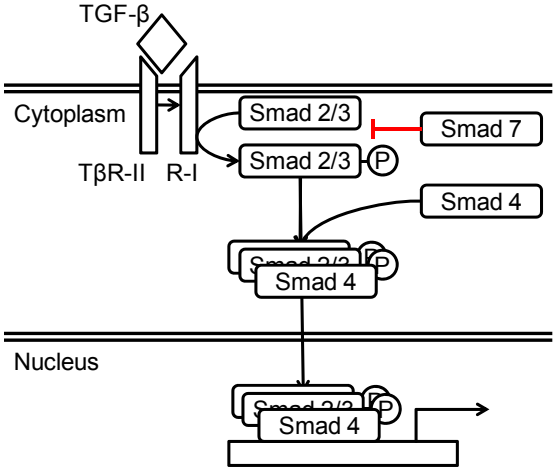


**Figure 1-1: TGF-β – Smad Signaling Pathway**
Adapted from Piek, et al. (60)

Treatment strategies based on the use of bone-marrow derived cartilage progenitor stem cells, such as MSCs, and growth factors have been extensively studied using well-established *in vitro* chondrogenic assays and *in vivo* animal models (61). Transforming growth factor-β (TGF-β) is the most extensively examined anabolic growth factor for hMSC induction into chondrogenic phenotype *in vitro* (57, 62), especially the TGF-$\beta_1$ isoform (63). Relevant TGF-$\beta_1$ signaling pathway (Fig. 1-1) include TGF-$\beta_1$ binding to its type II receptor (TGF-β-R-II), which then forms a complex with the type I TGF-β receptor (64). Upon the receptor activation, intracellular signaling molecule Smad2 or Smad3 gets phosphorylated, forms a complex with Smad4, and the complex then translocates to the nucleus to function as a transcription factor. Via this mechanism, TGF-$\beta_1$ stimulates collagen-II and proteoglycan expressions in MSCs (65). Smad7 inhibits Smad2 and Smad3 phosphorylation and prevents further signaling. In addition to its anabolic functions, TGF-$\beta_1$ also decreases the catabolic activity of inflammatory cytokines, such as IL-1, *in vitro* and *in vivo* (64). However, a number of deleterious side effects have been associated with uncontrolled high-dose TGF-$\beta_1$ administration *in vivo*, including synovial fibrosis and osteophyte formation (61, 66, 67). These side effects have been shown to be blocked when Smad7 was intracellularly overexpressed in the synovial lining while maintaining TGF-$\beta_1$ induced cartilage repair effects (68).

On the catabolic side, IL-1β and TNF-α are pro-inflammatory cytokines that activate the nuclear factor kappa-light chain enhancer of activated B cells (NF-κB) pathway, induce destructive processes in multiple cell types in the joint space, and thus play a critical role in the progression of OA (26, 69). These cytokines accelerate the switching of the anabolic to catabolic states of the cartilage, and it has been shown that each of their stimulation increases the expression of catabolic enzymes, such as ADAMTS-5 (69, 70) and MMP-13 (71). As well, IL-

1β and TNF-α have been shown to inhibit TGF-$\beta_1$-mediated hMSC chondrogenesis (71). Previous animal studies showed that TNF is a potent pro-inflammatory mediator and IL-1 a potent cartilage catabolic mediator (72). Arthritis induced by TNF-overexpression was completely blocked by antibodies targeting IL-1 receptor, suggesting that IL-1 is the pivotal downstream mediator in arthritis. IL-1 receptor antagonist (IL-1Ra) is a small 20-25 kDa secreted protein that competitively inhibits IL-1 by binding to and preoccupying type I IL-1 receptors, thus preventing IL-1 ligand-receptor interactions (73). It has no known agonist activity (74). However, although this strategy is straightforward, the efficacy is limited by the poor pharmacokinetics of the small molecule and the need for high dosing to fully occupy IL-1 receptors for prolonged periods of time.

## 1.4 PROJECT OBJECTIVES

The central hypothesis of this project is to test the hypothesis that modulation of various anabolic and catabolic factors involved in mesenchymal stem cell (MSC) chondrogenesis via adeno-associated virus (AAV) will enhance the outcomes of joint restoration.

### 1.4.1 Objective #1: To test the hypothesis that the transgene expression in articular cartilage joint is localized, persistent, and controllable following a single intra-articular injection of adeno-associated virus

Adeno-associated virus (AAV) is a promising delivery vehicle for articular cartilage. Most simple method to deliver the genetic material for cartilage viral gene therapy applications is by

direct injection for the resident cells within the joint to produce the therapeutic factor. Knowledge of the duration of transgene expression is critically important to develop efficient therapies. As well, while long-term transgene expression may be critical for disease treatment, it may not be ideal for cartilage repair strategies, where a growth factor may only be needed for a limited time period. In cases where a growth factor is needed for a specific period of time, it may be advantageous to use an inducible gene expression system, where the transgene expression can be controlled pharmacologically by oral administration of the inducing agent. The tetracycline-inducible gene regulation system has been efficient both *in vitro* and *in vivo* (75-77). Doxycycline, an analog of tetracycline, is widely accepted as an inducer due to its safe use in humans (78).

In this objective, AAV-mediated transgene persistence, duration, and controllability will be studied in intact rat diarthrodial joint using a reporter gene luciferase. Also, since the intact and undamaged articular cartilage is unlikely to require treatment, AAV transduction and transgene expression profiles in rat models of articular joint damage will provide invaluable information to improve gene therapy strategies, as they will more closely mimic the disease environment. Two different AAV injection time points, pre- and post-injury, will be investigated on osteochondral defect and anterior cruciate ligament transection models of joint damage.

### 1.4.2 Objective #2: To test the hypothesis that doxycycline reduces MMP, improves chondrogenesis of human bone marrow derived mesenchymal stem cells (MSC), and does not adversely affect repair of osteochondral defect (OCD)

New strategies to improve repair tissue quality after bone marrow cell based procedures such as microfracture may reduce later development of osteoarthritis (OA). Doxycycline can be used to

control intra-articular transgene expression and has been shown to reduce matrix metalloproteinases (MMP) and OA disease progression. In this study, MSCs will be cultured in chondrogenic media with either 0, 1 or 2-μg/mL doxycycline to assess the doxycycline effect on chondrogenic differentiation. Rats will be treated with or without oral doxycycline following osteochondral defect surgeries to assess the doxycycline effect on cartilage repair. These studies will evaluate the potential use of doxycycline either alone or in combination with AAV gene therapy applications to improve cartilage repair and delay OA.

### 1.4.3 Objective #3: To test the hypothesis that fibrin glue concentration alters the adeno-associated virus-release profile, which affects adeno-associated virus-bioavailability

Use of biodegradable scaffolds embedded with AAV can lead to direct and localized *in situ* delivery of bioactive vectors to the host cells in close proximity to the scaffold. Although numerous novel synthetic and natural polymers have been investigated for cartilage tissue engineering studies, usage of an FDA-approved and autologous biomaterial as an AAV-releasing scaffold can accelerate the transition of basic science research into human clinical studies. Fibrin glue (FG) is a biomaterial widely used in clinical practice and tissue engineering applications. Nonetheless, FG formulation for AAV delivery has not been optimized. FG hydrogels containing varying fibrinogen concentrations will be characterized for its function as an AAV-releasing scaffold *in vitro*. Specifically, alterations in FG scaffold microstructure via different dilutions and its effect on AAV-release capacity will be characterized. As well, usage of biodegradable FG scaffold for release and delivery of bioactive AAVs to hMSCs will be done by assaying for the induction of cartilage specific genes.

### 1.4.4 Objective #4: To test the hypothesis that chondrogenic potential of human mesenchymal stem cells will be enhanced by using adeno-associated virus encoding for anabolic factors and/or anti-catabolic factors

Anabolic growth factors have been extensively studied for hMSC chondrogenesis and cartilage repair (16, 42, 57, 65, 79). However, the catabolic side of the balance, which is increasingly recognized to be important, warrants additional investigation. Interleukin-1 (IL-1) is the pivotal inflammatory cytokine in articular cartilage pathologies, with its levels greatly upregulated within the joint in disease processes (71). Furthermore, it has been shown the IL-1β inhibits hMSC chondrogenesis (71, 80). Therefore, anti-IL-1 strategy like IL-1 receptor antagonist protein (IL-1Ra or IRAP), which competitively inhibits IL-1, holds further therapeutic potential (81). Transforming growth factor-β (TGF-β) is the most extensively examined anabolic growth factor for hMSC induction into chondrogenic phenotype and its use in chondrogenic media has long been established (61, 62). However, it has also been shown to blunt cytokine-mediated inhibition of hMSC chondrogenesis (71). As a basis to apply IRAP and TGF-$\beta_1$ anti-inflammatory strategies in clinical MSC-mediated cartilage repair, AAV-IRAP transduced hMSCs and AAV-TGF-$\beta_1$ transduced hMSCs will be investigated for their chondrogenic differentiation in an inflammatory environment.

# 2.0 SINGLE INTRA-ARTICULAR INJECTION OF ADENO-ASSOCIATED VIRUS RESULTS IN STABLE AND CONTROLLABLE IN VIVO TRANSGENE EXPRESSION IN NORMAL RAT KNEES

## 2.1 INTRODUCTION

Prevention of articular cartilage degradation or treatment of its damage in arthritis remains challenging due to the limited self-repair potential of articular cartilage. Currently, no therapeutic methods exist for complete re-establishment of cartilage function. Delivery of therapeutic agents that could promote articular cartilage repair or prevent its further degradation once damaged is an attractive therapeutic option. Protein biologics can be delivered systemically, or locally by direct injection or through polymer based delivery systems (82). However, due to the short half-life of proteins, administration of supra-physiological doses and/or repeated delivery are often necessary, significantly increasing the cost of these approaches. An attractive alternative is to deliver the genetic information to cells within the joints and engineer them to produce the therapeutic protein *in situ*.

Naked DNA, retrovirus, adenovirus, and herpes virus-based vectors have been explored for gene transduction *in vivo*; however, most were rendered suboptimal due to safety, efficacy, and duration issues. Recombinant adeno-associated virus (AAV) derived from an endemic and non-pathogenic parvovirus is emerging as a promising delivery vehicle for musculoskeletal

tissues, with the advantages of sustained transgene expression, reduced potential for host immune response, and the capacity to transducer both dividing and non-dividing cells *in vitro* and *in vivo* (83). Different serotypes of AAV exist, each having different preferential targets (83, 84). AAV5 has better transduction efficacy in rodent arthritic joints; however, AAV2 is currently used in human clinical trials for arthritis (85-88).

Many studies have genetically engineered cells *ex vivo* for implantation *in vivo*. Although this has led to cartilage repair in animal models (42, 89-92), culturing cells *ex vivo* prolongs the time before treatment and is also very expensive in a clinical setting. An alternative method would be direct injection and rely on the cells within the joint to produce the therapeutic factor. AAV vectors have a strong tropism for synoviocytes in vitro (93-96). However, few studies have identified the exact in vivo localization of the transgene, after intra-articular injection of AAV (44, 46, 79, 97-99). It is important to identify which cells or tissues are infected by AAV after intra-articular injection and to use this information to develop optimal treatment strategies for intra-articular disease processes such as inflammatory and degenerative arthritis.

Knowledge of the duration of transgene expression is also important to develop efficient therapies. It has been reported that parkinsonian nonhuman primates having received AAV2 encoding human L-amino acid decarboxylase (L-DOPA) into their brains were still expressing the transgene after 8 years (100). AAV-mediated erythropoietin delivery to rhesus monkey skeletal muscle has led to transgene expression for more than 6 years (77). Long-term transgene expression may be critical for disease treatment, but may not be ideal for cartilage repair strategies, where a growth factor may only be advantageous to use an inducible gene expression system, where the transgene expression can be controlled pharmacologically by oral administration of the inducing agent. The tetracycline-inducible gene regulation system has been

efficient both *in vitro* and *in vivo* (75-77). Doxycycline (Dox), an analog of tetracycline, is widely accepted as an inducer due to its safe use in humans (78). Only few studies have investigated the use of an AAV-based tetracycline-inducible gene system in the knee joint after direct injection.

Given the potential translational value of AAV for human clinical use, the aim of the present study was to investigate the presence, persistence, and ability to externally control transgene expression when using AAV2 delivered by a single intra-articular injection into the rat diarthrodial joint. The immunocompetent rat was chosen since it is a good animal model for future studies that will test the repair of articular cartilage, the prevention of its degradation, or the treatment of inflammatory arthritis by AAV-mediated gene therapy.

## 2.2 METHODS

### 2.2.1 AAV vector production

Double-stranded serotype 2 AAV (AAV2) vectors were produced using the three-plasmid cotransfection method (101). Depending on the AAV2 vector being produced, the first plasmid used was either the AAV-cytomegalovirus (CMV)-Luc plasmid with the luciferase (Luc) gene driven by the CMV promoter, the AAV-CMV-enhanced green fluorescent protein (GFP) plasmid, the AAV-CMV-reverse-tetracycline-controlled transactivator (rtTA) plasmid, or the AAV-TRE-Luc plasmid with the Luc gene driven by the tetracycline response element (TRE) promoter. The second plasmid used in the cotransfection was the pXX6 plasmid, which contains the helper genes from adenovirus, and the third plasmid was the pXX2, which supplies AAV2 rep protein

and capsid protein (101). Vector purification was performed as previously described and AAV genomic titers were determined by DNA dot-blot assay (101).

### 2.2.2 *In vitro* infection of rat articular chondrocytes

Primary rat articular chondrocytes were extracted from the tibial and femoral cartilage of 3-month-old male Sprague Dawley rats. Cartilage samples were washed in phosphate buffered saline (PBS; Invitrogen) with 2% penicillin-streptomycin (pen/strep; Invitrogen). To digest the cartilage, thin shavings were incubated in 0.2% pronase (Calbiochem) solution in F-12 medium (Invitrogen) supplemented with 5% fetal bovine serum (FBS) and 1% pen/strep for 90 min in a dry 37°C incubator. This was followed by overnight digestion in 0.025% collagenase P (Roche Applied Science) in F-12 medium supplemented with 5% FBS and 1% pen/strep. Recovered chondrocytes were seeded as monolayers in a T-75 flask in 50% Dulbecco's Modified Eagle medium/50% F-12 medium (DMEM/F-12; Invitrogen) supplemented with 10% FBS, and 1% pen/strep under normal growth conditions (37°C, 5% $CO_2$). Cells were grown to passage four and plated onto 96-well plates at a density of 2.0 x $10^4$ cells/$cm^2$ in growth medium (DMEM/F-12, 10% FBS, 1% pen/strep). On the following day, chondrocytes in plain DMEM/F-12 were infected with 3.2 x $10^5$ vector genomes per cell (vg/cell) of AAV-CMV-GFP, AAV-CMV-Luc, or AAV-CMV-rtTA + AAV-TRE-Luc for 1 h, after which the medium was changed to growth medium. This dose was selected because it gave the greatest gene expression in an *in vitro* dose response study ranging from 4 x $10^4$ – 3.2 x $10^5$ vg/cell (data not shown). After 2 days, cells infected with AAV-TRE-Luc were stimulated with Dox at concentrations of 0, 1, or 2 μg/mL for 36 h. Luciferase transgene expression was measured 4 days post-transduction by adding 50 μL of luciferin (30 mg/mL; D-Luciferin Firefly, Caliper Life Sciences) per well and imaging after 5

minutes with the IVIS® 200 optical imaging system (Xenogen Corp., Hopkinton, MA, USA). GFP signal was visualized on the same day using the epifluorescent Eclipse TE-2000U inverted microscopy (Nikon).

### 2.2.3 Animal experiments

All animal experiments were performed following a University of Pittsburgh Institutional Animal Care and Use Committee approved protocol. The study was divided into two parts.

In the first study, nine male Sprague Dawley rats (3 months old) received a 50 μL intra-articular injection containing 2.5 x $10^{10}$ vg of AAV-CMV-GFP or AAV-CMV-Luc into the right and left knee joint, respectively. For longitudinal evaluation of luciferase expression, rats were anesthetized with isoflurane inhalation, followed by a 50 μL intra-articular injection of luciferin (30 mg/mL). After 5 min, to allow proper distribution of luciferin, rats were placed in an IVIS® 200 optical imaging system. Photon emissions in the region of interest were quantified using Living Image software v.3.0 (Xenogen Corp.), and bioluminescent flux was reported as photons/sec. Rats were imaged every other week for 4 months, and monthly thereafter, until 1 year post-AAV injection. Rats were sacrificed at either 1 week (N = 1), 2 weeks (N = 2), 3 months (N = 1), 4 months (N = 1), or 1 year (N = 4) after AAV injection. On the day of sacrifice, rats received an intraperitoneal injection of 100 μL of luciferin to determine whether any signal was present outside of the intra-articular space. They also received an intra-articular injection of luciferin and imaged as previously described. The joint was then opened to image the intra-articular tissues. Tissues within the joint were also analyzed for GFP-positive cells using a fluorescent stereomicroscope (MVX-10 MacroView Systems, Olympus, Japan) equipped with a

DP71 camera (Olympus). All GFP images in Fig. 2-4 had the contrast increased by the same value in Adobe Photoshop to improve the GFP signal for print.

In the second animal experiment, the right and left knees of four male Sprague Dawley rats (3 months old) were divided into experimental and control groups. In the right knee, each rat received a 50 µL intra-articular injection containing 2.5 x $10^{10}$ vg of AAV-TRE-Luc and 2.5 x $10^{10}$ of AAV-CMV-rtTA. In the left knee, each rat received a 50 µL intra-articular injection containing 2.5 x $10^{10}$ vg of AAV-CMV-Luc and 2.5 x $10^{10}$ vg of AAV-CMV-rtTA, to have the same number of vg in both knees. To induce expression of luciferase in the right knee joint (injected with AAV-TRE-Luc), rats were administered drinking water containing Dox at a concentration of 2 mg/mL for 7 days, followed by its removal. To ensure fresh supply, the water was replaced every day and protected from light with amber drinking bottles. Rats were imaged twice a week as described above. Addition of Dox to the drinking water was performed at 14 days, 8 months, and 13 months post-AAV injection.

### 2.2.4 Statistical analysis

*In vitro* studies were repeated three times with 3 – 9 replicates. A representative experiment is shown in Fig. 2-1 (n = 9). *In vivo* studies were conducted and data observed using independent animals, with N = 4 – 8 for Fig. 2-2 due to animals being sacrificed at different time points during the study and N = 4 for Fig. 2-5. All data are represented as median and interquartile range boxplots with percentiles calculated using Tukey Hinge. The significant level used was $p < 0.05$, unless otherwise noted. Assumptions of parametric data were tested for all data: normality of data distribution using Shapiro-Wilk test and homogeneity of variance using Levene's test. For parametric data (Fig. 2-5), one-way analysis of variance (ANOVA) with *post-hoc* Tukey was

used. For non-parametric independent data (Fig. 2-1), a Kruskal-Wallis test and *post-hoc* pair-wise Mann-Whitney *U* with a Bonferroni correction was used. *P*-values less than 0.008 (0.05/6 total comparisons) were considered significant. For non-parametric data in the longitudinal study (Fig. 2-2), Friedman's ANOVA test was used with the Wilcoxon test and a Bonferroni correction applied for *post-hoc* analysis of each consecutive time point. *P*-values less than 0.005 (0.05/10 comparisons) were considered significant. Statistical evaluations were performed with SPSS software (IBM).

## 2.3 RESULTS

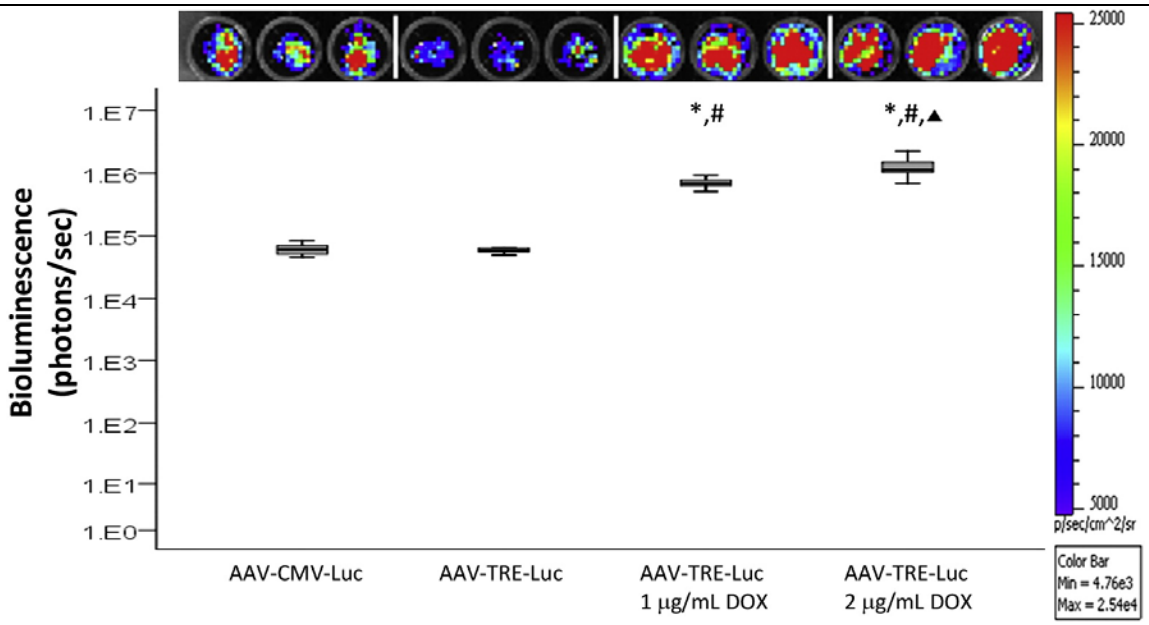


**Figure 2-1: *In vitro* response of rat articular chondrocytes to AAV2**
Rat articular chondrocytes were infected with AAV-CMV-Luc or AAV-TRE-Luc, stimulated with Dox (0, 1, or 2 µg/mL) for 36 h, and luciferase signal was detected. Upper panel: image of bioluminescence signal from the cells infected with (left to right) AAV-CMV-Luc, AAV-TRE-Luc (no Dox), AAV-TRE-Luc stimulated with 1 µg/mL Dox, and AAV-TRE-Luc stimulated with 2 µg/mL Dox. Lower panel: median and interquartile range of bioluminescence for the different cell groups. n = 9. *$p < 0.001$ for AAV-TRE-Luc: 1 µg/mL Dox vs AAV-TRE-Luc and for AAV-TRE-Luc: 2µg/mL Dox vs AAV-TRE-Luc. #$p < 0.001$ for AAV-TRE-Luc: 1 µg/mL Dox vs AAV-CMV-Luc and for AAV-TRE-Luc: 2µg/mL Dox vs AAV-CMV-Luc. ▲$p < 0.001$ for AAV-TRE-Luc: 2 µg/mL Dox vs AAV-TRE-Luc: 1 µg/mL Dox.

### 2.3.1 *In vitro* response of rat articular chondrocytes to AAV2 vectors

GFP expression was visualized in articular chondrocytes infected with AAV-CMV-GFP as early as 24 h post-infection (data not shown). Articular chondrocytes infected with AAV-CMV-Luc had luciferase expression (Fig. 2-1). Infection of articular chondrocytes with AAV-TRE-Luc led to weak bioluminescence when no Dox was added (Fig. 2-1, AAV-TRE-Luc). This signal was significantly increased when the cells were cultured with Dox at concentrations of 1 μg/mL and 2 μg/mL for 36 h (Fig. 2-1, $*p < 0.001$ for AAV-TRE-Luc: 1 μg/mL Dox and AAV-TRE-Luc: 2 μg/mL Dox compared to AAV-TRE-Luc). The bioluminescence observed in vitro with the AAV-TRE-Luc vector and addition of Dox was also greater than that obtained with the AAV-CMV-Luc vector (Fig. 2-1, $\#p < 0.001$ for AAV-TRE-Luc: 1 μg/mL Dox and AAV-TRE-Luc: 2 μg/mL Dox compared to AAV-CMV-Luc). A significant difference was also observed between the two concentrations of Dox tested (Fig. 2-1, $\blacktriangle p < 0.001$ for AAV-TRE-Luc: 2 μg/mL Dox compared to AAV-TRE-Luc: 1 μg/mL Dox).

### 2.3.2 Duration of *in vivo* transgene expression after a single intra-articular injection of AAV2

The IVIS® 200 optical imaging system enables *in vivo* tracking of luciferase expression in the same rat knee joints over a 1 year period. Bioluminescence was visualized as early as 14 days after intra-articular injection of AAV-CMV-Luc and persisted in all animals for 1 year, the study end point. Figure 2-2A shows bioluminescent images from a representative animal at 14 days, 1 month, 6 months, and 1 year after intra-articular injection of AAV-CMV-Luc. In all study animals, the luciferase signal remained constant throughout the duration of the study (Fig. 2-2B).

The contralateral AAV-CMV-GFP-injected knees did not show luciferase signal during the study. Intraperitoneal injection of luciferin and imaging before sacrifice also indicated that no luciferase signal was present outside the injected knee area.

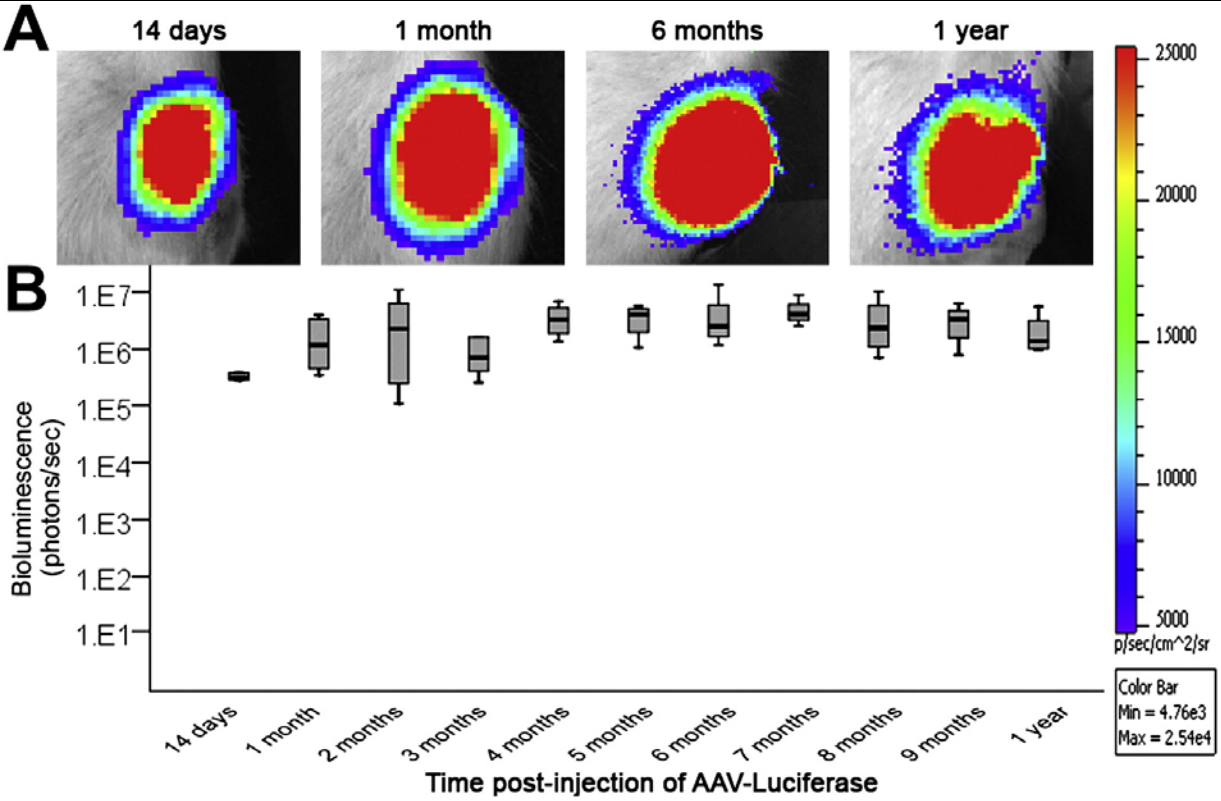


**Figure 2-2: Duration of *in vivo* transgene expression after a single intra-articular injection of AAV-CMV-Luc**

Transgene expression was observed and quantified using bioluminescence imaging to detect luciferase activity. **(A)** Bioluminescent images of the left knee joint of a representative rat at 14 days, 1 month, 6 months, and 1 year after a single intra-articular injection of AAV-CMV-Luc. **(B)** Median and interquartile range of bioluminescence observed in the left knee joint of all rats in the study over 1 year following intra-articular injection of AAV-CMV-Luc. N = 4 – 8 rats (N = 8 at 14 days, N = 6 at 1 and 2 months, N = 5 at 3 months, and N = 4 from 4 months to 1 year). No significant difference was observed between the different time points.

### 2.3.3 Localization of *in vivo* transgene expression after a single intra-articular injection of AAV2

To localize luciferase signal, knees were imaged intact (Fig. 2-3A) and after exposing the intra-articular space (Fig. 2-3B). Bioluminescence was concentrated in two areas (Fig. 2-3B and C). The majority of the signal was found in the exposed infrapatellar fat pad area, with some signal

in the intra-articular space containing the ligaments and meniscus. No bioluminescence was observed in articular cartilage.

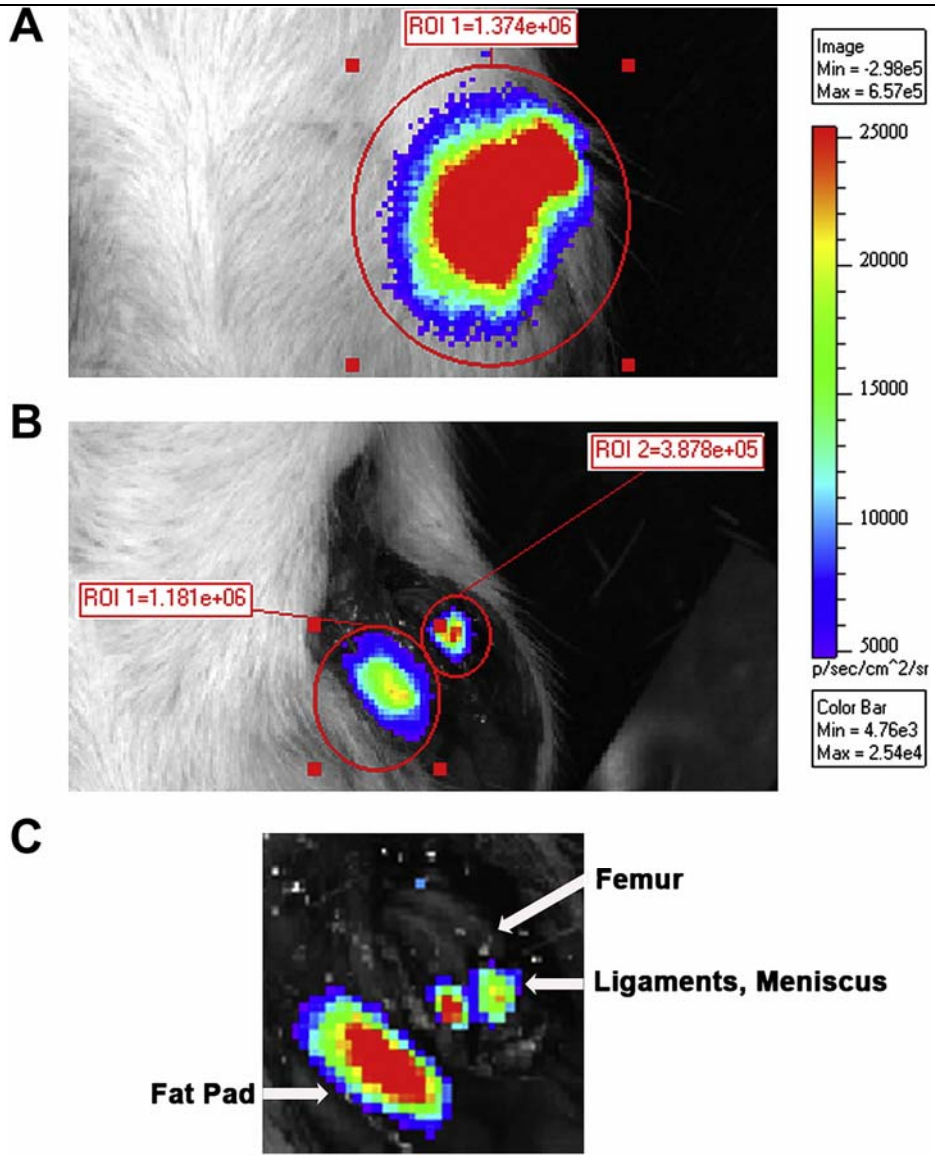


**Figure 2-3: Localization of *in vivo* luciferase expression after a single intra-articular injection of AAV-CMV-Luc by using the IVIS optical imaging system**
**(A)** Luciferase was detected in the intact left knee joint. **(B)** Exposure of the intra-articular space of the same knee joint in (A) revealed that the luciferase signal was located in two major areas. **(C)** A higher magnification of (B) indicated that the signal was mainly found in the infrapatellar fat pad and in the soft tissues between the femur and tibia, such as the ligaments and meniscus.

Tissues retrieved from the AAV-CMV-GFP-injected side provided more information on the localization of cells expressing the transgene. Abundant GFP-positive cells were found in soft tissues such as synovium, infrapatellar fat pad, and tissues within the intra-articular joint

space. Figure 2-4A shows a large area of GFP-positive cells within meniscus, while Figure 2-4B shows GFP-positive cells in soft tissues surrounding the tibial plateau. GFP-positive cells could be found when compared to soft tissues. As seen in Figure 2-4C, two small areas containing GFP-positive cells were found on the trochlear ridge of the femur. Large areas of GFP-positive cells in articular cartilage were not found in any of the study animals.

### 2.3.4 Controlled *in vivo* transgene expression following a single intra-articular injection of AAV2

Persistent luciferase expression was observed for the duration of the experiment, in all knee joints injected with AAV-CMV-Luc (Fig. 2-5A, B, and C). Intra-articular injection of AAV-TRE-Luc led to a weak luciferase signal before addition of Dox to the drinking water of the rats (Fig. 2-5A). Fourteen days post-AAV injection, Dox was added to the drinking water and led to a significant increase in the luciferase signal after 7 days (Fig. 2-5B and D, median fold increase of 11.28 and interquartile range of 16.34 (twenty-fifth-percentile = 8.20, seventy-fifth-percentile = 19.46) and $*p = 0.015$ compared to Day 0: Dox (-)). Removal of Dox significantly decreased the signal 7 days later (Fig. 2-5C and D, $\#p = 0.023$ compared to Day 7: Dox (+)). When measured 8 months post-AAV injection, addition of Dox to the drinking water of the rats for 7 days increased luciferase expression by a median fold increase of 4.31 and interquartile range of 5.45 (twenty-fifth-percentile = 2.16, seventy-fifth-percentile = 6.04) and $p = 0.099$ compared to Day 0: Dox (-). The luciferase signal returned to pre-Dox values after the inducer had been removed for 7 days. The induction cycle performed 13 months after the initial injection of AAV also showed increased luciferase signal on the AAV-TRE-Luc side 7 days after addition of Dox to the drinking water (Fig. 2-5E, median fold increase of 38.43 and interquartile range of 32.46

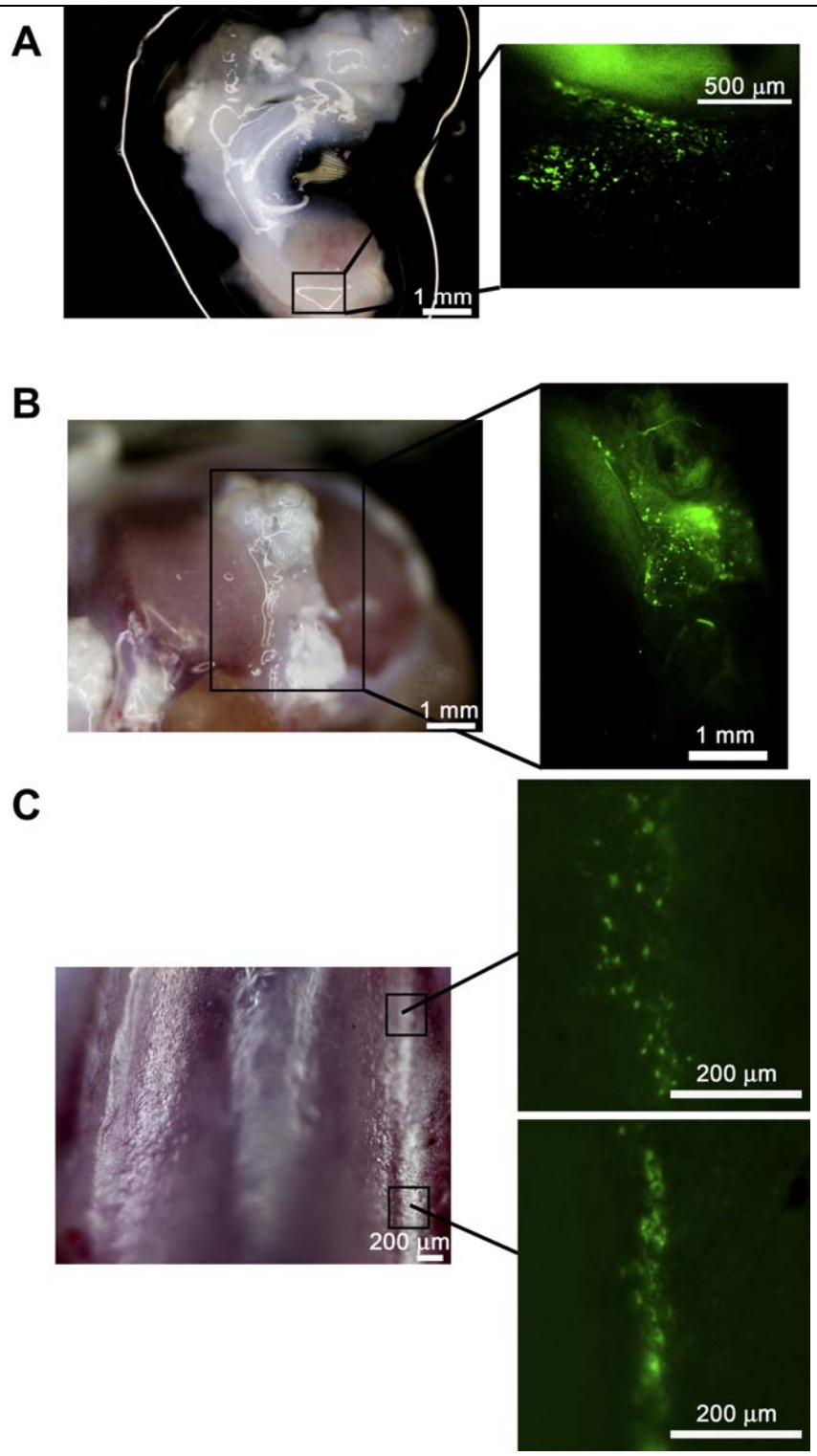


**Figure 2-4: GFP-positive cells in tissues harvested from the knee joint of rats injected with AAV-CMV-GFP, imaged with a stereomicroscope**

**(A)** Brightfield image (left panel) of meniscal tissue with the area located within the square enlarged to show the GFP-positive cells (right panel). **(B)** Brightfield image (left panel) of tibial plateau. Area within the square is magnified in the right panel and shows GFP-positive cells within the soft tissue. **(C)** Brightfield image of the trochea (left panel). GFP-positive cells were sparse in articular cartilage. Two small areas with GFP-positive cells were found on the trochlear ridge in this animal (right panel).

(twenty-fifth-percentile = 27.48, seventy-fifth-percentile = 54.90) and *$p$ = 0.003 compared to Day 0: Dox (-)). Removal of Dox decreased the signal to baseline levels (Fig. 2-5E, #$p$ = 0.016 compared to Day 7: Dox (+)).

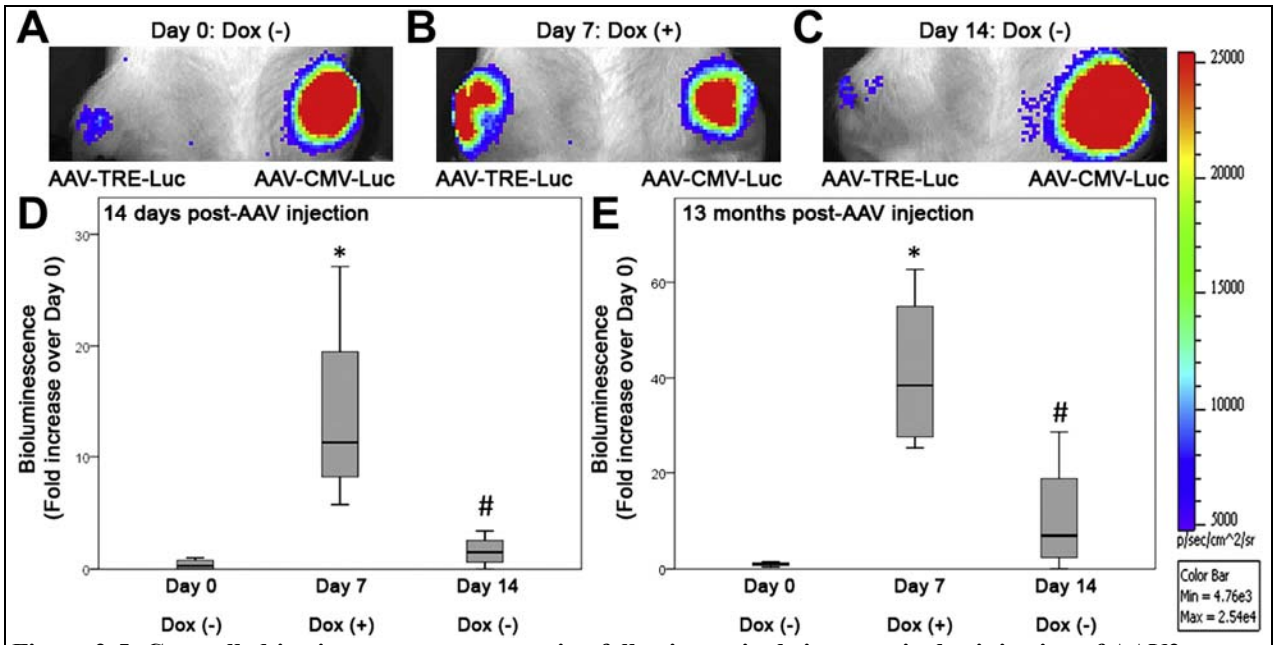


**Figure 2-5: Controlled *in vivo* transgene expression following a single intra-articular injection of AAV2**
**(A-C)** Bioluminescent images of a representative rat that received AAV-TRE-Luc in the right knee and AAV-CMV-Luc in the left knee 14 days prior. Images shown were taken (A) before addition of Dox to the drinking water (Day 0), (B) 7 days after Dox was added to the drinking water (Day 7) and (C) 7 days after Dox was removed from the drinking water (Day 14). Luciferase expression was stable in the knee joint injected with AAV-CMV-Luc, but varied with Dox administration in the knee joints injected with AAV-TRE-Luc. **(D)** Bioluminescence measured in the knee joint 14 days post-AAV-TRE-Luc injection. Bioluminescence is represented as a median fold increase over Day 0, when no Dox was present in the drinking water, and interquartile range. Luciferase expression increased with addition of Dox to the drinking water after 7 days (Day 7: Dox (+)). *$p$ = 0.015 compared to Day 0: Dox (-). After removal of Dox from the drinking water for 7 days (Day 14: Dox (-)), the luciferase signal decreased. #$p$ = 0.023 compared to Day 7: Dox (+). **(E)** Median and interquartile range of bioluminescence measured 13 months post-injection with AAV-TRE-Luc. Luciferase expression increased 7 days after Dox was present in the drinking water (Day 7: Dox (+)). *$p$ = 0.003 compared to Day 0: Dox (-). Luciferase expression decreased 7 days after removal of Dox (Day 14: Dox (-)). #$p$ = 0.016 compared to Day 7: Dox (+). N = 4 rats.

## 2.4 DISCUSSION

Prevention of articular cartilage degradation or promotion of its repair in inflammatory and degenerative arthritis remains challenging. Therapeutic strategies that rely on the delivery of

growth factors to enhance repair or inhibitory molecules that would prevent degradation are of interest. Ideally, the therapeutic protein should be produced *in situ*, to obtain a persistent and stable concentration, thus limiting the need for purification processes, repeated injections, and supra-physiological doses, which are not cost effective. Gene therapy is a promising alternative to the delivery of therapeutic factors, as it provides the genetic material necessary for protein synthesis *in situ*. In this study, we analyzed important aspects for efficient intra-articular gene delivery. These included the persistence and localization of transgene expression after a single intra-articular injection of AAV2, as well as the ability to control the transgene expression over time when using an inducible AAV2 vector.

Efficacy of AAV2 for *in vitro* chondrocyte transduction was evaluated using GFP and luciferase as reporter genes. In accordance with other studies on mice, rabbit, equine, and human chondrocytes (98, 102-104), rat articular chondrocytes were also capable of uptaking the AAV2 vector and producing the transgene protein, suggesting that AAV2 could be used to infect rat chondrocytes *in vivo*. The ability to induce transgene expression with addition of Dox to the cell culture medium demonstrated the potential to control the timing of transgene expression.

Studies in nonhuman primates indicate that administration of AAV to the brain leads to transgene expression for as long as 8 years (100), yet few studies have assessed the persistence of transgene expression after AAV administration to the rat knee joint past a few months (45, 79, 95, 99). Intra-articular injections into the rat stifle joint, while challenging, have previously been reported by our group and others (45, 46, 79, 105). Given this experience, we believe that AAV was delivered intra-articularly in this study, although it is possible that some leakage or partial extra-articular injection may have occurred. By using bioluminescence, the same animal could be imaged repeatedly, providing a clear profile of transgene persistence and

biodistribution. All animals had stable luciferase transgene expression for up to 1 year following intra-articular injection of AAV-CMV-Luc. A recent study employing recombinant lentivirus or adenovirus vectors did not observe such stable transgene expression in knees of immunocompetent rats (106). They observed strong transgene expression that diminished over a 3-week period. Injection of the same vectors into athymic rats led to an initially high transgene expression, which decreased to 20% and remained at that level for 6 months (106). Prolonged transgene expression in the current study suggests lower immunogenicity of AAV2 than lentivirus or adenovirus. Stability of transgene expression following AAV2 injection into the rat knee joint supports a potential role for AAV2 gene therapy in treatment strategies for inflammatory or degenerative arthritis by facilitating the synthesis of therapeutic factors within the joint space.

Consistent with previous reports of AAV injection into the knee joint of various animals, both luciferase and GFP transgene expressions were mostly localized to soft tissues (44, 46, 95, 97, 99). GFP imaging with the stereomicroscope provided a more precise localization than the bioluminescence imaging system and indicated that few sparse areas of GFP-positive cells could be found in articular cartilage. A recent study employing self-complementary AAV2 injected into the intra-articular joint of guinea pigs also demonstrated transgene expression by articular chondrocytes (97). Previous studies using AAV have shown higher levels of transgene expression in diseased cartilage compared to normal cartilage (44, 46). Seeing that intact and undamaged articular cartilage is unlikely to require treatment, future studies will test AAV in rat models of articular cartilage damage, as it will more closely mimic the osteoarthritic environment. Abundant transgene expression in soft tissues suggests that cells within these tissues, such as those within the infrapatellar fat pad, can uptake the AAV2 and lead

to transgene expression. Given the low turnover rate of these cells, intra-articular delivery of AAV2 targeted to soft tissues is of value for anti-inflammatory treatment strategies for arthritis conditions. For articular cartilage repair, it may be necessary to target more specifically the chondrocytes. This may be especially important if delivering genes encoding for bone morphogenetic proteins, as their expression in soft tissues could result in ectopic mineralization. We and other are exploring strategies for targeted delivery of transgenes to articular chondrocytes and chondral defects (42, 107, 108).

Lack of luciferase signal in the contralateral control knee that did not receive AAV-CMV-Luc, and lack of signal anywhere else in the animal suggests that intra-articular injection limits AAV2 delivery to tissues within the joint and does not travel systemically. This is advantageous, as bioactive factors present from viral transgene expression would not affect tissues outside of the joint, and possibly lead to negative side effects.

The dose of AAV used in this study of $2.5 \times 10^{10}$ vg/knee joint was chosen based on what was previously been shown to be effective in rats (45). This prior study employed $10^{10}$ vg of AAV/rat knee joint and reported transgene expression for at least 100 days. The dose chosen for our current rat study will need to be increased in order to be effective in a human joint, which is larger in size and in volume of synovial fluid, resulting in a larger volume of distribution.

Others have shown that it is feasible to administer AAV to humans through intra-articular injection. Human clinical trials for rheumatoid arthritis using a recombinant, single-stranded AAV2 vector have performed intra-articular injections at doses ranging from $10^{11}$ to $10^{13}$ vg/mL and 5 mL was injected per joint (88, 109). The authors reported these dosages to be safe and feasible, and although some improvement in patient-reported outcomes was observed, the transgene expression was not found to be sufficient. It should be noted that humans have serum

IgG and neutralizing factors against different types of AAV, representing a limiting factor to AAV gene therapy (110). In moving towards direct intra-articular injection of AAV to larger joints, it will be important to determine the optimal dose of AAV to deliver and the serotype that will face the least amount of neutralizing antibodies.

Studies involving inducible gene therapy for musculoskeletal application have mainly focused on genetic engineering of cells *ex vivo*, followed by their implantation *in vivo* (75, 111-113). Direct viral gene delivery is easier to administer, and does not require the additional time and cost associated with *ex vivo* cell-mediated gene delivery. As shown in this study, the transgene expression can last for up to a year, which is not the case with implanted cells (42). By persisting for a prolonged period of time, there is the possibility to perform multiple cycles of transgene expression with a single injection of AAV, as shown in this study.

We observed increased transgene expression with addition of Dox to the drinking water and reduction of transgene expression following its removal at both 14 days and 13 months post-AAV injection. A similar trend was observed after 8 months. These data demonstrate the persistence of the transgene and controllability of its expression. The variability in observed transgene expression between the 14 days, 8 months, and 13 months time points could reflect type II error due to the small sample size or potentially be related to a difference in Dox intake. Adding Dox to the drinking water, while simple and shown in this study to be capable of controlling *in vivo* intra-articular transgene expression, may however lead to some degree of variability since free water intake is less well controlled than oral administration as a pill or measured suspension. Future studies with inducible gene expression systems may need to use direct injection of Dox in small animals and oral suspension or pill administration in larger animals.

Induction of gene expression 13 months post-AAV injection is of clinical relevance when a therapeutic protein needs to be re-administered to further promote cartilage repair, or in cases where cartilage resumes degrading or inflammation increases and another round of treatment is necessary. An inducible AAV2 gene expression system is also of interest for the delivery of multiple factors. Different biological molecules could be synthesized at different time points, depending on the regulatory transcriptional activator. This would provide a controlled environment for cartilage repair, where multiple growth factors are involved. A limitation of the inducible AAV2 gene expression system used in this study is the observed leakiness without the addition of Dox. This can potentially be addressed in future studies by newer rtTA vectors that have been developed to reduce basal activity and that require less Dox to be activated (114).

## 2.5 CONCLUSIONS

In summary, AAV2 delivered by a single intra-articular injection to a normal rat knee joint led to persistent and stable transgene expression that was mainly localized to soft tissues of the joint, with some expression in chondrocytes. Intra-articular injection of an inducible AAV2 vector demonstrated the ability to regulate *in vivo* transgene expression by oral administration of Dox, a compound that is safely used in humans. This regulation was possible immediately after delivering the AAV to the knee joint, and 13 months later. Ability to achieve stable yet high regulatable long-term intra-articular transgene expression is of potential clinical utility for development of new treatment strategies for intra-articular disease processes, such as inflammatory and degenerative arthritis.

# 3.0 PERSISTENCE, LOCALIZATION, AND EXTERNAL CONTROL OF TRANSGENE EXPRESSION AFTER SINGLE INJECTION OF ADENO-ASSOCIATED VIRUS INTO INJURED JOINTS

## 3.1 INTRODUCTION

Traumatic and degenerative injuries to articular cartilage are a leading source of disability. The limited healing potential of articular cartilage often leads to development of osteoarthritis (OA). OA is a chronic and progressive disease, and patients need to be on medications for a long period of time. Common medications for OA include non-selective non-steroidal anti-inflammatory drugs (NSAIDs) (115, 116). Chronic and often daily use of these drugs; however, is not without significant complications. NSAID therapy results in systemic side effects and is responsible for 16,500 deaths per year in the US (117). As well, there are no disease modifying treatments for osteoarthritis nor a method to completely re-establish cartilage function (79). Cartilage injuries or OA affects only a limited number of joints, without major extra-articular or systemic symptoms. Hence, delivery of bioactive agents in a localized manner to the injured joints is an attractive therapeutic option. It is therefore of critical interest to investigate an effective delivery vehicle that targets articular joints.

A potentially novel and innovative treatment strategy is gene therapy, utilizing viral vectors, such as adeno-associated virus (AAV) to deliver therapeutic proteins of interest to

affected joints to enhance joint repair or to prevent cartilage degradation. Recombinant AAV is a promising delivery vehicle for articular cartilage with the advantages of sustained transgene expression, reduced potential for host immune response, and the capacity to transduce both dividing and non-dividing cells *in vivo* and *in vitro* (108, 118). The viral vector is derived from an endemic, non pathogenic parvovirus, and intra-articular injection of AAV has been used in clinical trials for delivery of bioactive substances (88, 119). Numerous serotypes of AAV exist, each serotype with different preferential targets (44). AAV5 has recently been suggested to have better transduction efficiency in rodent arthritic joints; however, AAV2 has the best defined safety profile as it is used in clinical trials (48).

A recently published study from our laboratory has shown both stable and persistent reporter transgene expression at one year after a single intra-articular injection of AAV (47). Most of the AAV transduction occurred in the intra-articular soft tissues covered with synovial lining, with limited articular chondrocyte transduction. This is consistent with other studies, as vector penetration through the dense cartilage extracellular matrix is restricted (44, 116). However, high level expression of transgene product was possible from the soft tissues. Nonetheless, there are potential safety issues concerning long-term or high-dose expression of transgenes, in that overexposure could result in undesirable side effects. For this reason, controllable vectors have been developed to limit treatment time/dosage to the minimal needed to achieve therapeutic efficacy. One novel system is the Tetracycline (Tet)-on promoter, in which control is facilitated by using tetracycline molecule as an activator of the promoter, stimulating transgene expression only in the presence of the drug (76). Previous studies in our laboratory have successfully modulated gene expression utilizing the Tet-on system and doxycycline, a tetracycline analog (47). However, as intact/undamaged articular cartilage is

unlikely to require treatment, AAV administration strategies in the setting of joint injury will provide invaluable information to improve gene therapy strategies for joint restoration.

This study tests the hypotheses that 1) *in vivo* AAV transgene expression localizes to damaged cartilage when AAV is administered post-injury, 2) AAV injection pre-injury leads to the creation of a soft tissue reservoir that persistently expresses transgene products at high levels, and 3) *in vivo* transgene signal can be externally controlled after joint injury using oral doxycycline. Two surgically created unilateral joint injuries of high clinical relevance will be studied: osteochondral defect (OCD) and anterior cruciate ligament transection (ACLT).

## 3.2 METHOD

### 3.2.1 AAV preparation

Double stranded AAV serotype 2 (AAV2) vectors were produced, purified, and vector genome (vg) titer determined as previously described (120). AAV2s with constitutively active cytomegalovirus (CMV) promoter included AAV2-CMV-Luciferase (Luc) and AAV2-CMV-reverse-tetracycline-controlled transactivator (rtTA). AAV2 with tetracycline response element (TRE) promoter included AAV2-TRE-Luc.

### 3.2.2 Explant study

Femoral cartilage samples from three month old male Sprague Dawley rats (Harlan) were harvested, washed in phosphate buffered saline (PBS, Gibco) with 2% penicillin-streptomycin

(pen/strep, Gibco) and incubated for 2 – 3 days in 37°C, 5% $CO_2$ in 1:1 ratio Dulbecco's modified Eagle medium (DMEM) and F-12 (DMEM/F-12, Gibco), 10% fetal bovine serum (FBS, Gibco), 2% pen/strep, and 1% amphotericin B (Invitrogen). The explants were divided into three groups in triplicate: No Injury/No AAV Control, No Injury/AAV-CMV-Luc, Scratch injury with AAV-CMV-Luc. The explants from the latter group had the femoral condyles scratched with a blade. The explants from the No Injury/AAV-CMV-Luc and Scratch/AAV-CMV-Luc groups were transduced with AAV-CMV-Luc at a concentration of 80,000 vg/cell in serum-free DMEM/F-12. After one hour incubation, the culture media was replaced with fresh DMEM/F-12, 10% FBS, 2% pen/strep, and 1% amphotericin B. The culture media was changed after two days. The explants were imaged after 96 hours post-AAV transduction, using IVIS® Imaging System 200 (Xenogen) by adding 10 μL of 30 mg/mL D-Luciferin Potassium Salt (Caliper Life Sciences) per 1 mL of culture media. The images were taken at 1 min exposure.

### 3.2.3 Animal studies

Animal experiments were performed following a University of Pittsburgh Institutional Animal Care and Use Committee (IACUC)-approved protocols 0901937 and 1103868. Longitudinal *in vivo* study was performed using forty-eight three month old male Sprague Dawley rats.

### 3.2.4 Animal surgeries

Twenty-four rats underwent unilateral OCD surgeries, while the other twenty-four rats underwent ACLT surgeries as previously described (121, 122). Briefly, all the procedures were carried out while the animals were anesthesized with inhalation of isoflurane (Phoenix

Pharmaceuticals): 2-5% for induction and 0.25-4.0% for maintenance. Rat knee joints were exposed via medial parapatellar and medial patellar tendon approaches. The patella was dislocated laterally and the knee was flexed. For the OCD surgeries, the midpoint of the femoral trochlea was identified and a 1.5 mm carbide tipped drill (Emil Lange/ELA) was used to create an OCD approximately 1.0 mm deep. The subchondral bone was penetrated and bleeding bone was observed. For the ACLT surgeries, ACL and posterior cruciate ligament (PCL) were visualized with the aid of a 3x surgical loupe (Carl Zeiss). Forceps were used to protect the PCL and the ACL was severed using a 1.5 mm Cutting Edge Beaver Needle Blade (Becton, Dickinson and Company). ACLT was confirmed with an anterior drawer test. Following injury creation for both OCD and ACLT, the joint spaces were washed with sterile saline, and both capsule and skin were sutured using monofilament 4-0 monocryl (Ethicon). An intramuscular injection of 0.2 – 0.5 mg/kg buprenorphine (Hospira) was administered twice per day for two days following surgery for analgesia.

### 3.2.5 AAV injections

AAV2-CMV-Luc was used to characterize the persistence and localization of the transgene signal while AAV2-TRE-Luc was used to characterize the external controllability of the transgene signal using oral doxycycline.

Two different AAV injection time points were investigated to compare the transgene expression levels: post-injury AAV injection and pre-injury AAV injection. For the post-injury AAV injection group, the viral vectors were injected bilaterally into both injured and intact joints at one week post-injury for OCD rats and three weeks post-injury for ACLT rats. For the pre-injury AAV injection group, the AAVs were injected bilaterally into the joint. After twenty-eight

days, when the transgene expression level has stabilized, the animals underwent unilateral joint surgeries, either OCD or ACLT.

Each knee was given a total of 50 μL of AAVs, containing 2.5 x $10^{10}$ vg of either AAV2-CMV-Luc or AAV2-TRE-Luc and an equal amount of AAV2-CMV-rtTA by single intra-articular injection. During the injection procedures, animals were anesthesized with gaseous isoflurane. Six rats were used for each viral construct per injury model per AAV injection time points (Table 3-1).

**Table 3-1: Animal study design**
Two AAV-injection time points were investigated on OCD and ACLT models of joint damage, with *N* = 6/injury type/AAV-injection time point/AAV-construct.

| AAV-injection Timepoint | Injury | AAV2 construct | N |
|---|---|---|---|
| **Post-injury** | OCD | AAV2-CMV-Luc | 6 |
| | | AAV2-TRE-Luc | 6 |
| | ACLT | AAV2-CMV-Luc | 6 |
| | | AAV2-TRE-Luc | 6 |
| **Pre-injury** | OCD | AAV2-CMV-Luc | 6 |
| | | AAV2-TRE-Luc | 6 |
| | ACLT | AAV2-CMV-Luc | 6 |
| | | AAV2-TRE-Luc | 6 |
| **Total number of rats:** | | | 48 |

### 3.2.6 External control of transgene expression

To induce expression of luciferase in the animals injected with AAV2-TRE-Luc, the rats were administered drinking water containing doxycycline (Sigma) at a concentration of 2 mg/mL for seven days, followed by its removal. To ensure fresh supply of doxycycline, the water was replaced every day and protected from light using amber drinking bottles. Addition of doxycycline to the drinking water was performed at 14 days, 3 months, and 6 months post-AAV injection. Rats injected with AAV2-CMV-Luc had regular drinking water for the duration of the study.

### 3.2.7 Longitudinal *in vivo* live animal imaging

At each imaging time point, rats were anesthetized with isoflurane inhalation, followed by a 50 µL intra-articular injection of 30 mg/mL D-Luciferin Potassium Salt substrate. After 5 minutes, rats were placed in and imaged with an IVIS® 200 optical imaging system. Rats injected with AAV2-CMV-Luc were imaged every week for the first month, and monthly thereafter, until six months post-AAV injection, when the rats were sacrificed. On the day of sacrifice following regular imaging as detailed above, rats received a 400 µL intra-peritoneal injection of 30 mg/mL D-Luciferin Potassium Salt substrate (Goldbio) to determine if any signal was present outside the joint. The joint was then opened to image the intra-articular tissues. Rats injected with AAV2-TRE-Luc were imaged three times for every oral doxycycline stimulation cycle: pre-doxycycline time point prior to addition of doxycycline, 7 days following doxycycline addition, and 7 days following doxycycline removal. These rats were sacrificed at six months post-AAV injection as well, following the third doxycycline stimulation cycle. All the rats were sacrificed via $CO_2$ asphyxiation and subsequent thoracotomy.

### 3.2.8 Statistical analyses

All the statistical analyses were performed using Statistical Packages for Social Studies (SPSS) 17.0 (IBM). Results were judged for significance at $p < .05$, unless otherwise noted. Explant data were observed in triplicate (Fig. 1, $n = 3$). *In vivo* animal data were observed using independent animals, with $N = 6$ per group. All the data were tested for assumptions of parametric data: Shapiro-Wilk for normality of data distribution and Levine's for homogeneity of variance. The parametric bioluminescence data for the explant study is represented as median and interquartile

range boxplots, and analyzed using one-way independent analysis of variance (ANOVA) with *post hoc* Tukey (Fig. 3-1). The longitudinal bioluminescence data for the animal studies assessing the persistence and magnitude of the AAV-transgene are represented as line graphs ± standard error of mean (SEM) and were analyzed using two-way mixed ANOVA, with main independent variables of joint injury status as paired variable and time as repeated variable (Fig. 3-2 and 3-4). Friedman's ANOVA test with a Bonferroni correction was used as a *post hoc* test to assess effect of time on each of the injured and intact joints ($p < .025$ considered significant) and Wilcoxon Signed Ranks test with a Bonferroni correction was used as a *post hoc* test to assess the effect of joint injury status at each outcome time points when the interaction effect of time between the time and joint injury status was significant (Fig. 3-4B). The bioluminescence data assessing controllability of transgene expression were analyzed using one-way repeated measured ANOVA (Fig. 3-6).

## 3.3 RESULTS

### 3.3.1 *In vitro* AAV transduction of explants

Transgene expression was observed from femoral cartilage explants transduced with AAV-CMV-Luc (Fig. 3-1). The bioluminescence signal was greater in No Injury/AAV-CMV-Luc group ($p = .046$) and Scratch/AAV-CMV-Luc group ($p = .008$) compared to No Injury/No AAV Control group. While no difference was observed between the two AAV-CMV-Luc transduced groups ($p = .313$), the mechanical scratch injury model where the condyles were scratched with a blade showed brighter bioluminescence at both lateral and medial condyles.

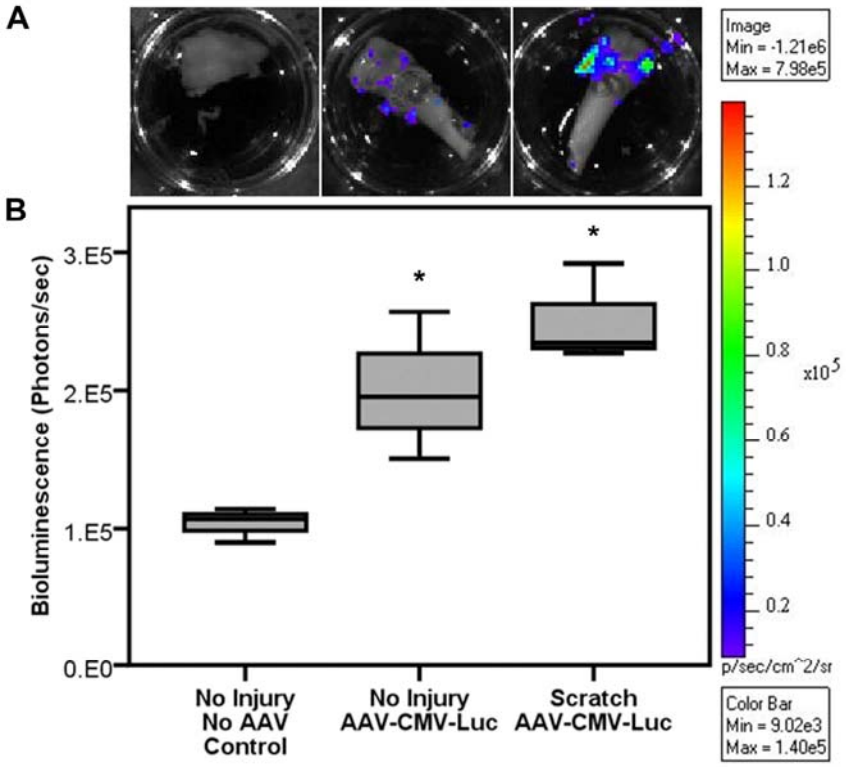


**Figure 3-1: Explant AAV transduction of rat femoral cartilage**
Rat femoral cartilage explants were either scratched or kept intact (No Injury), after which they were transduced with AAV-CMV-Luc. Luciferase signal was detected after 96 h. **(A)** Representative images of bioluminescence signal from the explants. **(B)** Median and interquartile range of bioluminescence for the different explant groups. $n = 3$. *$p < .05$ versus No Injury/No AAV Control group.

### 3.3.2 AAV transduction in osteochondral defect injury

AAV transgene expression was persistent in both the OCD and intact joints whether the AAV was injected post- or pre-OCD injury (Fig. 3-2). However, the magnitude of the transgene expression levels in the OCD joints was different between the two AAV injection time points. For the knees with AAV injected post-OCD, there was a significant main effect of the injury status on the bioluminescence level ($p = .015$), where the OCD knees had lower signal than the intact knees (Fig. 3-2B). On the other hand, for the knees with AAV injected pre-OCD, the main effect of the injury status on the bioluminescence level was non-significant ($p = .924$, Fig. 3-2D). As well, the luciferase expression remained unchanged from the pre-OCD time points. For both

the AAV injection time point groups, there was a non-significant main effect of time on the bioluminescence level ($p$ = .175 for post-OCD AAV injection and $p$ = .185 for pre-OCD AAV injection): the transgene magnitude remained constant throughout the duration of the study for each of the joints. The interaction effect between the joint injury status and the time was non-significant in both cases as well ($p$ = .182 or post-OCD AAV injection and $p$ = .921 for pre-OCD AAV injection).

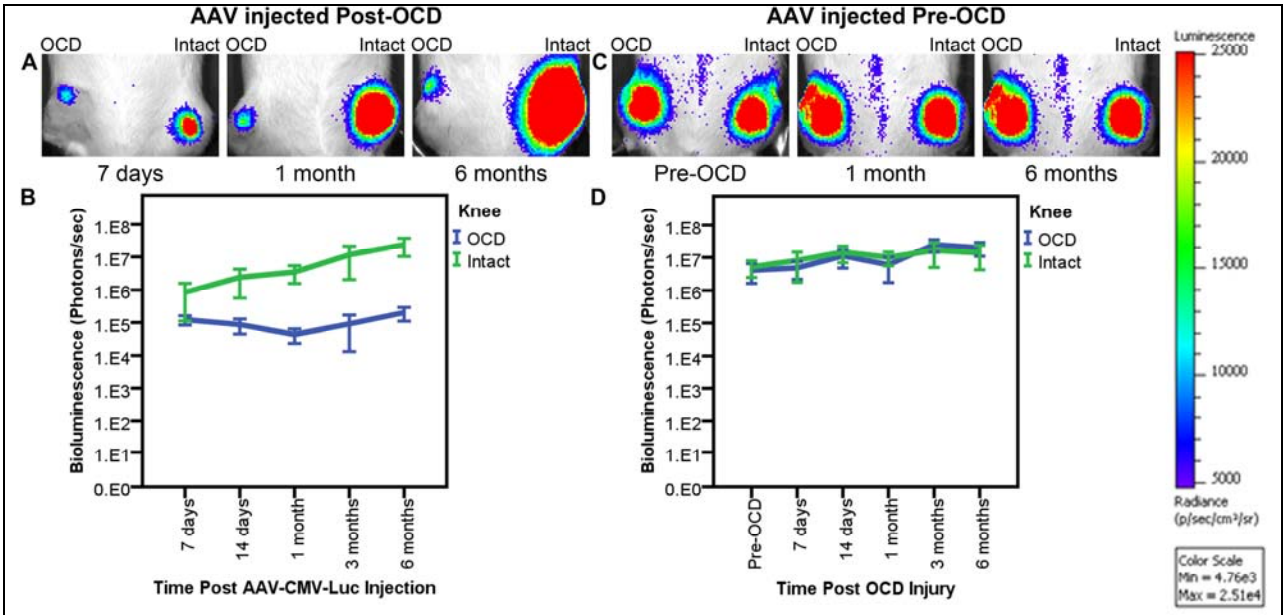


**Figure 3-2: Persistence of AAV transgene in osteochondral defect injury model**
Persistence of *in vivo* transgene expressions in OCD injured joints with a single intra-articular injection of AAV-CMV-Luc post-OCD **(A and B)** or pre-OCD **(C and D)** were assessed via bioluminescence. **(A)** Representative images of transgene signal from the OCD and intact joints at 7 days, 1 month, and 6 months following AAV-CMV-Luc injection 1 week after OCD injury. **(B)** Mean and SEM of bioluminescence observed in the OCD and intact joints of all rats in the group over 6 months following AAV-CMV-Luc injection 1 week after OCD injury. **(C)** Representative images of transgene signal from the OCD and intact joints injected with AAV-CMV-Luc 4 weeks prior to OCD injury at pre-OCD, 1 month, and 6 months time points. **(D)** Mean and SEM of bioluminescence observed in the OCD and intact joints of all rats in the group over 6 months following OCD injury in joints injected with AAV-CMV-Luc 4 weeks prior. $N$ = 6/group.

Upon exposing the intra-articular space, the location of transgene expression was different in the OCD injured knees between the two different AAV injection time points (Fig. 3-3). For both of the AAV injection time points, the intact joints had the diffuse and high magnitude signal in the exposed infrapatellar fat pad. However, for the OCD injured joints, the

bioluminescence signal was concentrated to the injured cartilage and the associated OCD repair tissue in the post-OCD AAV-injected knees (Fig. 3-3A), whereas the signal was more diffusely found in intra-articular soft tissues, mainly the fat pad in the pre-OCD AAV-injected knees, with no bioluminescence observed in the injured cartilage (Fig. 3-3B). Hence, the pre-OCD AAV-injected knees had transgene signal location similar to those of the intact joints.

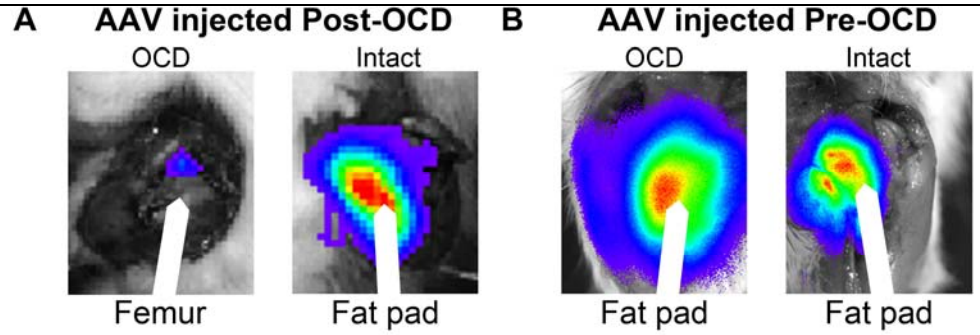


**Figure 3-3: Localization of AAV transgene in osteochondral defect injury model**
Intra-articular localization of transgene expressions in OCD injured joints with a single intra-articular injection of AAV-CMV-Luc were assessed after exposing the joint on the day of sacrifice using the IVIS optical imaging system. **(A)** Representative intra-articular images of transgene signal from the exposed OCD and intact joints that were injected with AAV-CMV-Luc 1 week after OCD injury. **(B)** Representative intra-articular images of transgene signal from the exposed OCD and intact joints that were injected with AAV-CMV-Luc 4 weeks prior to OCD injury.

### 3.3.3 AAV transduction in anterior cruciate ligament transection injury

Similarly to the OCD injury model, the transgene expression was persistent in both the ACLT and intact joints, and for both post-ACLT and pre-ACLT AAV injections (Fig. 3-4). The magnitude of the bioluminescence levels in the ACLT joints was again different between the two AAV injection time points. For the joints with AAV injected post-ACLT, there was a significant main effect of the injury status ($p$ = .001): the ACLT joints had lower signal than the intact (Fig. 3-4B). For the knees with AAV injected pre-ACLT, on the other hand, the main effect of the injury status was non-significant, with no change in transgene expression from the pre-ACLT time points ($p$ = .717, Fig. 3-4D). The main effect of time on the bioluminescence level was

significant for the post-ACLT AAV injected group ($p$ = .010) and non-significant for the pre-ACLT AAV injected group ($p$ = .401). The interaction effect between the joint injury status and the time was significant for post-ACLT AAV injection study group ($p$ = .011) and non-significant for pre-ACLT AAV injection study group ($p$ = .872). Further *post hoc* testing of the post-ACLT AAV injection study group showed that the effect of time on the bioluminescence level of the ACLT joints is non-significant for the ACLT injured joints ($p$ = .992). Hence, the transgene magnitude remained constant throughout the study period in the ACL injured joints for both post-ACLT and pre-ACLT AAV injection groups.

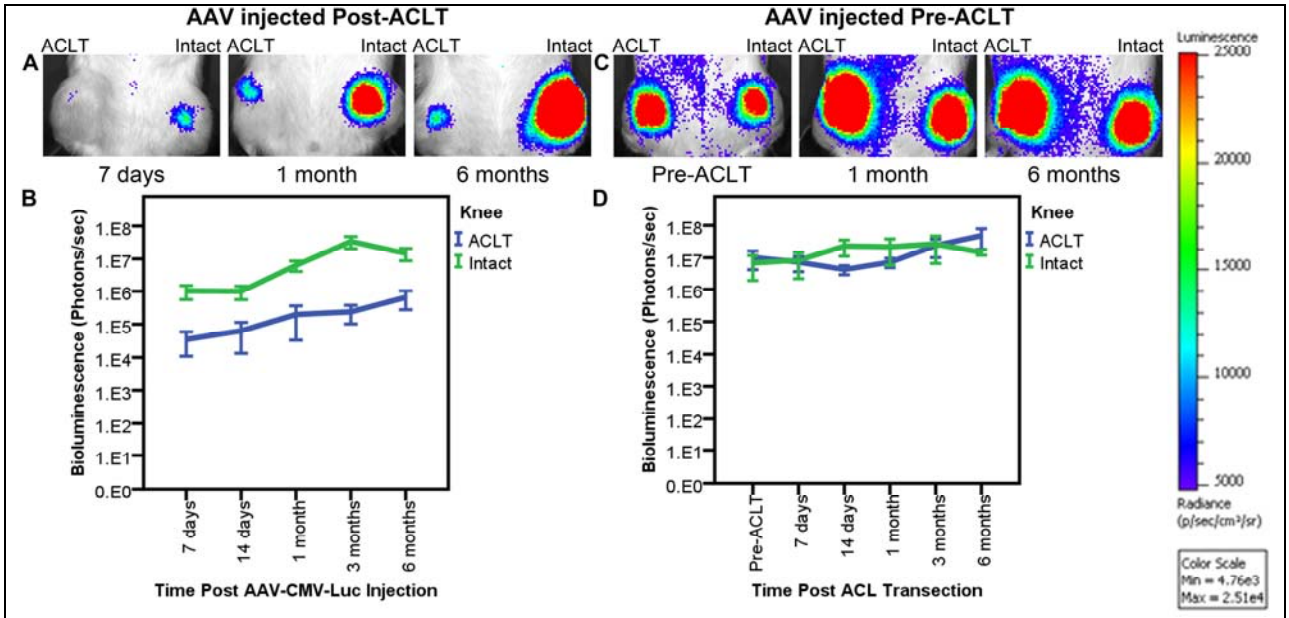


**Figure 3-4: Persistence of AAV transgene in anterior cruciate ligament transection injury model**
Persistence of *in vivo* transgene expressions in ACL transected joints with a single intra-articular injection of AAV-CMV-Luc post-ACLT **(A and B)** or pre-ACLT **(C and D)** were assessed via bioluminescence. **(A)** Representative images of transgene signal from the ACLT and intact joints at 7 days, 1 month, and 6 months following AAV-CMV-Luc injection 3 weeks after ACL transection. **(B)** Mean and SEM of bioluminescence observed in the ACLT and intact joints of all rats in the group over 6 months following AAV-CMV-Luc injection 3 weeks after ACL transection. **(C)** Representative images of transgene signal from the ACLT and intact joints injected with AAV-CMV-Luc 4 weeks prior to ACL transection at pre-ACLT, 1 month, and 6 months time points. **(D)** Mean and SEM of bioluminescence observed in the ACLT and intact joints of all rats in the group over 6 months following ACL transection in joints injected with AAV-CMV-Luc 4 weeks prior. $N$ = 6/group.

When the intra-articular space was exposed, the localization of bioluminescence signal was different in the ACLT joints between the two different AAV injection time points as well

(Fig. 3-5). Consistent with the intact sides of the OCD injury model animals, the intact joints showed diffuse signal in the exposed infrapatellar fat pad for both of the AAV injection time points. As well, the diffuse bioluminescence signal was found in the infrapatellar fat pad for the pre-ACLT AAV-injected ACL transected joints, with no signal found in the cartilage (Fig. 3-5B). However, for the post-ACLT AAV-injected ACL transected joints, the bioluminescence signal was lower in the intra-articular soft tissues but some region of concentrated signal in the injured cartilage (Fig. 3-5A).

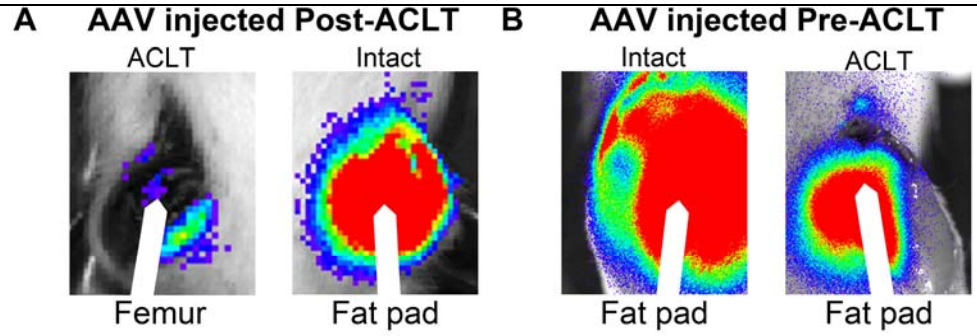


**Figure 3-5: Localization of AAV transgene in anterior cruciate ligament transection injury model**
Intra-articular localization of transgene expressions in ACL transected joints with a single intra-articular injection of AAV-CMV-Luc were assessed after exposing the joint on the day of sacrifice using the IVIS optical imaging system. **(A)** Representative intra-articular images of transgene signal from the exposed ACLT and intact joints that were injected with AAV-CMV-Luc 3 week after ACL transection. **(B)** Representative intra-articular images of transgene signal from the exposed ACLT and intact joints that were injected with AAV-CMV-Luc 4 weeks prior to ACL transection.

### 3.3.4 External control of AAV-transgene expression in injured joints

Rats that received the inducible AAV2-TRE-Luc showed gene expression upregulation with addition of Dox and downregulation following its removal from the drinking water from both the OCD and ACLT injured joints (Fig. 3-6). This finding was consistent between the two AAV injection time points.

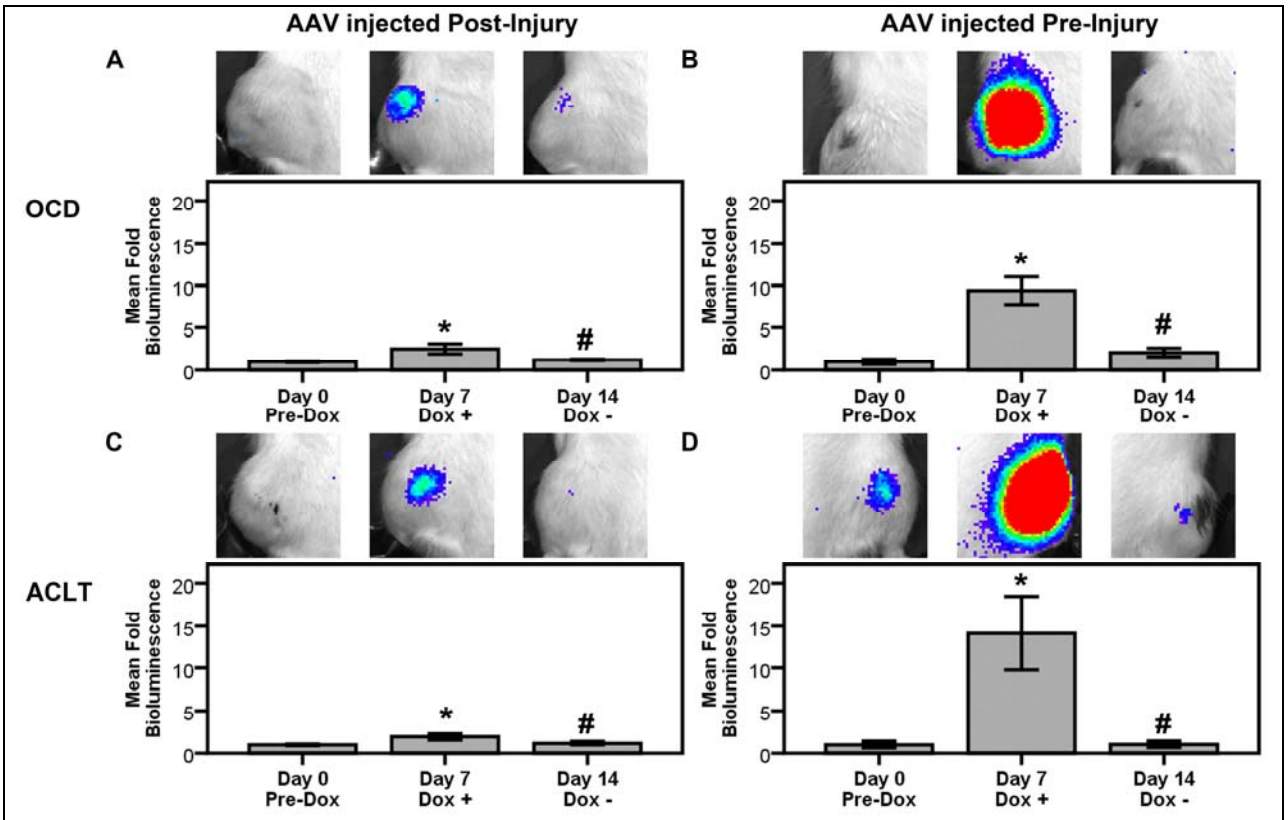


**Figure 3-6: Controllability of AAV transgene in joint injury models**
Intra-articular transgene expressions in injured joints with a single intra-articular injection of AAV-TRE-Luc post-injury **(A and C)** or pre-injury **(B and D)** were assessed after a cycle of doxycycline addition and removal using the IVIS optical imaging system. **(A)** Representative intra-articular images of transgene signal from the OCD joints that were injected with AAV-TRE-Luc 1 week after OCD injury. **(B)** Representative intra-articular images of transgene signal from the OCD joints that were injected with AAV-TRE-Luc 4 weeks prior to OCD injury. **(C)** Representative intra-articular images of transgene signal from the ACLT joints that were injected with AAV-TRE-Luc 3 weeks after OCD injury. **(D)** Representative intra-articular images of transgene signal from the ACLT joints that were injected with AAV-TRE-Luc 4 weeks prior to ACL transection. *$p < 0.05$ compared to Day 0: Pre-Dox. #$p < 0.05$ compared to Day 7: Dox +. N = 6 rats.

## 3.4 DISCUSSION

Treatment or prevention strategies of pathologic processes within articular joints are severely limited. Hence, a successful delivery strategy for adequate levels of therapeutic molecules in a localized manner is critically important. Gene therapy strategies, therefore, has gained a lot of attention for arthritis treatment (44, 116). Numerous vectors are available for *in vivo* gene transfer, such as naked DNA, retrovirus, adenovirus, etc.; however, most are limited in term of

safety, efficacy, and duration (123). AAV, on the other hand, is a very promising vector system that may provide the best balance between safety and *in vivo* gene delivery efficiency (116). Methods to localize and control *in vivo* transgene expression are important to enhance the therapeutic efficiency and safety of intra-articular AAV gene therapy. This has been achieved in intact joints (47). However, to more closely mimic the osteoarthritic environment, AAV transduction to injured cartilage and joints has been investigated.

We initially characterized the efficacy of AAV transduction in explants culture of femoral cartilage. With 80,000 vg/cell AAV2-CMV-Luc, significant transduction was observed for rat femoral explants. There was no significant difference with transduction efficacy between the two AAV-transduced groups; however, the mechanical injury model where the condyles were scratched with a blade showed high intensity of luciferin flux at both lateral and medial condyles. This is potentially due to the scratch injury creating a more permeable path to articular chondrocytes for AAV transduction. Thus, we expected to have more AAV-transduction in damaged areas of articular cartilage.

For the *in vivo* animal studies, we chose two commonly used joint injury models of high clinical relevance: OCD and ACLT. The timing of AAV injection, pre- or post-joint injury, permitted us to characterize the effect of injury on AAV transduction and localization of transgene expression. For both of the injury models, AAV transduces and is mainly expressed by intra-articular soft tissues in the intact sides, as shown in the previous study (47). However, if the AAV is injected after joint injury, as would likely be the case in a clinical setting, the transgene signal localizes to the vicinity of the injured cartilage and associated repair tissue. As in the case for the explants study, the injured cartilage, with more permeable extracellular matrix, would have allowed AAV to travel and traduce the chondrocytes/injury activated repair cells. The

transgene expression from the soft tissues was limited for both OCD and ACLT injured joints. This can also be due to a number of reasons, such as increased volume of synovial fluid in injured joints diluting the intra-articular viral concentrations, injury-activated macrophages clearing up the virus prior to effective transduction, or the viral gene promoter shut off in response to the injury (124). When the AAV is injected before injury, the transgene signal magnitude as well as localization was no different from those of the intact joints. All of the transgene expression was found in the soft tissues with no detectable signal from the injured cartilage or associated repair tissue. This pre-injury AAV injection data makes the theory that promoter shuts off in response to injury less likely.

The differential transgene location between the two AAV-injection timepoints can be used to optimize AAV-mediated cartilage repair strategies. The highly localized gene expression following AAV injection post-injury is advantageous for gene therapy strategies that deliver anabolic growth factors that would aid in cartilage repair, especially genes that need to specifically target chondrocytes to be effective. Such strategies may include RNA interference against various cartilage catabolites, such as aggrecanases/ADAMTSs (70), or chondrogenic growth factors that have adverse effects on other intra-articular soft tissues, such as transforming growth factor (TGF)-$\beta_1$. TGF-$\beta_1$ has been shown to increase chondrocyte matrix synthesis when its gene vector was injected in the joint; however, its overexpression from the synovium resulted in adverse fibrosis (66).

Diffuse signal, seen when AAV is injected before creation of injury, is also of potential value, as it provides a model to study the delivery of protective factors to individuals that may be at high risk for cartilage degeneration. Although the virus does not specifically transduce chondrocytes, a high level of transgene expression from surrounding soft tissues still allows for

preventative therapeutic approaches by using the soft tissue as a drug depot to release protective molecules. The high intra-articular concentrations of secreted products, such as a cytokine antagonist like interleukin-1 receptor antagonist protein, can protect the cartilage by competing with catabolic factors in the joint (74). Moreover, since synoviocytes release numerous pro-inflammatory molecules in arthritic conditions, a strong tropism of AAV for the synovium can be utilized to suppress expression of any of these injurious compounds (125).

The controllability of gene expression in intact and injured joints is also important since gene expression may not be needed for a prolonged period of time to have a beneficial effect, and it provides added means of safety. We have shown this controllability in all the injury models, whether the AAV was injected post- or pre-injury using oral administration of doxycycline in drinking water. Doxycycline is an analog of tetracycline, an anti-microbial agent that is safely used in humans (78). In addition, the use of doxycycline as the transgene inducer molecule may have added beneficial effect for cartilage protection. Doxycycline inhibits collagen degrading enzymes, such as matrix metalloproteinases (MMPs), and has shown beneficial effects in both OCD and ACLT injury models by preventing MMP upregulation (121, 126).

The studies investigating AAV transduction in injured joints are limited, and only rheumatoid arthritis injury setting has been explored (44, 46, 127). Two groups used a transgenic mice model that spontaneously develops arthritis due to tumor necrosis factor (TNF)-α overexpression (44, 127). Goater et. al. reported increased AAV transduction efficiency with increased degree of the joint disease following an intra-articular injection of AAV, with synoviocytes as the primary target. As well, *in vitro* transduction efficiencies of synoviocytes extracted from the transgenic mice increased with the treatment of these cells with damaging

agents, such as irradiation and TNF-α. However, their study was done using single stranded AAV, where the second strand synthesis is the limiting step in AAV transgene expression. Hence, the injurious agents promote DNA synthesis and thus transgene expression as well. The use of double stranded or self complementary AAV has been shown to improve AAV transgene expression (73). Zhou et al. showed persistent transgene expression for 120 days following AAV-Luc injection in the transgenic mice joints; however, they did not compare their bioluminescence level to intact joints, preventing a comparison to our study. Another study investigated intra-articular AAV transduction in Sprague Dawley rats damaged via a joint injection of lipopolysaccharide (LPS) (46). This study showed positive correlations between disease severity and AAV transduction and between disease severity and transgene expression. Again, however, these injury models mimic inflammatory/rheumatoid arthritis rather than osteoarthritis.

Limitations of the current investigation include that the models of joint injury were surgically induced, which is removed from most human idiopathic osteoarthritis cases. Hence, the relevance of the results from this study may be more applicable to joint injuries secondary to trauma. However, post-traumatic arthritis, with a known date of onset/injury, is more amenable for early intervention strategies such as AAV-mediated gene therapy compared to idiopathic OA with less definable time of onset (128). Our current focus was mainly for the characterization of AAV-transgene expression in the injured joints. The mechanism behind differential gene expression localization between the post-injury and pre-injury AAV injection time points remains unresolved and needs further elucidation with sham operated animals, as well as various other control groups.

## 3.5 CONCLUSIONS

While AAV transgene expression was localized to the soft tissues of the uninjured joint and injured joints when AAV was injected pre-injury, AAV was able to transduce articular chondrocytes within the cartilage matrix when injected following injuries. The explant data showing AAV-transduction of articular chondrocytes in damaged cartilage suggests that cartilage matrix injury may have facilitated entry of more AAV into the cartilage. The *in vivo* data supports use of AAV for persistent, regulated, and safe intra-articular release of bioactive factors from injured joint tissues for cartilage repair/protection. Differential transgene expression localizations can be used to optimize AAV-mediated cartilage repair strategies: post-injury AAV injection approaches would directly target articular chondrocytes in diseased and injured cartilage and pre-injury AAV injection would allow intra-articular delivery of secreted anti-inflammatory factors for sustained release from soft tissues to protect the joint. This information can aid in the design of transgene product that could be used for joint strategies. Overall, these data support further study of the *in vivo* therapeutic potential of AAV for safe and localized delivery of bioactive substances to injured joints. This can aid in cartilage repair, which may delay or prevent the onset of debilitating osteoarthritis.

# 4.0 EFFECTS OF DOXYCYCLINE ON MESENCHYMAL STEM CELL CHONDROGENESIS AND CARTILAGE REPAIR

## 4.1 INTRODUCTION

Annually, nearly one million people in the United States are affected by articular cartilage injuries. These injuries result in significant disability and have a substantial disease and financial burden for the healthcare system and the economy. Articular cartilage has limited capability to regenerate or repair following injury, and therefore presents a great therapeutic challenge (129, 130). Furthermore, focal cartilage injuries are known to accelerate the degeneration of surrounding cartilage, hastening onset of osteoarthritis. Microfracture (bone marrow stimulation) is the simplest and most commonly used surgical procedure for many focal cartilage injuries. This technique involves the recruitment of bone marrow derived mesenchymal stem cells (MSCs) to the defect area in an attempt to stimulate chondrogenesis. However, the repair does not restore pristine hyaline cartilage containing type II collagen, but instead results in formation of a mechanically inferior fibrocartilage scar primarily composed of type I collagen (129, 130). Therefore, new and innovative clinical strategies are needed to improve the type and quality of repair tissue in order to prevent the development of osteoarthritis.

Doxycycline is a widely available and inexpensive anti-microbial agent that is safely used in humans (78). In addition, doxycycline is a commonly used inducer molecule for the

tetracycline-inducible gene regulation system for controlled gene therapy applications in the articular joint as well as other organ systems across multiple animal models (47, 131). Besides these anti-microbial and gene-inducing functions, doxycycline may also have intrinsic benefits to cartilage. It has been well established that the tetracycline class of medications have the ability to inhibit matrix metalloproteinases (MMPs), specifically MMP-1 (collagenase-1), MMP-3 (stromelysin), and MMP-13 (collagenase-3), independent of their anti-microbial activity (132-137). Doxycycline is the tetracycline analog that is most studied for MMP-inhibition, and it has been shown to exert a beneficial effect against extracellular matrix (ECM) degradation in arthritic diseases, as MMPs are shown to be upregulated in arthritis and following cartilage injury (133, 136-139). Down-regulation of MMPs increases the amount of collagens produced and retained in the ECM (136). However, despite the existing studies suggesting high potential for doxycycline to exert a protective effect against cartilage degeneration, there are limited studies evaluating the effects of doxycycline on the repair tissue formed by MSCs following bone marrow stimulation.

This study tests the hypothesis that doxycycline reduces MMP expression, enhances human mesenchymal stem cell (hMSC) chondrogenesis and improves *in vivo* cartilage repair.

## 4.2 METHOD

### 4.2.1 *In vitro* studies

#### 4.2.1.1 hMSC chondrogenic differentiation

Human MSCs were obtained, processed, and maintained as previously described (57). MSCs at passage 3 underwent chondrogenesis as previously described pellet culture assay (57). Briefly, 2.5 x $10^5$ hMSCs were pelleted by centrifugation in 15 mL conical polypropylene tubes at 500 x *g* for 15 min. The pellets were cultured in 0.5 mL of pre-defined chondrogenic medium containing high-glucose Dulbecco's modified Eagle medium (DMEM, Gibco), with 1% penicillin-streptomycin (Gibco), $10^{-7}$ M dexamethasone (Sigma-Aldrich), 50 µg/mL L-ascorbic acid-2-phosphate (Sigma-Aldrich), 40 µg/mL proline (MP biomedicals), and 1% BD™ ITS+ Premix (Becton-Dickinson), 10 ng/mL transforming growth factor-beta1 (TGF-$\beta_1$, R&D Systems). The chondrogenic medium was supplemented with 0, 1, or 2 µg/mL of doxycycline. The pellets were incubated at 37°C in 5% $CO_2$ for 3, 7, 14, or 21 days, and the media was refreshed every 2 – 3 days.

#### 4.2.1.2 Chondrogenic hMSC pellet assessments

##### 4.2.1.2.1 Pellet area and histological evaluation

After 14- and 21-days of chondrogenic culture, three hMSC pellets per group were collected and assessed macroscopically using stereomicroscopy (MVX-10 MacroView Systems, Olympus)

equipped with a DP71 camera (Olympus). The pellet area was measured using DP2-BSW software (Olympus). The pellets were subsequently fixed in 10% buffered formalin and embedded in paraffin for histological analyses. Five-μm cross-sections were stained with Safranin O-Fast green for sulfated glycosaminoglycan (GAG) and alizarin red for calcium, and immunostained for MMP-13 according to standard protocols. Briefly for MMP-13 immunohistochemistry (IHC), sections were de-paraffined and rehydrated via conventional methods. Antigen retrieval was performed by heating and cooling the slides in 10-mM sodium citrate (pH 6.0) with 0.05% Tween-20 buffer (Sigma-Aldrich) for 20 minutes each at 85°C and room temperature. The sections were then digested in 1 mg/mL hyaluronidase in 0.1 M sodium acetate buffer (both from Sigma-Aldrich) for 30 minutes in 37°C. The hyaluronidase-digested sections were blocked with 10% goat serum (Vector Laboratories) and 1% bovine serum albumin (BSA, Fisher Scientific) for 1 hour. The sections were incubated with a rabbit polyclonal antibody against MMP-13 (Abcam) at 1:100 dilution in 1% BSA solution overnight at 4°C. Endogenous peroxidase was blocked using 0.3% hydrogen peroxide (Sigma) in tris-buffered saline (TBS, Calbiochem) for 15 minutes at room temperature. The slides were then treated with secondary goat polyclonal anti-rabbit antibody (Abcam) in 1% BSA solution in 1:100 dilution for an hour, then developed using ImmPACT™ AEC Peroxidase Substrate (Vector Laboratories), according to the manufacturer's instructions. The slides were counterstained with hematoxylin (Vector Laboratories). Images of all the stained sections were captured using TE-2000U Eclipse microscope (Nikon) equipped with a DP71 camera. The MMP-13 IHC images in Fig. 4 had the contrast increased by the same value in Adobe Photoshop CS4 to improve MMP-13-positive and -negative cell contrast for print.

#### 4.2.1.2.2 Biochemical analyses

After 3, 7, 14, and 21 days of chondrogenic culture, three hMSC pellets per group were washed with phosphate buffered saline (PBS, Gibco) and each dry pellet was frozen at -80°C until biochemical analyses. Each frozen pellet was incubated overnight in 0.25 mL papain buffer (50 mM sodium phosphate buffer (Sigma-Aldrich), 5 mM ethylenediaminetetraacetic acid (EDTA, Gibco), 5 mM cysteine HCl (Sigma-Aldrich), and 0.5 mg/mL papain (Sigma-Aldrich)) in 60°C shaking water bath (200 RPM). The papain-digested pellets were vortexed. GAG content was quantified using the standard dimethylmethylene blue (DMMB) assay using VersaMax UV-Vis spectrophotometer (Molecular Devices) (57), and DNA content was quantified using Quanti-iT™ PicoGreen® dsDNA Reagent and Kits (Molecular Probes) per manufacturer's protocol using a VICTOR™ X3 Multilabel Plate Reader (Perkin Elmer). The GAG/DNA ratios were calculated from the results of these two assays.

#### 4.2.1.2.3 Gene expression analyses

Three hMSC pellets per group at 3, 7, 14, and 21 days of chondrogenic culture were washed with PBS and frozen at -80°C until gene expression analyses. Total RNA was extracted from each frozen pellets using TRIzol (Invitrogen). Briefly, pellets in 0.3 mL TRIzol were grinded using microtube pestles (USA Scientific), and the ground pellet samples were homogenized using QIAshredder columns (Qiagen). The lysate was transferred to a new 1.5 mL tube and incubated at room temperature for 5 minutes, after which the contents were centrifuged at 12,000 x *g* for 10 min at 4°C. RNease Mini Kit (Qiagen) was used for the rest of the RNA isolating process per manufacturer's protocol. The pre-designed human *aggrecan*, *collagen-II*, *collagen-I*, *collagen-X*,

mmp-13 and *18S* TaqMan primers were purchased from Applied Biosystems. Custom human *sox-9* primers and probe (108) and human *transforming growth factor-beta receptor II* primers (forward: TCCACGTGTGCCAACAACATCAAC; reverse: TGCCACTGTCTCAAACTGCTCTGA) and FAM-labeled probe (ACAACACAGAGCTGCTGCCCATTG) were purchased from Integrated DNA Technologies. qRT-PCR reactions were done in duplicate in 384 well plates in a total volume of 10 μL as previously described (108) using 2x real-time TaqMan PCR Master Mix with an ABI PRISM 7700 Sequence Detection System (Applied Biosystems). Relative expression levels normalized to *18S* were calculated using the $2^{-\Delta Ct}$ method.

### 4.2.2 *In vivo* studies

#### 4.2.2.1 Animal surgeries

All longitudinal animal experiments were performed following a University of Pittsburgh Institutional Animal Care and Use Committee (IACUC) approved protocol (Protocol No. 1103868) using the previously established OCD model (42, 140). Briefly, OCD creation on twenty-four three-month old Sprague Dawley rats (Harlan) was performed under general gaseous anesthesia (Isoflurane, Phoenix Pharmaceuticals). The knees were shaved and swabbed with betadine and ethanol. A medial parapatellar approach was utilized to access the stifle joint. The patella was dislocated laterally and the knee was flexed to greater than 90-degrees to deliver the femoral trochlea into operative view. The trochlear groove was identified and the midpoint of the trochlea, which was the midpoint in the superior to inferior dimension at the center of the trochlear groove, was marked. A 1.5-mm drill was used to create the OCD, at a depth of 1.0-mm.

The subchondral bone was penetrated until bleeding bone was identified. Sterile saline was used to gently irrigate the area to remove any osteochondral fragments, and the incision was closed in layers. The animals were placed in standard cages with full access to food and water post-operatively. Subcutaneous buprenorphine (Reckitt Benckiser Healthcare) at 0.5 mg/kg dosage was injected twice daily for the first two-days following surgery as post-operative analgesia. Most of the study animals survived the OCD surgeries, except for one death associated with anesthesia complication. Hence, the number of animals per group in the *in vivo* study were N = 11 for No Doxycycline Control group and N = 12 for 12 Week Doxycycline group. The animals received either regular drinking water or 2 mg/mL doxycycline (Sigma-Aldrich) in the drinking water. Doxycycline water was replaced daily to ensure fresh supply of doxycycline.

**Table 4-1: ICRS Cartilage Repair Scoring System**

| Criteria | Points | Scores |
|---|---|---|
| **Degree of defect repair** | In level with surrounding cartilage | 4 |
| | 75% repair of defect depth | 3 |
| | 50% repair of defect depth | 2 |
| | 25% repair of defect depth | 1 |
| | 0% repair of defect depth | 0 |
| **Integration to border zone** | Complete integration with surrounding cartilage | 4 |
| | Demarcating border < 1mm | 3 |
| | ¾ of repair tissue integrated, ¼ with a notable border > 1 mm | 2 |
| | ½ of repair tissue integrated with surrounding cartilage, ½ with a notable border > 1 mm | 1 |
| | From no contact to ¼ of repair tissue integrated with surrounding cartilage | 0 |
| **Macroscopic appearance** | Intact smooth surface | 4 |
| | Fibrillated surface | 3 |
| | Small, scattered fissures or cracks | 2 |
| | Several, small, or few but large fissures | 1 |
| | Total degeneration of defect area | 0 |

#### 4.2.2.2 Repair tissue assessments

Following sacrifice by carbon dioxide asphyxiation at 12 weeks post-OCD surgery, the joints were dissected and the repair tissue was examined grossly using three-dimensional (3D) optical coherence tomography (OCT) scanning system with a 1,310 nm center wavelength (Bioptigen) as previously described (141). The specimens were also analyzed with the aforementioned stereomicroscopy and camera, with/without india ink staining for gross grading using the ICRS-Cartilage Repair Assessment system (Table 4-1) (142). The harvested femurs were then fixed, decalcified, embedded in paraffin, and subsequently sectioned. The sections were stained using traditional hematoxylin and eosin (H&E) staining, as well as immunostained using rabbit polyclonal antibody against MMP-13. The stained sections were imaged using DP71 camera and Eclipse TE2000-U microscope, and evaluated using modified Holland histological scoring system (Table 4-2) (42). Three independent blinded individuals graded both the gross and sectioned histologic specimens, and the scores were averaged for statistical analyses. For the estimate percentages of MMP-13-positive cells, the sections from four selected knees from each treatment groups were imaged at high-power fields (magnification, x 20). Positive and negative cells were counted using ImageJ software (NIH), and percentages were calculated by dividing the numbers of MMP-13-stained cells by the sum of the numbers of MMP-13-stained and unstained cells. On average, 304 cells were counted per OCD repair tissue. The MMP-13 IHC images in Fig. 4-6C had the contrast increased by the same value in Adobe Photoshop CS4 to improve MMP-13-positive and -negative cell contrast for print and cell counting.

| Table 4-2: Modified Holland Histological Scoring System | | |
|---|---|---|
| **Criteria** | **Points** | **Scores** |
| **Overall defect evaluation (throughout the entire defect depth)** | | |
| **Percentage filling with neoformed tissue (%)** | 100 | 3 |
| | >50 | 2 |
| | <50 | 1 |
| | 0 | 0 |
| **Subchondral bone evaluation** | | |
| **Percentage filling with neoformed tissue (%)** | 100 | 3 |
| | >50 | 2 |
| | <50 | 1 |
| | 0 | 0 |
| **Subchondral bone morphology** | Normal trabecular bone | 4 |
| | Trabecular, with some compact bone | 3 |
| | Compact bone | 2 |
| | Compact bone and fibrous tissue | 1 |
| | Only fibrous tissue or no tissue | 0 |
| **Extent of neotissue bonding with adjacent bone** | Complete on both edges | 3 |
| | Complete on one edge | 2 |
| | Partial on both edges | 1 |
| | Without continuity on either edge | 0 |
| **Cartilage evaluation** | | |
| **Morphology of neoformed surface tissue** | Extensively articular cartilage | 4 |
| | Mainly hyaline cartilage | 3 |
| | Fibrocartilage (spherical morphology observed with >75% of cells) | 2 |
| | Only fibrous tissue (spherical morphology observed with <75% of cells) | 1 |
| | No tissue | 0 |
| **Thickness of neoformed cartilage** | Similar to the surrounding cartilage | 3 |
| | Greater than surrounding cartilage | 2 |
| | Less than the surrounding cartilage | 1 |
| | No cartilage | 0 |
| **Joint surface regularity** | Smooth, intact surface | 3 |
| | Surface fissures (<25% neosurface thickness) | 2 |
| | Deep fissures (25-99% neosurface thickness) | 1 |
| | Complete disruption of the neosurface | 0 |

### 4.2.3 Statistical analyses

All the statistical analyses were conducted using Statistical Package for Social Studies (SPSS) 17.0 for Windows (IBM). Assumptions of parametric data were tested for all data: normality of data distribution with Shapiro–Wilk and homogeneity of variance with Levene's tests. *P*-values

of less than 0.05 were considered significant, unless otherwise noted. *In vitro* studies were performed in triplicate (n = 3), and data are reported as line graphs with mean ± standard error of mean (SEM) (Figs. 4-1 – 3). *In vivo* studies were conducted and data observed using independent animals, with N = 11 for No Doxycycline Control group and N = 12 for 12 Week Doxycycline group, and data are reported as bar graphs with mean ± SEM for parametric data (Fig. 4-5) and as a boxplot with median and interquartile range for non-parametric data (Fig. 4-6B). For comparison among three groups and multiple time points for the *in vitro* data, two-way independent analysis of variance (ANOVA) was used with doxycycline concentration and time points as main independent variables. For variables that were considered significant, *post-hoc* Tukey was used to further evaluate the data. For comparisons between two groups for the *in vivo* data, unpaired Student's *t*-test was used for parametric data (Figs. 4-5C) and Mann-Whitney U test was used for non-parametric data (Fig. 4-6B).

## 4.3 RESULTS

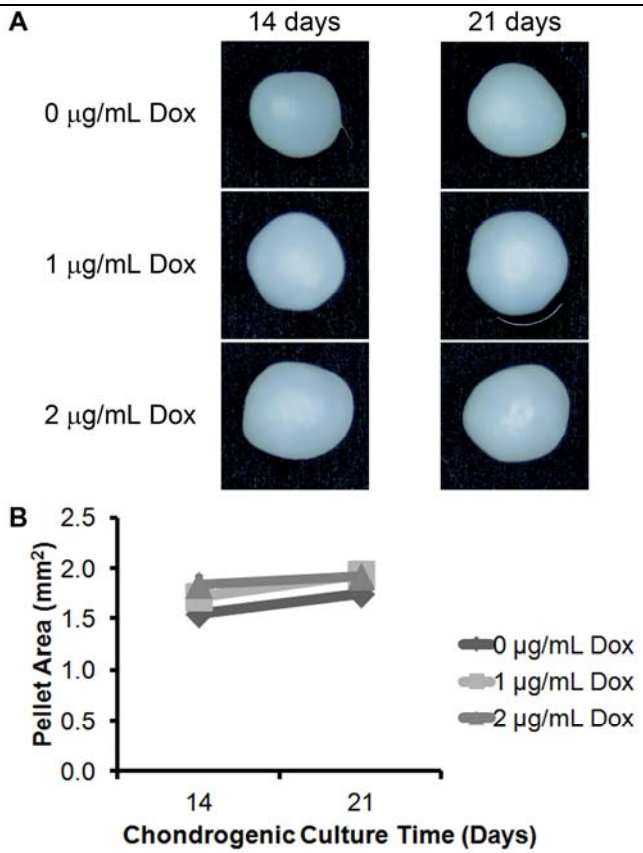


**Figure 4-1: Macroscopic appearance of hMSC pellets and pellet area analysis**
**(A)** Macroscopic images of hMSC pellets cultured in chondrogenic media with 0, 1, or 2 μg/mL doxycycline (Dox) for 14 and 21 days. **(B)** Pellet area measured from the macroscopic images of hMSC pellets cultured in chondrogenic media with 0, 1, or 2 μg/mL Dox for 14 and 21 days. Pellet area increased from 14 to 21 days in chondrogenic culture period ($p$ = 0.002). As well, the pellet area was significantly affected by the doxycycline concentration in the chondrogenic media ($p$ = 0.002): 0 μg/mL Dox pellets were smaller than the 1 μg/mL ($p$ = 0.014) and 2 μg/mL ($p$ = 0.002) Dox pellets. There was no difference in sizes between the 1 and 2 μg/mL Dox pellets ($p$ = 0.535). $n$ = 3/group.

### 4.3.1 Gross evaluation of hMSC chondrogenic pellets (Fig. 4-1)

Gross images of the hMSC chondrogenic pellets were taken at 14 and 21 days of culture in chondrogenic media supplemented with 0, 1, or 2 μg/mL of doxycycline (Fig. 4-1A). When the pellet areas were measured, an increasing trend in pellet areas from 14 to 21 days in chondrogenic culture was seen (Fig. 4-1B). The areas of hMSC chondrogenic pellets were

significantly affected by both the concentration of doxycycline ($p$ = 0.002) and the time in chondrogenic culture ($p$ = 0.002). The *post-hoc* Tukey test revealed that the pellet areas were significantly larger for those cultured in 1 μg/mL ($p$ = 0.014) and 2 μg/mL ($p$ = 0.002) of doxycycline compared to those cultured without any addition of doxycycline. There was no significant difference in pellet areas between those cultured in 1 and 2 μg/mL doxycycline. The interaction effect between the two main variables, doxycycline concentration and culture time, was also non-significant ($p$ = 0.377).

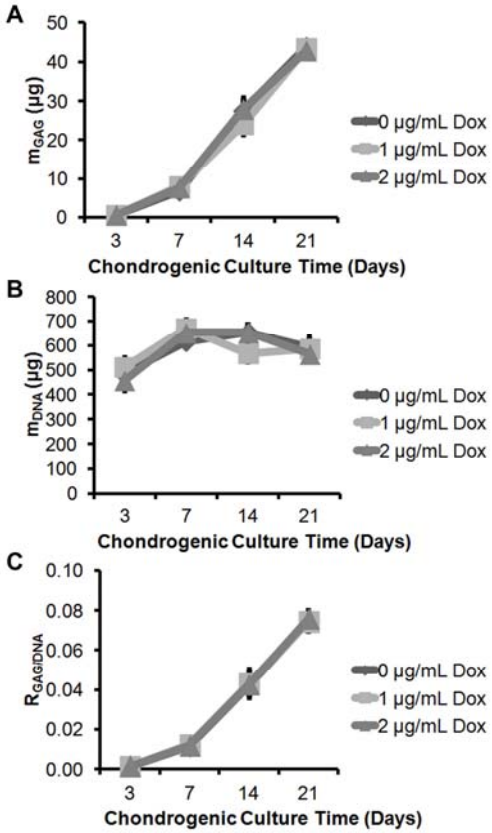


**Figure 4-2: Biochemical quantification of GAG and DNA in hMSC pellets**
**(A)** Total GAG content per hMSC pellets showed increasing GAG content with longer chondrogenic culture time ($p$ < 0.001), with GAG content of the 7 day pellets significantly greater than those of the 3 day pellets ($p$ < 0.001), those of 14 day pellets significantly greater than those of the 7 day pellets ($p$ < 0.001), and those of 21 day pellets significantly greater than those of the 14 day pellet ($p$ < 0.001). There was no significant effect of doxycycline (Dox) concentration on the total GAG content ($p$ = 0.412). **(B)** Total DNA content per hMSC pellets showed significant effect of chondrogenic culture time on the DNA contents ($p$ < 0.001): DNA content of the 3 day pellets were significantly lower than those of the 7 ($p$ < 0.001), 14 ($p$ < 0.001), and 21 ($p$ = 0.009) day pellets. There was no difference in DNA content among 7, 14, and 21 day pellets. As well, there was no significant effect of doxycycline concentration on the DNA content ($p$ = 0.314). **(C)** Normalized GAG content with respect to the DNA content showed that there is significant effect of chondrogenic culture time ($p$ < 0.001); however, the effect of doxycycline concentration was not significant ($p$ = 1.000). $n$ = 3/group.

### 4.3.2 Biochemical analyses of hMSC chondrogenic pellets (Fig. 4-2)

Total GAG (Fig. 4-2A) and DNA (Fig. 4-2B) content per pellet samples and their ratio (Fig. 4-2C) were measured and calculated on 3, 7, 14, and 21 day old chondrogenic pellets to analyze the effect of doxycycline on hMSC chondrogenesis and proliferation/viability. For all three outcome measures, there was a significant main effect of the time in chondrogenic culture ($p$s < 0.001); however, the main effect of doxycycline concentration and the interaction effects were non-significant. The *post-hoc* Tukey tests for total GAG content and GAG/DNA ratio revealed significant differences of these outcome variables between all the different time points ($p$s < 0.001). On the other hand, the *post-hoc* Tukey test for total DNA content showed significant differences between day 3 and day 7 ($p < 0.001$), day 14 ($p < 0.001$), and day 21 ($p = 0.009$), but no significant differences between any other days.

### 4.3.3 Gene expression analyses of hMSC chondrogenic pellets (Fig. 4-3)

Various mRNA levels were measured on 3, 7, 14, and 21 day old chondrogenic pellets to analyze the effect of doxycycline on hMSC chondrogenesis. The time in chondrogenic culture had significant effect on gene expressions for all the assayed genes: *sox-9* ($p = 0.001$), *tgf-βRII* ($p = 0.003$), *aggrecan* ($p < 0.001$), *collagen-II* ($p < 0.001$), *collagen-I* ($p = 0.028$), *collagen-X* ($p < 0.001$), and *mmp-13* ($p < 0.001$). The main effect of doxycycline concentration as well as interaction effects between the two main independent variables were non-significant for *sox-9, tgf-βRII, aggrecan, collagen-II, collagen-I*, and *collagen-X* mRNA levels. For the *mmp-13* gene expression, on the other hand, there was a non-significant main effect of doxycycline concentration but a significant interaction effect between the time in chondrogenic culture and

doxycycline concentration ($p$ = 0.025). This indicates that the doxycycline concentration affected *mmp-13* mRNA level differently on various chondrogenic culture time points. Specifically, *mmp-13* levels for all three doxycycline concentrations were similar for day 3, 7, and 14 hMSC pellets; however, they were different for day 21 pellets ($p$ = 0.012). The 2 μg/mL doxycycline pellets had significantly lower *mmp-13* mRNA level compared to 0 μg/mL doxycycline pellets ($p$ = 0.010). It was lower compared to 1 μg/mL doxycycline pellets as well, however not to a significant extent ($p$ = 0.078).

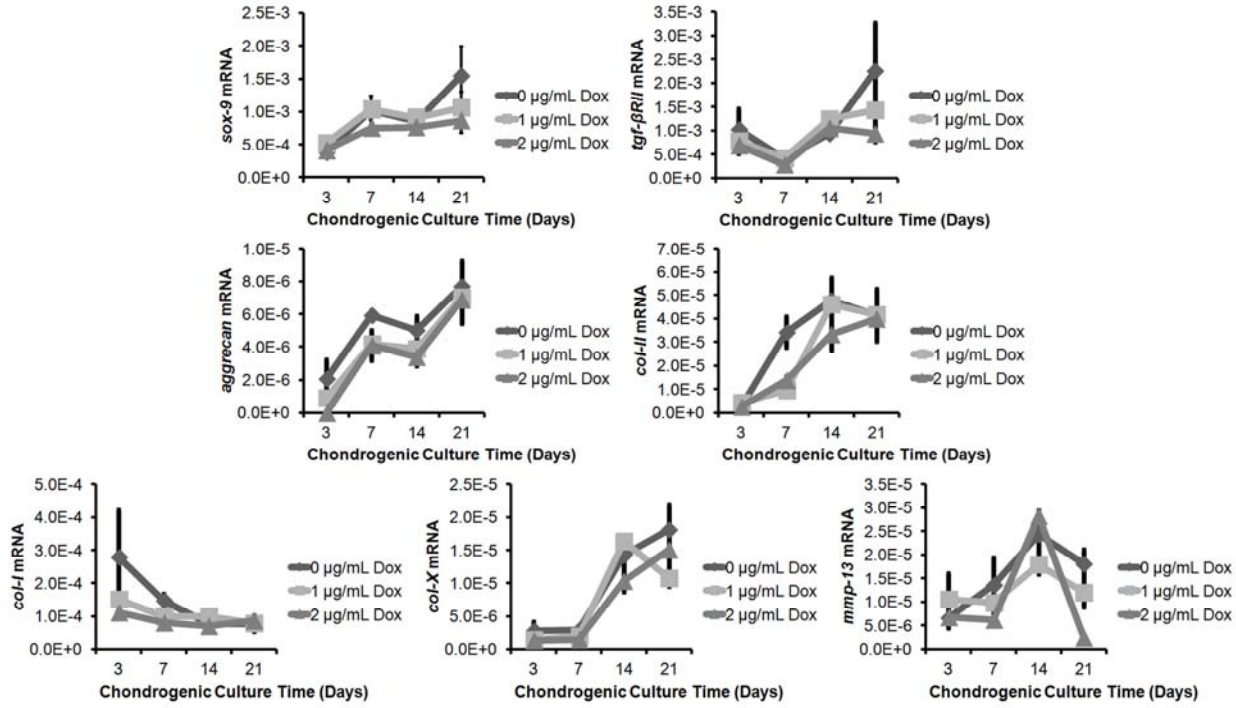


**Figure 4-3: Gene expression analyses of hMSC pellets**
Messenger RNA levels of chondrogenic inducers *sox-9* and *tgf-βRII*, chondrogenic genes *aggrecan* and *col-II*, fibrocartilage marker *col-I*, and hypertrophic chondrocyte marker *col-X*, and catabolic gene *mmp-13*. There was an increasing trend in *sox-9*, *tgf-βRII*, *aggrecan*, *col-II*, and *col-X* levels ($p$s < 0.01), and a decreasing trend in *col-I* level ($p$ = 0.028) over chondrogenic culture time. There was no significant effect of doxycycline concentration on these gene expressions ($p$s > 0.05). For *mmp-13* level, there was an upward trend until day 14, with mRNA level in the 14 day pellets significantly higher than those of the 3 ($p$ < 0.001) and 7 ($p$ < 0.001) days. However, on day 21, there was a reduction in the mRNA level from day 14 ($p$ < 0.001). The *mmp-13* mRNA levels on day 21 pellets were also significantly different among different doxycycline concentrations: 2 μg/mL doxycycline (Dox) pellets had significantly lower *mmp-13* levels compared to 0 μg/mL Dox pellets ($p$ = 0.01). $n$ = 3/group.

### 4.3.4 Histological analyses of hMSC chondrogenic pellets (Fig. 4-4)

Safranin O-fast green staining of sulfated GAGs showed increased amount of staining for 21 day versus 14 day hMSC pellets (Fig. 4-4A). However, no differences in staining intensities were appreciable among the three different doxycycline concentrations. These results confirm the biochemical analysis of total GAG content (Fig. 4-2A). The MMP-13 IHC showed more MMP-13-positive cells for the 0 and 1 μg/mL doxycycline pellets at Day 21 (Fig. 4-4B), confirming the mRNA results (Fig. 4-3). As upregulation of MMP-13 in MSC chondrogenesis has also been linked to terminal differentiation of hypertrophic chondrocytes (143-145), alizarin red staining was performed. However, there were no positively stained pellets at either doxycycline concentration at both 14 and 21 days chondrogenic culture time points (Fig. 4-4C).

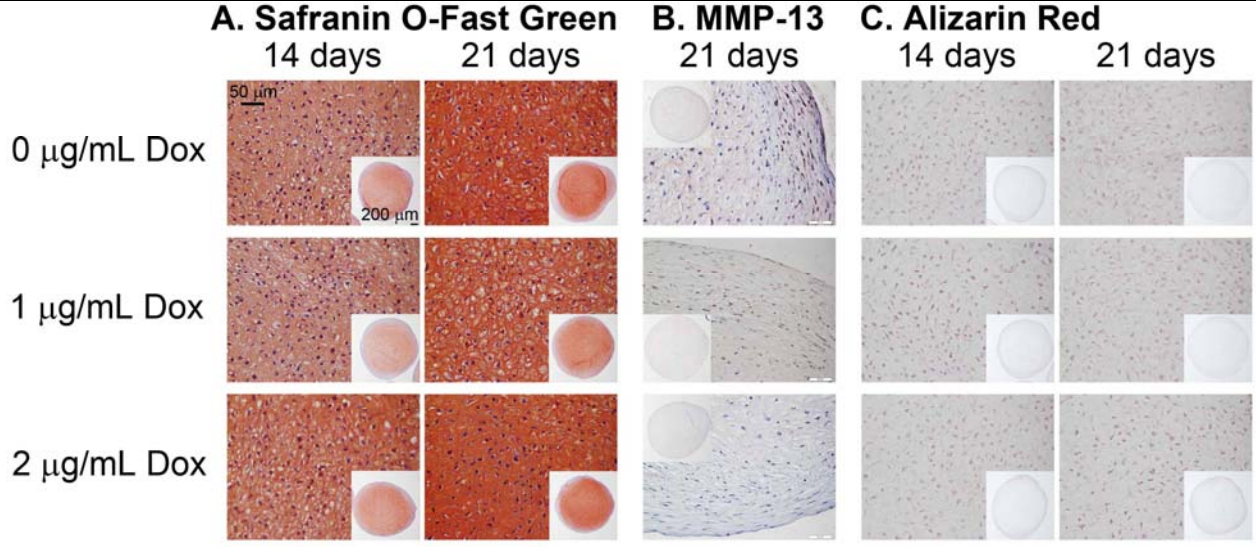


**Figure 4-4: Histological analyses of hMSC pellets**
Representative images of **(A)** safranin-O fast green, **(B)** MMP-13 immunohistochemistry, and **(C)** alizarin red staining of hMSC pellets at 20x (larger box) and at 4x (smaller inset). There was no difference in staining intensities for Safranin-O fast green and alizarin red staining among different doxycycline concentration groups at each time point. However, more MMP-13-positive cells were found in the periphery of the hMSC pellets cultured in 0 and 1 μg/mL doxycycline compared to those cultured in 2 μg/mL doxycycline.

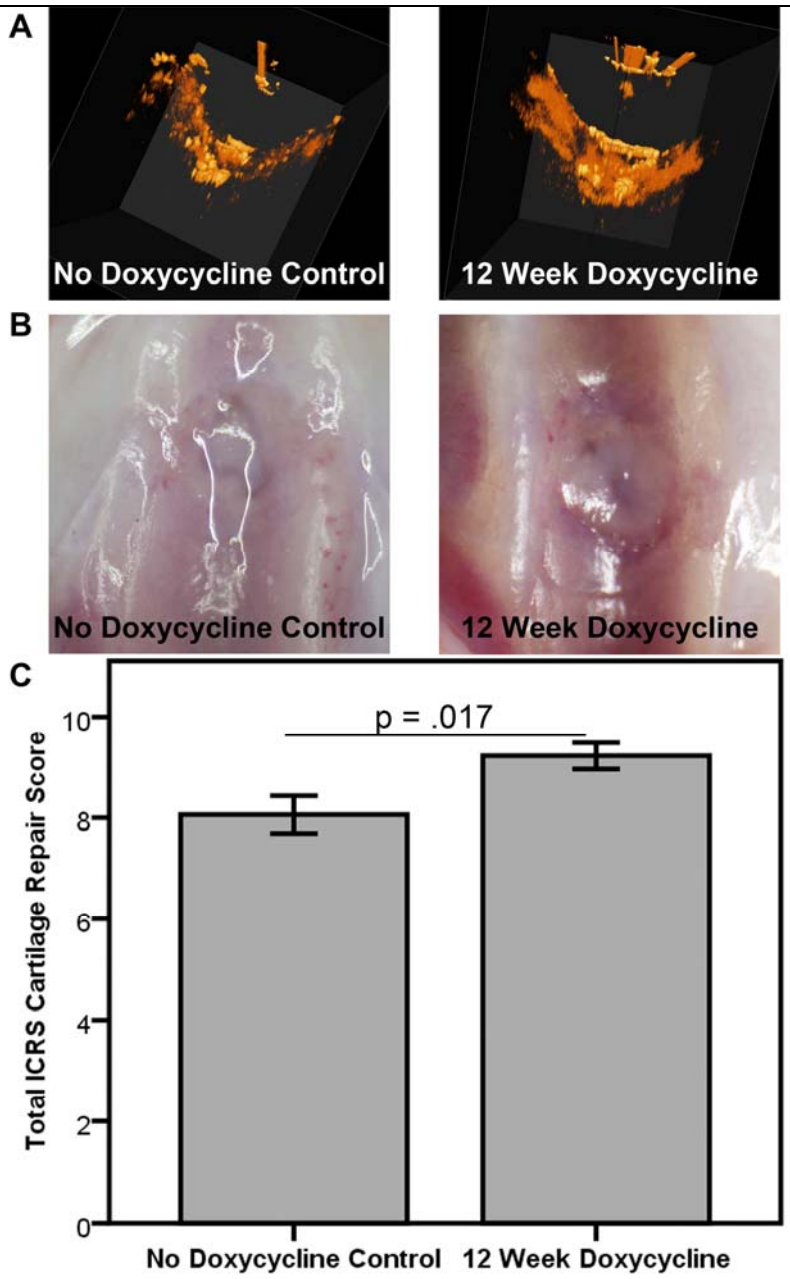


**Figure 4-5: Gross assessment of osteochondral defect repair tissues**
Representative images of repair tissues from No Doxycycline Control and 12 Week Doxycycline groups evaluated using **(A)** 3D OCR and **(B)** stereomicroscopy. **(C)** Gross grading of OCD repair tissues using ICRS Cartilage Repair Assessment grades showed better repair tissue for the 12 Week Doxycycline group. $N = 11 – 12$/group.

### 4.3.5 Evaluation of osteochondral defect repair tissue (Fig. 4-5)

The OCD repair tissues from the 12 Week Doxycycline group showed more complete repair tissue within the femoral trochlear groove by gross inspection and *in situ* Optical Coherence

Tomography (Fig. 4-5A). The animals that received doxycycline for 12 weeks post-op had higher mean total ICRS Cartilage Repair Scores reflecting better quality repairs than the No Doxycycline Control group (Fig. 4-5C, $p$ = .017). Qualitative evaluation using the modified Holland Histological scoring of the H&E stained OCD repair tissue showed similar scores between the two groups ($p$ = .116).

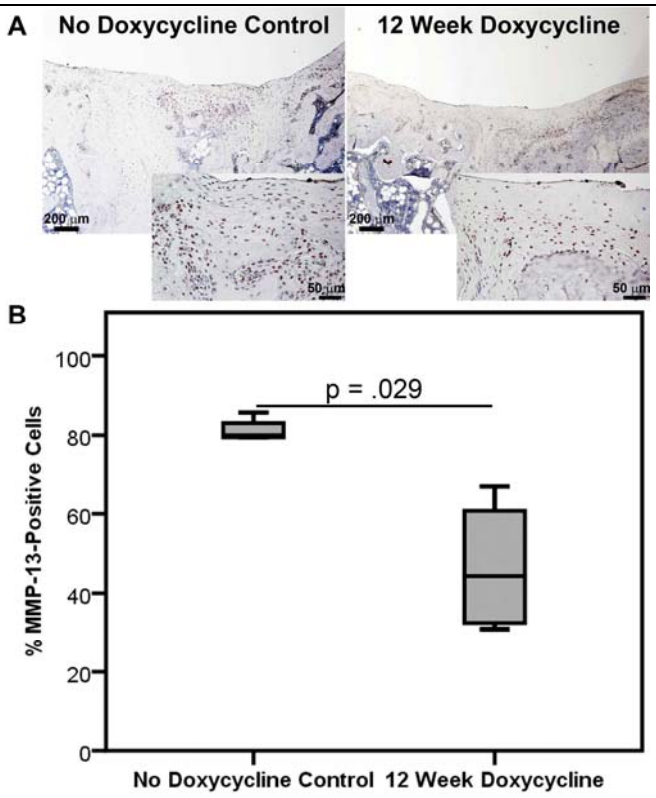


**Figure 4-6: MMP-13 of osteochondral defect repair tissues**
**(A)** Representative 4x (larger box) and 20x (smaller inset) images of MMP-13 immunohistochemical staining of repair tissues from No Doxycycline Control and 12 Week Doxycycline groups (**B)** Median and interquartile range of percentage of MMP-13-positive cells in different treatment groups. More MMP-13-positive cells were found in the newly formed repair tissues of No Doxycycline Control group compared to those of 12 Week Doxycycline group ($p$ = 0.029). $N$ = 4/group.

### 4.3.6 MMP-13 of OCD repair tissue (Fig. 4-6)

The repair tissues from No Doxycycline Control group showed more MMP-13-positive cells compared to those of 12 Week Doxycycline group (Fig 4-6A): No Doxycycline Control group

had 80% MMP-13-positive cells, whereas 12 Week Doxycycline group had 44% MMP-13-positive cells (Fig 4-6B, $p$ = .029). This *in vivo* OCD repair tissue MMP-13 content result correlates to the *in vitro* hMSC pellet data (Fig. 4-4B).

## 4.4 DISCUSSION

Osteoarthritis currently affects 27 million adults and costs 3% of the GDP in the US (5, 146). The prevalence of osteoarthritis will continue to rise, especially with the aging population and the growing epidemic of obesity. By 2030 it is projected to affect 67 million, with 3.5 million total knee arthroplasties performed annually (5, 146). Therefore there is significant clinical as well as research interest in finding novel ways to improve the quality of cartilage repair. Articular cartilage repair with MSCs is widely studied; however, results are often suboptimal to prevent osteoarthritis.

Oral administration of doxycycline has been postulated to have beneficial effects on articular cartilage by inhibiting important classes of MMPs (132, 147). Doxycycline administration *in vivo* has resulted in significant decreases in MMP levels in small animal models, as well as in human osteoarthritic patients (148, 149). When doxycycline was administrated prophylactically in several animal models, the decreased activities of MMPs were correlated to reduced proteoglycan loss from cartilage extracellular matrix, as well as reduced degenerative changes in the weight-bearing areas of cartilage (126, 150). In a randomized, double-blinded, placebo-controlled study that evaluated the effects of doxycycline on the progression of joint space narrowing in mildly arthritic knees, the doxycycline treatment group had a decreased rate of narrowing by 40% at 16-months and 33% at 30-months as compared to

placebo ($p$ = .017) (133). On the other hand, however, a number of other studies show lack of any effect on joint disease and/or MMP activities with doxycycline treatment. In a prospective clinical study involving dogs with stifle joint instability, there was no significant difference in MMP activity levels in synovial fluid for doxycycline versus no doxycycline treatment groups (144). In another study involving guinea pigs, oral doxycycline treatment for 4 – 8 months lead to no significant OA changes compared to controls (151). Hence there are numerous studies on the effect of doxycycline on cartilage degeneration, with conflicting results. Nonetheless, doxycycline effect on cartilage repair with MSCs as well as MSC chondrogenesis is largely unknown.

Our laboratory has also previously utilized doxycycline as a control molecule for external control of adeno-associated virus (AAV)-mediated transgene expression, as potential strategy to deliver therapeutic proteins of interest to affected joints to enhance MSC chondrogenesis, thereby improving cartilage repair (47). Intra-articular injection of AAV has been used in clinical trials for delivery of bioactive substances (88), and our previous study has shown both stable and persistent reporter transgene expression at one year after a single intra-articular injection of AAV (47). Nonetheless, there are potential safety issues concerning long-term or high-dose expression of transgenes, such as overexposure resulting in undesirable side effects. For this reason, controllable vectors have been developed to limit treatment time/dosage to the minimal needed to achieve therapeutic efficacy. One novel system is the Tet-on promoter, in which control is facilitated by using tetracycline-class drugs as activators of the tetracycline response element (TRE)-promoter, stimulating transgene expression only in the presence of the drug. Previous studies in our laboratory have successfully modulated gene expression utilizing the Tet-on

system with oral administration of 2 mg/mL doxycycline (47), providing an added measure of safety, as well as the ability to alter the timing and duration of exposure to bioactive factors.

Our comprehensive *in vitro* study shows that doxycycline reduced the MMP-13 gene as well as protein expressions at day 21 of chondrogenic culture period. This is consistent with MMP-13 suppressing activity of doxycycline found in other tissue types, such as chondrocytes and synoviocytes (134, 136). We also observed larger hMSC pellets in the doxycycline group. The larger hMSC pellet sizes may be in part due to improved matrix synthesis through inhibition of MMP-13 production. As the predominant function of MMP-13 in cartilaginous ECM is collagen-II breakdown (134, 144), this MMP-13 inhibition would ultimately lead to reduction of excessive collagen-II degradation or enhancement of collagen-II accumulation. MMP-13 is also a marker of terminal differentiation of MSCs into hypertrophic chondrocytes (143-145). However, lack of differences in *col-X* gene expression level and lack of alizarin-red positive staining among hMSC pellets cultured in various doxycycline concentrations suggest that doxycycline is not principally involved in inhibition of MSC hypertrophy.

Our *in vivo* data additionally suggests that oral administration of doxycycline potentially improves the repair. As well, MMP-13 expression in OCD repair tissue samples was significantly greater in No Doxycycline Control than in 12 Week Doxycycline groups. This can potentially explain the higher quality repairs reflected in the ICRS scores in the doxycycline treated rats. Furthermore, this *in vivo* finding is correlated to the *in vitro* findings of MMP-13 levels in control versus doxycycline-treated MSC pellets.

## 4.5 CONCLUSIONS

In summary, we showed in both *in vitro* and *in vivo* study that doxycycline inhibited MMP-13 and potentially improved in chondrogenesis and cartilage repair. There was significant inhibition of MMP-13 on both mRNA and protein levels in hMSC cultured with 2-μg/mL doxycycline, which would lead to reduction of collagen-II degradation and hence larger pellet size potentially due to enhanced collagen-II retention. The doxycycline-mediated inhibition of MMP-13 expression in MSCs is consistent with other studies using doxycycline on other joint cell and tissue types. Oral administration of doxycycline visibly improved osteochondral defect repair tissues *in vivo*. The doxycycline-mediated downregulation of MMP-13 expression was observed in OCD repair tissues. These findings suggest that doxycycline can be used as an agent for external control of transgene expression in cartilage repair studies incorporating AAV-mediated gene therapy strategies without interfering with the repair process. Doxycycline inhibition of MMP-13 may even potentially improve *in vivo* cartilage repair. As such, continued evaluation of the potential benefits of doxycycline to articular cartilage may lead to novel treatment strategies improve cartilage repair and delay development of osteoarthritis.

# 5.0 RELEASE OF BIOACTIVE ADENO-ASSOCIATED VIRUS FROM FIBRIN SCAFFOLDS: EFFECTS OF FIBRIN GLUE CONCENTRATIONS

## 5.1 INTRODUCTION

Articular cartilage has a limited self-regeneration capacity and recombinant adeno-associated virus (AAV) is a promising vehicle for articular cartilage and the surrounding soft tissues to deliver bioactive factors to promote joint restoration. There are three approaches for AAV administration to articular cartilage: direct, indirect, and hybrid. The direct method involves an intra-articular injection of viral vectors into the articular joint space for their transduction of local cells. Although long-term persistence and transgene expression has been observed with direct injection of AAV (47), most of the transduction occurs in soft tissues and it is difficult to localize the transduction to specific cell types. Further, rapid dispersion of viral particles from the joint space would prevent effective transduction of repair cells that are recruited to the defect site over time. Thus, the *in vivo* transduction efficiency remains low and non-specific transduction of adjacent tissues and their transgene expression at undesired sites is usually observed (53). The indirect approach involves implantation of cells that were genetically modified *ex vivo*, and faces high clinical translational barriers. The hybrid approach, involving implantation of bioscaffold embedded with genetic material in the site of defect, leads to direct and localized transduction of host cells *in situ* and sustained expression of the transgene. Further, scaffolds can act as support

for injury-activated repair or progenitor cells, such as bone marrow-derived mesenchymal stem cells (BM-MSCs), to migrate, attach, and differentiate at the defect site. Thus, the hybrid method offers the advantages of site-specific localization, direct transduction of host repair cells, and sustained transgene expression, while limiting the disadvantages of indiscriminate transduction and requirement of *ex vivo* manipulations.

Our group has previously shown that AAV2-transforming growth factor-β1 (AAV2-TGF-$\beta_1$) transduced human MSCs (hMSCs) implanted into a 1.5-mm diameter osteochondral defect significantly improved cartilage regeneration over 12 weeks *in vivo* (42). These results demonstrated that AAV2 is a suitable vector for gene delivery to improve the cartilage repair potential of the MSCs. However, although the *ex vivo* gene transfer is effective, the regulatory barriers for using genetically modified cultured human cells for therapeutic purposes clinically are extremely high. In addition, extraction and expansion of MSCs prolong the time before treatment can be applied and are very expensive. Therefore, we have explored the use of biodegradable scaffolds for release and delivery of bioactive substances to host MSCs within cartilage wound (140, 152-154).

Fibrin glue (FG) is used in a variety of clinical applications and in the laboratory for localized and sustained release of factors potentially important for tissue engineering. It has been shown that diluted FG produces a more open fibrin network compared to undiluted FG scaffolds (155), and that FG can act as an efficient scaffold for gene delivery (156-158). However, the effect of different fibrinogen concentrations on FG scaffold delivery of bioactive AAVs has not been established.

In the current study, we investigated the effect of different fibrinogen dilutions during the preparation of FG scaffold on the delivery of AAV2 and their early effects on human BM-MSC

(hBM-MSC) chondrogenesis *in vitro*. The aim of this study was to test the hypotheses that diluted FG scaffolds will release more viral particles, resulting in higher transduction efficiency, and increase the chondrogenic potential of transduced hBM-MSCs.

## 5.2 METHODS

### 5.2.1 Preparation of FG

Chemicals were purchased from Sigma-Aldrich unless otherwise stated. Twenty-four well plates and 24-well plate inserts were purchased from BD biosciences. Commercially available Tisseel® human fibrin sealant (Baxter) was used to construct FG hydrogels. Fibrinogen (100% of the original material concentration, lyophilized human fibrinogen reconstituted in aprotinin fibrinolysis inhibitor) was prepared by serial dilution with phosphate buffered saline (PBS, Gibco) into four different concentrations: 25%, 50%, 75%, and 100% fibrinogen. Different dilutions of fibrinogen were subsequently mixed with an equal volume (1:1 volume ratio) of thrombin solution provided in the Tisseel kit (human thrombin 400 – 625 IU/mL and calcium chloride 36 – 44 μmol/mL). The resultant FG constructs were named 25%, 50%, 75%, and 100% FG, according to the fibrinogen dilution before thrombin activation.

### 5.2.2 Characterization of different FG concentrations

#### 5.2.2.1 Clotting time

100 µL of different fibrinogen dilutions was mixed with 100 µL Thrombin-$CaCl_2$ in a 96 well plate to make 25%, 50%, 75%, and 100% FG scaffolds. Change in the turbidity of the FG scaffold solution was immediately measured by a VersaMax UV-Vis spectrophotometer (Molecular Devices) at 550 nm wavelength (159). The clotting time was defined as the time at which the maximum value was reached in the absorbance curve. Three replicates of each FG scaffold concentrations were examined in this study.

#### 5.2.2.2 Scanning electron microscopy

Three FG scaffolds constructed from 200 µL of different fibrinogen dilutions and 200 µL Thrombin-$CaCl_2$ were used for scanning electron microscopy (SEM) analysis. After fixation in 2.5% gluteraldehyde for 1 h and rinsing in PBS, FG scaffolds were dehydrated in increasing alcohol concentrations (30%, 50%, 70%, 90%, and 100%) for 15 min each, followed by hexamethyldisilazane for 1 h. Once hexamethyldisilazane was removed, the scaffolds were air-dried for an hour. Each FG scaffold was coated with an ultra-thin gold layer containing a gold sputter coater for 2 min at 25 mA and observed under an SEM (JSM-6335F; Jeol USA, Inc). Two separate images of each scaffold were captured. Pore size diameter and thickness of fibrin fibers were measured for each image using image analysis software, Metamorph 7.6.2.0 (Molecular Devices).

#### 5.2.2.3 FG dissolution

##### 5.2.2.3.1 Wet weight measurement

Different fibrinogen dilutions were mixed with an equal volume of thrombin-$CaCl_2$ and injected into uncoated 24 well plate inserts with 8 μm pores at 200 μL FG/insert, and incubated at 37°C for 15 min to form hydrogels. The weight of each insert was measured before injection of the fibrinogen/thrombin solutions. Once the FG scaffolds had solidified, 500 μL PBS was added on top of each inserts, and the inserts were placed in a 24 well plate containing 1 mL PBS/well. After incubation at 37°C for 10 min, inserts were removed, PBS aspirated, surface PBS absorbed by a filter paper, and the initial weight of the hydrogels ($W_0$) was recorded. FG hydrogels were re-weighed ($W_t$) every 2 days to estimate the wet weight fraction, which as defined as ($W_0 - W_t$)/$W_0$. Five replicates of each FG concentration were examined in this study.

##### 5.2.2.3.2 Protein dissolution

The conditioned PBS from each well, in which the FG hydrogels were incubated, was also collected at the time of hydrogel wet weight measurement. The amount of the protein dissolved and released into the PBS was measured by UV-Vis spectroscopy (NanoDrop) at 278 nm, which measures the absorbance of the phenyl group of fibrinopeptide proteins. Fresh PBS was used as blank control.

### 5.2.3 AAV2-CMV-GFP *in vitro* transduction

#### 5.2.3.1 AAV2-CMV-GFP-loaded FG preparation

Double-stranded AAV2-GFP with a cytomegalovirus promoter (dsAAV2-eGFP, hereunder referred to as AAV2-CMV-GFP) was prepared as previously described (120). The AAV2 particles were packaged and purified using the adenovirus-free, triple plasmid transfection method. The titer (vector genome per milliliter [vg/mL]) was determined by viral DNA dot blot method (101). The stock AAV2-CMV-GFP titer was $3 \times 10^{12}$ vg/mL.

The AAV2-CMV-GFP vector stock was added to the various fibrinogen preparations (25%, 50%, 75%, and 100%) to obtain a final concentration of $6.25 \times 10^{10}$ vg/mL. After vortexing for 3 min, the AAV2-CMV-GFP-loaded fibrinogen solutions were mixed with an equal volume of thrombin-$CaCl_2$ and injected into uncoated 24 well plate inserts with 8 μm pores, at 200 μL/well. After gelation at 37°C for 15 min, pre-warmed 500 μL Dulbecco's modified Eagle's medium (DMEM, Gibco)-1% penicillin-streptomycin (pen/strep, Gibco) was added to each insert. Three replicates were examined in this study.

AAV2-CMV-GFP released from the AAV2-CMV-GFP loaded FGs and their direct transduction of mammalian cells were assessed over 21 days. HEK-293 cells (ATCC) were maintained in DMEM, 10% fetal bovine serum (Atlanta Biologicals), and 1% pen/strep at 37°C and 5% $CO_2$. Each day, ~ $2.4 \times 10^6$ cells were seeded onto 24 well plates at a seeding density of 100,000 cells/well and incubated for 24 h, after which the medium was changed to serum-free DMEM-1% pen/strep. Inserts containing AAV2-CMV-GFP-loaded FGs were placed into the wells of the 24 well plate seeded with HEK-293 cells and incubated for additional 24 h at 37°C. The medium was placed below and in the inserts to allow migration of AAV2-CMV-GFP from

the FG hydrogels to the seeded cells. Photomicrographs of GFP-expressing cells were taken daily using an Olympus DP71 camera and Nikon Eclipse TE2000-U microscope. All GFP images presented in Figure-5-4C – F had the contrast increased by the same value in Adobe Photoshop CS4 to improve the GFP signal for print.

#### 5.2.3.2 AAV2-CMV-GFP release from FG

Each day, the conditioned serum free medium from each well was collected and preserved at -80°C until analysis. The amount of AAV2-CMV-GFP released into the conditioned medium from AAV2-CMV-GFP-loaded scaffolds was quantified by quantitative polymerase chain reaction (qPCR). All PCRs containing 0.5 μL of conditioned medium in a total volume of 10 μL using a commercially available pre-prepared 2x Real-time TaqMan PCR Master Mix (Applied Biosystems). GFP-specific custom TaqMan forward (GTCCGCCCTGAGCAAAGA) and reverse (TCCAGCAGGACCATGTGATC) primers as well as FAM-labeled probes (CCCAACGAGAAGCG) were used. All qPCRs were performed with an ABI PRISM 7700 Sequence Detection System (Applied Biosystems) according to the following program: 12 min at 95°C, followed by 40 cycles of 15 s at 95°C and 1 min at 60°C. Three replicates of each experimental group were examined in this study.

#### 5.2.3.3 *In vitro* transduction of AAV2-CMV-GFP released from FG

Transduction efficiency was quantified using flow cytometry and expressed as percentage of GFP-positive cells. Both AAV2-CMV-GFP-transduced and non-transduced control cells were trypsinized, washed, and resuspended in 400 μL of PBS with 1% bovine serum albumin and 2 %

paraformaldehyde (both from Fisher Scientific). Ten thousand events were collected using a BD Biosciences LSR II (BD Biosciences). The percentage of GFP-positive cells was determined by defining GFP-negative cells and gating out debris with Flow Jo 7.6.1 software (Tree Star, Inc.). Three replicates of each experimental group were examined in this study.

### 5.2.4 AAV2-CMV-TGF-$\beta_1$ *in vitro* transduction

#### 5.2.4.1 AAV2-CMV-TGF-$\beta_1$-loaded FG preparation

Double-stranded AAV2-TGF-$\beta_1$ with a cytomegalovirus promoter (dsAAV2-TGF-$\beta_1$, hereunder referred to as AAV2-CMV-TGF-$\beta_1$) was prepared and purified as described above for AAV2-CMV-GFP preparation. The stock AAV2-CMV-TGF-$\beta_1$ titer was 2.5 x $10^{12}$ vg/mL.

The AAV2-CMV-GFP and AAV2-CMV-TGF-$\beta_1$ vector stocks were separately added to 50% and 100% fibrinogen preparations to obtain a final concentration of 1.25 x $10^{11}$ vg/mL. After vortexting for 3 min, the AAV2-loaded fibrinogen solutions were mixed with an equal volume of thrombin-$CaCl_2$ and injected into uncoated 6 well plate inserts with 8 μm pores, at 1 mL/well. After gelation at 37°C for 15 min, pre-warmed 3 mL chondrogenic medium: High-Glucose DMEM (Gibco) supplemented with 1% pen/strep (Gibco), $10^{-7}$ M dexamethasone (Sigma-Aldrich), 50 μg/mL L-ascorbic acid-2-phosphate (Sigma-Aldrich), 40 μg/mL proline (MP Biomedicals), and 1% ITS+ Premix (BD) was added to each insert. Three replicates of 50% and 100% AAV2-CMV-TGF-$\beta_1$-loaded FGs were examined in this study against the 50% and 100% AAV2-CMV-GFP-loaded FGs.

AAV2-CMV-TGF-$\beta_1$ released from the AAV2-CMV-TGF-$\beta_1$-loaded FGs and their direct transductions of hBM-MSCs were assessed. The hBM-MSCs were obtained, maintained,

and characterized as previously described (57, 160). About 4.8 x $10^6$ cells were seeded onto 6 well plates at a seeding density of 200,000 cells per well and incubated for 24 h in their normal growth medium, after which the medium was changed to a chondrogenic medium. Inserts containing AAV2-CMV-GFP-loaded FGs and AAV2-CMV-TGF-$\beta_1$-loaded FGs were placed into the wells of the 6 well plates seeded with hBM-MSCs and incubated for 24 h. The medium was placed below and in the inserts to allow migration of AAV2s from the FG hydrogels to the seeded cells. After the removal of the inserts, the cells were incubated for an additional 48 h at 37°C. The conditioned serum free medium and hBM-MSCs from each well were collected separately and preserved at -80°C until analysis.

#### 5.2.4.2 *In vitro* transduction of AAV2-CMV-TGF-$\beta_1$ released from FG

The level of TGF-$\beta_1$ expression from hBM-MSCs was assessed by determining the level of TGF-$\beta_1$ in cell culture supernatant using a commercially available ELISA (R&D Systems, Inc) according to the manufacturer's description, and using a CCL-64 mink lung epithelial growth inhibition assay as previously described with slight modification (161, 162). Briefly, the CCL-64 cell line (ATCC, CRL-1573) was grown in DMEM, 10% FBS, and 1% pen/strep at 37°C in 5% $CO_2$. CCL-64 cells were plated at 5,000 cells per well in 96 well plates and cultured in 100 µL of normal growth media for 3 h. The medium was then changed to 100 µL of serum-free DMEM-1% pen/strep supplemented with 10% of conditioned media from hBM-MSC culture. The plates were incubated at 37°C in 5% $CO_2$ for 24 h, and then 20 µL reconstituted XTT reagent from *In Vitro* Toxicology Assay Kit (Sigma-Aldrich) was added to each well for 2 h incubation. The absorbance at 450 nm was measured using VersaMax UV-Vis spectrophotometer.

Cartilage-specific gene expression was measured from hBM-MSCs by quantitative reverse transcription-polymerase chain reaction (qRT-PCR). Total RNA from the collected hBM-MSC samples was extracted using the RNeasy Mini Kit (Qiagen). The pre-designed human *aggrecan* and *18S* TaqMan primers were purchased from Applied Biosystems. Human *sox-9* custom forward (TGACCTATCCAAGCGCATTACCCA) and reverse (ATCATCCTCCACGCTTGCTCTGAA) primers as well as FAM-labeled probed (AGGCCAACCTTGGCTAAATGGAGCA) were purchased from Integrated DNA Technologies (IDT). All samples contained 1 μL of extracted RNA in a total volume of 10 μL using a commercially available pre-prepared 2x Real-time TaqMan PCR Master Mix. All qRT-PCRs were performed with an ABI PRISM 7700 Sequence Detection System according to the following program: 12 min at 95°C, followed by 40 cycles of 15 s at 95°C and 1 min at 60°C. Relative expression levels normalized to *18S* were calculated using the $2^{-\Delta Ct}$ method.

### 5.2.5 Statistical analysis

Data are expressed as mean ± standard error of mean. Statistical analysis was performed using independent samples *t*-test for comparison between two samples (Fig. 5-5), and one-way independent analysis of variance or one-way repeated measures analysis of variance with *post hoc* Tukey for multiple comparisons (Figs. 5-1 – 5-4) using Statistical Package for Social Studies (SPSS) 17.0 for Windows (IBM). The significance level was set as $p < 0.05$.

## 5.3 RESULTS

### 5.3.1 Clotting time

After activation of the different fibrinogen dilutions with thrombin-$CaCl_2$, there was an immediate change in the turbidity of the solution. The clotting time, or the time of maximal turbidity, was dependent on the fibrinogen concentration ($p < 0.001$). Absorbance of the fibrin gel at 550 nm increased with time for all fibrinogen dilutions until it reached a plateau. The clotting time as a function of fibrinogen concentration is displayed in Figure 5-1. Clotting time of the 100% FG was significantly higher ($p < 0.05$) than the diluted (25%, 50%, and 75%) FG scaffolds. Although there was no significant difference in clotting time between the dilute FG scaffolds, there was an increasing trend in clotting time with increasing FG concentrations.

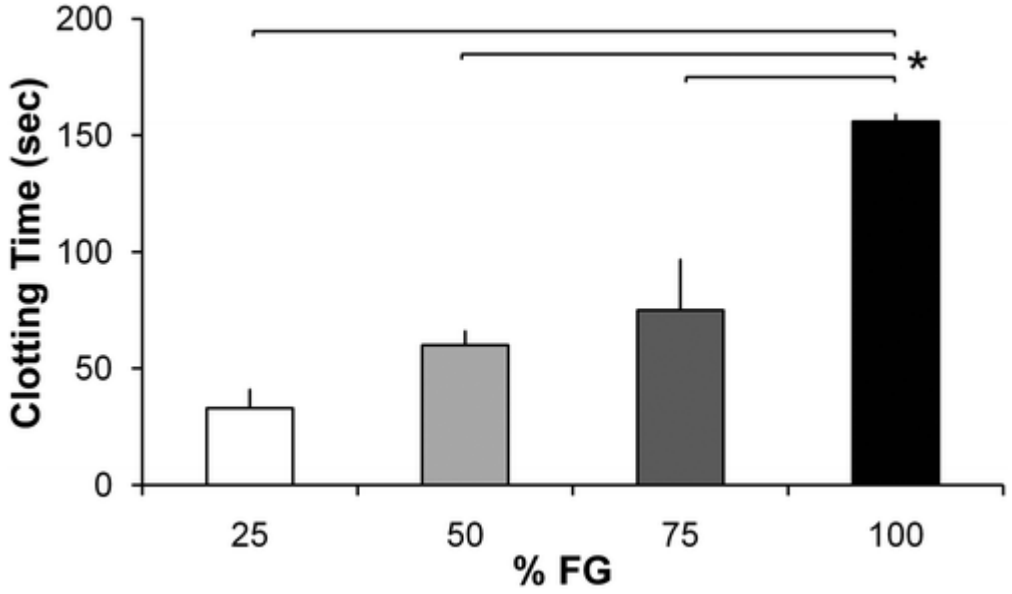


**Figure 5-1: Clotting time of FG hydrogels as a function of fibrinogen concentration**
Clotting time showed an increasing trend with increasing fibrin glue (FG) concentrations. Clotting time of 100% FG was statistically higher than diluted FGs. Bars represent mean ± standard error of mean; $n = 3$. *$p < 0.05$ compared with 100% FG.

### 5.3.2 SEM analysis of the FG hydrogel microstructure

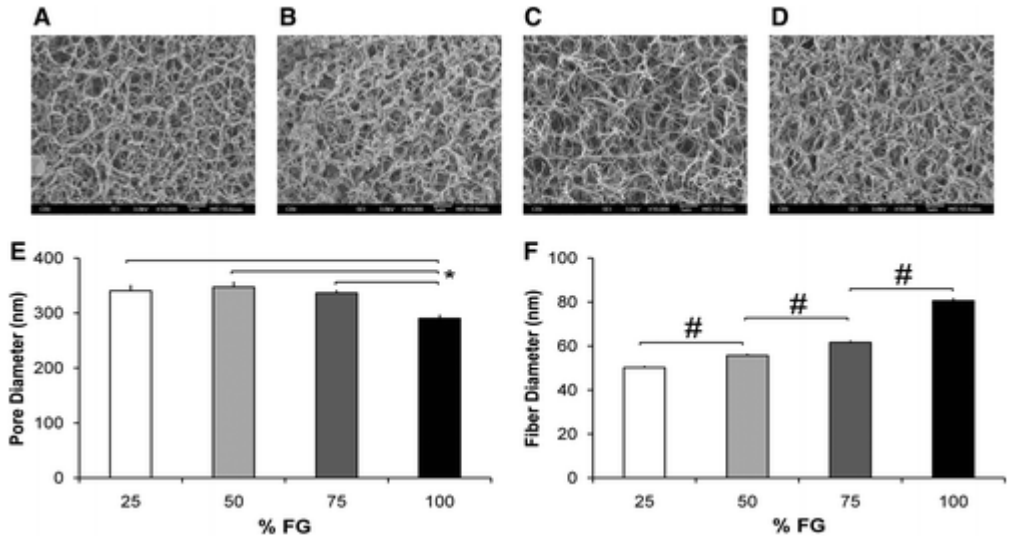


**Figure 5-2: Scanning electron microscopy analyses of FG hydrogels**
**(A-D)** SEM photographs of freeze-dried 25%, 50%, 75%, and 100% FGs, respectively. **(E)** Pore size analysis of the FG cross-sections showed that the pore diameter of the 100% FG was significantly lower than those of the diluted FGs. **(E)** FG fiber thickness analysis showed an increasing trend with increasing concentration of FG. The fiber thickness of each group was statistically different from each other. Bars represent mean ± standard error of mean; $n = 3$. $^{*}p < 0.05$, $^{\#}p < 0.001$.

SEM analysis of pore size diameter of the FG scaffolds showed that all four scaffolds had pore size diameters ranging 50 – 1,200 nm. However, there was a denser, heterogeneous distribution of pores in the 100% FG (Fig. 5-2D) compared with the diluted FG hydrogels, which displayed a more homogeneous and larger pore size diameters (Fig. 5-2A – C). The pore size of the 100% FG was significantly smaller in diameter ($p < 0.05$) than those of the diluted FG scaffolds (Fig. 5-2E). The fiber thickness of the scaffolds, also assessed by SEM, increased with increasing FG concentrations (Fig. 5-2F). The increases in fiber thickness were significant between scaffolds with different fibrinogen concentrations ($p < 0.001$).

### 5.3.3 *In vitro* dissolution of the FG hydrogels

Analysis of *in vitro* FG dissolution in PBS showed a biphasic pattern (Fig. 5-3A). Wet weight fraction result showed that the dissolution rate is significantly affected by different concentrations of FG scaffolds ($p < 0.001$): 25% and 50% fibrinogen concentrations displayed a significantly higher rate of dissolution than 75% and 100% FG scaffolds. The first spike in dissolution occurred at day 2 for the 25% and 50% FG scaffolds, where the hydrogels lost ~35% and 15% of their initial weight, respectively. This was followed by a second spike at day 8, when the hydrogels lost ~80% of their initial weight. For the 75% and 100% FG scaffolds, the two spikes in dissolution occurred later at days 6 and 12, with loss of 20% and 90% of the initial weight for the respective time points. The pattern of protein released, observed by UV-Vis spectroscopy (Fig. 5-3B), correlates well with the wet weight fraction finding, by being significantly affected by the percentage of fibrinogen ($p < 0.001$). As well, the biphasic pattern of absorbance peaks that reflects most weight dissolution into the conditioned PBS can be noted.

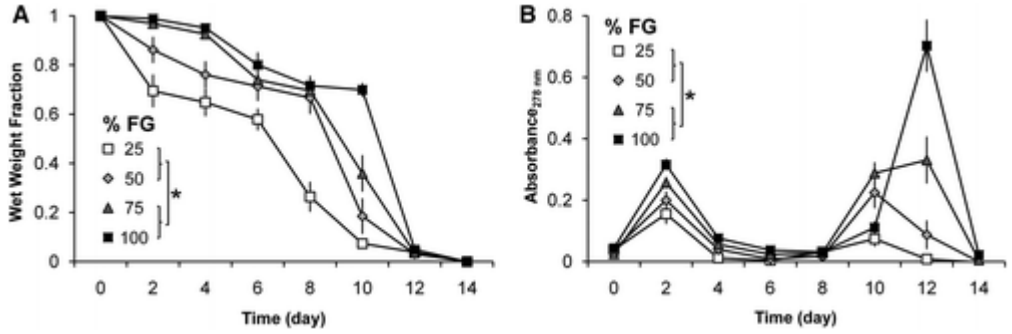


**Figure 5-3: *In vitro* FG dissolution**
**(A)** Wet weight fraction analysis and **(B)** absorbance at 278 nm, reflecting the amount of phenyl group of fibrinopeptide proteins dissolved in the conditioned PBS, showed a biphasic dissolution pattern for all FGs. Data markers represent mean ± standard error of mean; $n = 5$. *$p < 0.05$ between 25% and 50% FGs and 75% and 100% FGs.

### 5.3.4 Quantification of the amount of released AAV2-CMV-GFP from FG hydrogels

The amount of AAV2-CMV-GFP released into the conditioned media from the AAV2-CMV-GFP-loaded FG scaffolds is significantly affected by different concentrations of FG scaffolds ($p < 0.001$), and also displays a biphasic pattern (Fig. 5-4A). The spikes in the amount of AAV2-CMV-GFP released into the media occurred at day 2 and 9 for 25% and 50% scaffolds. In contrast, the spikes in the amount of AAV2-CMV-GFP released into the media occurred at day 2 and 15 for 75% and 100% FG scaffolds. Approximation of the area under the curves in Figure 5-4A suggests that the vector genomes of AAV2-CMV-GFP released into the media from 75% and 100% FG scaffolds were lower than that of 25% and 50% FG scaffolds.

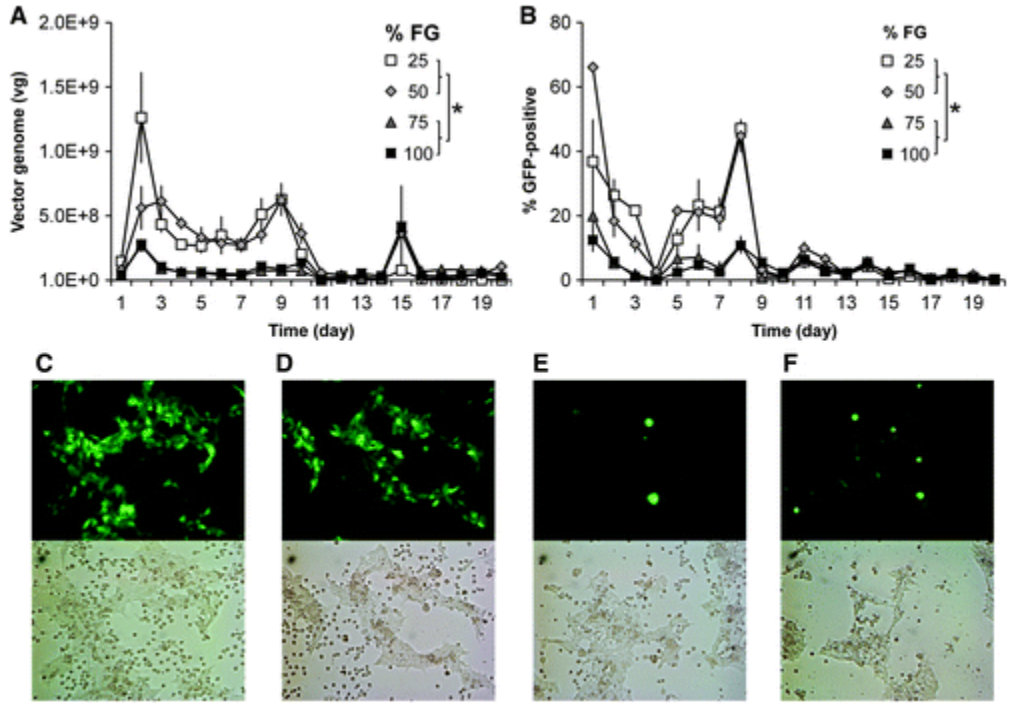


**Figure 5-4: *In vitro* characterization of AAV2-CMV-GFP-loaded FG scaffolds**
**(A)** Vector genomes (vg) of AAV2-CMV-GFP released into 1 mL of conditioned media and **(B)** percentage of GFP-positive HEK-293 cells show biphasic AAV2-CMV-GFP release and corresponding spikes in percentage of GFP-positive cells. Data markers represent mean ± standard error of mean; $n$ =3. *$p < 0.05$ between 25% and 50% FGs and 75% and 100% FGs. **(C-F)** Fluorescent and bright-field photomicrographs of HEK-293 cells incubated with AAV2-CMV-GFP-loaded 25%, 50%, 75%, and 100% FGs at day 8 correlates with the quantitative findings in A and B.

### 5.3.5 Quantification of mammalian cell transduction efficiency of released AAV2-CMV-GFP

The percentage of GFP-positive cells from transduction of AAV2-CMV-GFP released into the conditioned media from the AAV2-CMV-GFP-loaded FG scaffolds is also significantly affected by different concentrations of FG scaffolds ($p < 0.001$), and showed a biphasic pattern (Fig. 5-4B). This pattern is similar to those of the FG dissolution (Fig. 5-3) and AAV2-CMV-GFP release (Fig. 5-4A). FG scaffolds with 25% and 50% fibrinogen concentrations yielded significantly higher percentage of GFP-positive cells than the 75% and 100% FG scaffolds. There were spikes in the percentage of GFP-positive cells at days 1 and 8 for all FG scaffolds, which correlate with the biphasic release pattern of high amounts of AAV2-CMV-GFP at these time points (Fig. 5-4A). Although 75% and 100% FG scaffolds showed similar biphasic spikes in the percentage of GFP-positive cells, the response was significantly lower compared with 25% and 50% FG scaffolds. Photomicrographs of GFP-expressing cells taken daily confirmed quantitative findings by flow cytometry (Fig. 5-4C – F).

### 5.3.6 Quantification and functional analysis of TGF-$\beta_1$ expression from hBM-MSCs transduced with released AAV2-CMV-TGF-$\beta_1$

The amount of TGF-$\beta_1$ synthesized by hBM-MSCs and released into the conditioned medium is significantly affected by different concentrations of FG scaffolds (Fig. 5-5A, B). Cells incubated with 50% FG loaded with AAV2-CMV-TGF-$\beta_1$ made 2.5-fold more active TGF-$\beta_1$ than those incubated with 100% FG loaded with AAV2-CMV-TGF-$\beta_1$ ($p = 0.017$, Fig. 5-5A). As well, the conditioned medium from the hBM-MSC culture that was incubated with the 50% FG loaded

with AAV2-CMV-TGF-$\beta_1$ resulted in greater inhibition of CCL-64 cell proliferation (Fig. 5-5B), measured via mitochondrial activity ($p$ = 0.002). The different concentrations of AAV2-CMV-TGF-$\beta_1$-loaded FG scaffolds also affected the cartilage-specific gene expression of the hBM-MSCs (Fig. 5-5C). Human *sox-9* and *aggrecan* mRNA expressions were significantly higher for 50% FG versus 100% FG ($p$ = 0.049 and $p$ = 0.009, respectively). All the results were normalized against values from AAV2-CMV-GFP-loaded FG scaffolds of the same percentage fibrinogen concentration to account for the effects of viral transduction, FG, and endogenous TGF-$\beta_1$ production by hBM-MSCs.

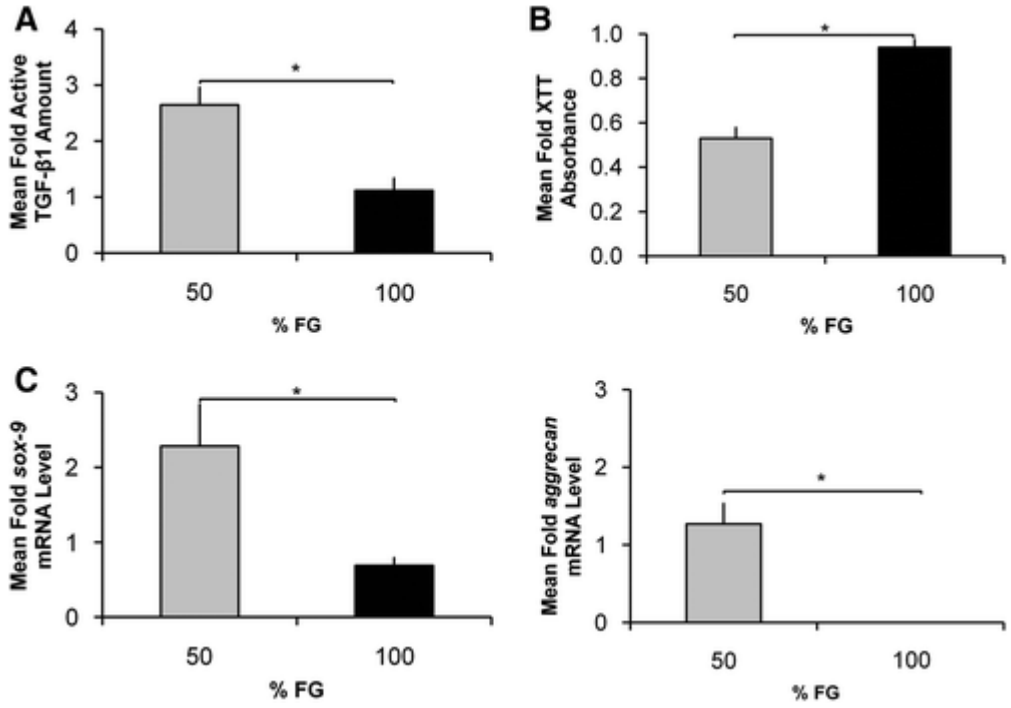


**Figure 5-5: *In vitro* characterization of AAV2-CMV-TGF-$\beta_1$-loaded FG scaffolds**
**(A)** Mean fold amount of active TGF-$\beta_1$ released into the conditioned media showed increased production of TGF-$\beta_1$ from hBM-MSCs incubated with 50% FG. **(B)** Mean fold XTT absorbance measurement from CCL-64 cells showed higher TGF-$\beta_1$-mediated growth inhibition in samples incubated with conditioned media from 50% FG. **(C)** Mean fold human *sox-9* and *aggrecan* mRNA expressions from hBM-MSCs incubated with AAV2-CMV-TGF-$\beta_1$-loaded FG scaffolds showed increased expression of relevant chondrogenic genes in cells incubated with 50% FG. Data were normalized against values from AAV2-CMV-GFP-loaded FG scaffolds of the same percentage fibrinogen concentration to account for the effects of viral transduction, FG, and endogenous TGF-$\beta_1$ production by hBM-MSCs. Bars represent mean ± standard error of mean; $n$ = 3. *$p$ < 0.05 between 50% and 100% FGs.

## 5.4 DISCUSSION

Tissue engineering scaffolds allow for the delivery of cells or diffusible factors that can act locally to promote tissue regeneration (163, 164). The combination of gene therapy and tissue engineering offers the potential to direct progenitor cells' proliferation and differentiation into functional tissue replacement (53). We have previously shown that hMSCs transduced with AAV-TGF-$\beta_1$ improved the *in vivo* cartilage repair when the *ex vivo* transduced cells were implanted into osteochondral defects of athymic rats (42). However, in an effort to move beyond *ex vivo* gene transfer, the current focus of the project is on *in situ* delivery of therapeutic transgenes, such as TGF-$\beta_1$, directly to host MSCs residing in cartilage wounds using biodegradable scaffolds. This strategy can be thought of as "augmenting" microfracture, which is an accepted human clinical standard for treatment of full-thickness cartilage defects (165). The goal of this strategy is to induce localized exogenous transgene expression in repair/progenitor cells infiltrating into the scaffold for sustained release of these factors at the site of injury. Strategies that combine scaffolds, drug delivery technology, and gene therapy have the potential to provide more effective tissue regeneration with significant improvements on safety and cost issues compared to currently available therapies.

Although numerous novel synthetic and natural polymers have been investigated for cartilage tissue engineering studies (140, 153, 154), usage of an FDA-approved and autologous biomaterial as an AAV2-releasing scaffold can accelerate the transition of basic science research into human clinical studies. FG is a biomaterial widely used in clinical practice and tissue engineering applications. As well, dilute FG has been successfully used to treat cartilage wounds in a pilot human clinical study (152). However, studies on its use as a delivery scaffold for gene vectors are limited, and only adenovirus delivery has been investigated for delivery of viral

vectors (55). FG has been investigated as a delivery scaffold for controlled release of adenovirus in a rabbit ear ulcer model (156) and for perivenous adventitial gene transfer (158), and was shown to provide enhanced *in vivo* transgene expression over adenovirus transduction without FG scaffold. For cartilage tissue engineering purposes, FG scaffolds with non-viral copolymer-protected polyethylenimine-DNA vectors achieved sustained release of the gene over 20 day period and successful *in vitro* transfection of human keratinocytes and rabbit articular chondrocytes (157).

Nonetheless, FG formulation for AAV2 delivery has not been optimized. The fibrinogen/thrombin concentration in the FG preparation has been shown to affect the structural properties of the scaffold, and in turn influence the proliferation rate and morphology of hMSCs (155). Therefore, alterations in FG scaffold microstructure can influence its function as a delivery scaffold for AAV2. The aim of the current study was to assess, *in vitro*, the structural characteristics of FG hydrogels containing varying fibrinogen concentrations, their AAV2-particle release kinetics, and subsequent transgene expression in target cells for articular cartilage tissue engineering.

Undiluted 100% FG scaffold had longer gelation time compared with diluted scaffolds, which may be explained by data from SEM analysis, which showed that 100% FG scaffolds formed a denser scaffold with smaller pore sizes and thicker fibrin fibers than diluted FG scaffolds. In contrast, diluted FG scaffolds had a more open fibrin network, which was reflected by their shorter clotting times. Consistent with another finding (155), diluted FGs had a more homogenous structure than undiluted 100% scaffold.

FG scaffolds dissolved over time in PBS, which was shown by the decrease in the wet weight over time and by the change in absorbance measurements of the phenyl group of the

fibrinopeptide over time. Dissolution of the FG scaffolds coincided with the amount of AAV2-CMV-GFP released into the conditioned media. In addition, both the dissolution of the scaffold and the amount of AAV2-CMV-GFP released into the media occurred in a biphasic burst fashion, consistent with a typical hydrogel bulk-degradation pattern. The burst release pattern of AAV2-CMV-GFP was similar to the percentage of GFP-positive HEK-293 cells. There were more GFP-positive cells when a greater amount of AAV2-CMV-GFP was released into the media. Both the amount of AAV2-CMV-GFP released and the number of GFP-positive cells is higher in wells with 25% and 50% FG scaffolds than in those with 75% and 100% FG scaffolds. In addition to dissolution pattern of the FG scaffold, the more open fibrin network of the 25% and 50% FG scaffolds may contribute to greater release of AAV2-CMV-GFP and the higher percentage of GFP-positive cells compared with 75% and 100% FG scaffolds. These *in vitro* studies showed that commercial strength 100% as well as 75% FGs are less efficient at releasing AAV2 particles, and that dilute 25% and 50% FGs are more effective. Viral particles released from dilute FGs retained the ability to transducer HEK-293 cells up to 17 days *in vitro*.

In contrast to our findings with AAV2, a previous study investigating different concentrations of FG scaffold loaded with adenovirus had achieved optimal viral releasing properties with the higher fibrinogen concentration (166). However, this was observed with adenovirus vector and with a diluted thrombin concentration. Compared with adenovirus, AAV is much smaller and has the advantages of improved safety profile and longer transgene persistence (47). In addition, lower thrombin concentration decreases the rate of fibrin cross-linking (55). Since *in vivo* FG decomposition will be accelerated via plasmin-mediated fibrin degradation in addition to diffusion-mediated dissolution, FGs prepared with undiluted thrombin are more likely to persist and release AAV2 particles longer for animal or human applications.

Although many more dilutions of FG at smaller increments could be studied to further assess the AAV2 release kinetics, especially with lower concentrations of FG, the four dilutions were chosen to support the goal of evaluating FG concentrations potentially useful for *in vivo* clinical applications. As well, FG dilutions of 25% approach the lower limit to achieve a clinically functional scaffold structure (166). For this reason, 50% and 100% FGs were chosen for subsequent studies with AAV2-CMV-TGF-$\beta_1$.

As our ultimate goal is to develop a localized AAV2 delivery system for cartilage tissue engineering, we further explored the concentrations of 50% and 100% FGs for delivery of AAV2 encoding for a therapeutic gene useful for cartilage regeneration. Transforming growth factor-$\beta_1$ (TGF-$\beta_1$) has long been shown to consistently induce BM-MSC chondrogenesis *in vitro* (57, 167). We also have previously shown that implantation of AAV2-CMV-TGF-$\beta_1$-transduced hMSCs into osteochondral defects has improved cartilage repair *in vivo* (42). Therefore, we compared AAV2-CMV-TGF-$\beta_1$ delivery from the 50% and 100% FGs to hBM-MSCs *in vitro*. The studies on FG scaffold delivery of therapeutic AAVs versus reporter gene AAVs, especially for their chondrogenic effects, have been limited to date (166). hBM-MSCs cultured with 50% FG-AAV2-CMV-TGF-$\beta_1$ construct had higher concentration of active TGF-$\beta_1$, which resulted in greater inhibition of CCL-64 cell proliferation, and higher cartilage-specific gene expression levels in tranduced hBM-MSCs.

## 5.5 CONCLUSIONS

In summary, we have demonstrated that varying the fibrinogen concentrations in FG constructs changes the structural and functional characteristics of the scaffold for gene delivery. Diluting

the fibrinogen concentration yields a scaffold with a network of larger pores and thinner fibers, which reduces entrapment and subsequently enhances the release of AAV2 particles. Lower concentration FG scaffolds have also been shown to promote greater proliferation of hMSCs, which are the principal cell types recruited for *in situ* chondrogenesis (155). Therefore, implantation of diluted FG scaffolds containing bioactive AAV2 vectors have the potential to improve articular cartilage regeneration and be translated for clinical cartilage tissue engineering. Further *in vivo* studies are planned using small and large animal models to validate the enhanced repair potential of diluted FG scaffolds with therapeutic AAV2-TGF-$\beta_1$ for localized *in situ* cartilage tissue engineering before translation into the clinical setting.

# 6.0 INTERLEUKIN-1BETA-MEDIATED INHIBITION OF HUMAN MESENCHYMAL STEM CELL CHONDROGENESIS IS BLUNTED BY ADENO-ASSOCIATED VIRUS GENE TRANSFER OF INTERLEUKIN-1 RECEPTOR ANTAGONIST AND TRANSFORMING GROWTH FACTOR-BETA1

## 6.1 INTRODUCTION

Articular cartilage plays the essential role of forming a smooth surface between two bones, permitting frictionless joint motion. It is mainly composed of chondrocytes, as well as collagen type II and aggrecan that form a dense and avascular extracellular matrix (ECM). Due to the dense and avascular nature of ECM, the healing capacity of articular cartilage once damaged, is severely limited. Cartilage injuries, from trauma or degeneration, lead to debilitating osteoarthritis, often regardless of treatment status.

Microfracture is a commonly used surgical technique to promote cartilage repair (168). This technique involves perforation of the subchondral bone to allow bone marrow contents to access and fill the defect and undergo chondrogenic differentiation. The bone marrow contents include bone marrow-derived mesenchymal stem cells (MSCs) and various growth factors. Numerous *s*tudies have shown successful MSC differentiation into the chondrogenic phenotype using various growth factors in a controlled *in vitro* environment with pre-defined chondrogenic differentiation media (61). The microfracture technique resulted in improved cartilage repair in

*in vivo* studies as well; however, the remodeled cartilage remains inferior to the native articular cartilage in terms of matrix composition and biomechanical quality (169). Microfracture, nonetheless, remains popular due to its convenience and minimally invasive nature (168).

The altered homeostatic environment of the diseased joint may be responsible for the inconsistency between the *in vitro* and *in vivo* results of MSC chondrogenesis (80). In contrast to a healthy joint or a pre-defined *in vitro* environment, catabolic/inflammatory mediators are upregulated in diseased joints or from the surgical intervention itself, further impairing the ability of cartilage repair (170, 171). Indeed, addition of inflammatory cytokines, such as interleukin (IL)-1β and tumor necrosis factor (TNF)-α, in pre-defined chondrogenic media inhibited chondrogenic differentiation of MSCs in a dose-dependent manner (71, 80). When the cytokine actions were blocked using antagonist molecules *in vitro*, the inhibitory effect on chondrogenesis was restored to a certain extent (80).

The anti-inflammatory molecules used in this study include IL-1 receptor antagonist protein (IRAP) and transforming growth factor (TGF)-$\beta_1$. IRAP is a small 20 – 25 kDa secreted protein with no known agonist function (74). It competitively inhibits IL-1 signaling via competitive inhibition of IL-1 ligand and receptor interactions (73). TGF-$\beta_1$, on the other hand, is a well-established anabolic growth factor that induces MSC chondrogenesis, and is often included in chondrogenic differentiation media (42, 57). In addition to its anabolic functions, TGF-$\beta_1$ has also been shown to decrease the catabolic activity of inflammatory cytokines *in vitro* and *in vivo* (64). However, although these anti-inflammatory strategies are straightforward, the *in vivo* efficacy is limited by the poor pharmacokinetics of the small molecule and the need for sustained high concentrations.

To overcome this limitation, genetic modification of MSCs has been explored for sustained delivery of the bioactive factors. Numerous vector carriers, such as adenovirus, lentivirus, and retrovirus, have been studied for gene transfer; nonetheless, significant safety concerns associated with these viruses limit their application to clinical gene therapy (123). Adeno-associated virus (AAV), in contrast, is a non-pathogenic virus that is already used in numerous human clinical trials (47, 119). AAV transduction of MSCs has also been extensively studied by us and others (16, 42, 108).

In the current study, we investigated the chondrogenic differentiation of AAV-transduced MSCs in the presence of inflammatory cytokines *in vitro*. IRAP and TGF-$\beta_1$ molecules were overexpressed in the MSCs via AAV-gene transfer. The aim of the study was to test the hypothesis that chondrogenic potential of MSCs will be enhanced by using AAV-encoding for anti-catabolic factors, such as IRAP and TGF-$\beta_1$.

## 6.2 METHOD

### 6.2.1 hMSC cell culture

Human MSCs were obtained, processed, and maintained as previously described (57). Briefly, femoral bone marrow reaming tissues were obtained according to an exempt IRB-approved protocol at the University of Pittsburgh for discarded tissue. The bone marrow was minced, washed in phosphate buffered saline (PBS, Gibco), and vortexed. Then the cell suspension was passed through a cell strainer, loaded onto Histopaque-1077 density gradient (Sigma-Aldrich), and centrifuged at 400 x *g* for 30 min at 4°C to fractionate. Mononucleated cells were collected

and cultured in MSC growth media composed of Minimum Essential Medium Alpha (α-MEM, Gibco), 16.5% fetal bovine serum (FBS, Atlanta Biologicals), 1% penicillin-streptomycin (pen/strep, Gibco), and 2 mM L-glutamine (Invitrogen). Freshly isolated cells were allowed to adhere to the tissue culture flask for 5 – 7 days at 37°C and 5% $CO_2$ prior to media change. Cells were passaged after 10 days of initial plating via detaching with 0.25% trypsin (Invitrogen) and replating at 100 cells/$cm^2$ density. Medium was changed every 3 – 4 days. The cells were expanded for two passages, when hMSCs reached 70% confluence, and then frozen in FBS, 10% dimethyl sulfoxide (DMSO, Sigma). For the experiments in this study, the frozen passage 2 hMSCs were thawed and grown in MSC growth media for 8 days, with media change at days 4 and 6.

### 6.2.2 AAV preparation and hMSC transduction

Double-stranded serotype 2 AAVs encoding for enhanced green fluorescence protein (GFP) with cytomegalovirus (CMV) promoter (AAV-GFP), human IRAP with CMV enhancer/beta-actin (CB) promoter (AAV- hIRAP), and human TGF-$\beta_1$ with CMV promoter (AAV-TGF-$\beta_1$) were prepared and purified as previously described (120). The vector titers, determined using viral DNA dot blot method (101), were 6 x $10^{12}$ vector genomes (vg)/mL for AAV-GFP, 2 x $10^{12}$ vg/mL for AAV-hIRAP, and 1 x $10^{12}$ vg/mL for AAV-TGF-$\beta_1$. AAV transductions were performed when the thawed passage 2 hMSCs reached 80% confluence in T-225 flasks at a 50,000 – 100,000 vg/cell concentration in 10 mL of serum and antibiotic-free α-MEM. The untransduced control cells were treated with 10 mL serum and antibiotic-free α-MEM only. After one hour incubation, 20 mL of hMSC growth media was added to the tissue culture flasks.

**Table 6-1: Experimental conditions**

| Groups | AAV transgene | Cytokine Stimulation | Chondrogenic Media |
|---|---|---|---|
| 1 | Untransduced CTRL | None | CM + TGF-$\beta_1$ |
| 2 | | IL-1β | CM + TGF-$\beta_1$ + IL-1β |
| 3 | GFP | None | CM + TGF-$\beta_1$ |
| 4 | | IL-1β | CM + TGF-$\beta_1$ + IL-1β |
| 5 | hIRAP | None | CM + TGF-$\beta_1$ |
| 6 | | IL-1β | CM + TGF-$\beta_1$ + IL-1β |
| 7 | TGF-$\beta_1$ | None | CM |
| 8 | | IL-1β | CM + IL-1β |

### 6.2.3 Chondrogenic pellet culture

Fourty-eight hours post-AAV-transduction, MSCs were pelleted for chondrogenic culture as previously described (42, 57, 121). Briefly, AAV-transduced MSCs in tissue culture flasks were washed, trypsinized, and washed again in PBS and counted. The cells were divided into 8 groups (Table 6-1) and were separately aliquoted in 15-mL polypropylene conical tubes at a density of 2.5 x $10^5$ hMSCs in 0.5 mL of chondrogenic media. The composition of basal chondrogenic media (CM + TGF-$\beta_1$) are high-glucose Dulbecco's Modified Eagle Medium (DMEM, Gibco), with 1% penicillin-streptomycin (Gibco), $10^{-7}$-M dexamethasone (Sigma-Aldrich), 50-μg/mL L-ascorbic acid-2-phosphate (Sigma–Aldrich), 40-μg/mL proline (MP Biomedicals, Solon), and 1% BD™ ITS + Premix (Becton-Dickinson), and 10 ng/mL human TGF-$\beta_1$ (R&D Systems). For the cytokine groups, 10 ng/mL of human IL-1β (R&D Systems) were supplemented in CM + TGF-$\beta_1$ media (CM + TGF-$\beta_1$ + IL-1β). Of note, TGF-$\beta_1$ was excluded from the chondrogenic media for chondrogenic culture of hMSC transduced with AAV-TGF-$\beta_1$ (CM and CM + IL-1β). The aliquots were centrifuged at 500 x *g* for 5 min, after which the tubes with loose caps were incubated at 37°C and 5% $CO_2$. The media was refreshed every 2-3 days.

### 6.2.4 Longitudinal transgene expression

The transgene expression from AAV-transduced hMSCs over the chondrogenic culture period was assessed by detecting GFP expression by live fluorescence with a MVX-10 MacroView Systems stereomicroscopy equipped with DP71 camera (both from Olympus), and determining the level of hIRAP in conditioned media at different time points using a commercially available ELISA (R&D Systems) according to the manufacturer's description. The GFP images in Fig. 1A had the contrast increased by the same value in Adobe Photoshop CS4 to improve image contrast for print.

### 6.2.5 Gross and histological assessments of hMSC pellets

At the end of 21 days of chondrogenic culture, hMSC pellets were grossly assessed with stereomicroscopy and DP71 camera. The pellet area was measured using ImageJ (NIH). The pellets were subsequently fixed and processed for histological analyses using Safranin O-Fast green staining for sulfated glycosaminoglycan (GAG) according to standard protocols.

### 6.2.6 Biochemical analyses of hMSC pellets

Chondrogenic hMSC pellets were also collected for biochemical analyses. Each pellet was papain-digested overnight in a 60°C shaking water bath (200 RPM) in 0.25 mL papain buffer. The composition of papain buffer was the following: 50 mM sodium phosphate (Sigma-Aldrich), 5 mM Ethylenediaminetetraacetic acid (EDTA, Gibco), 5 mM cysteine HCl (Sigma-Aldrich), and 0.5 mg/mL papain (Sigma-Aldrich). The total GAG content from the digested pellets was

quantified with the dimethylmethylene blue (DMMB) assay using VersaMax UV-Vis spectrophotometer (Molecular Devices) as previously described (57). The DNA content was also quantified with Quant-iT™ PicoGreen® dsDNA Reagent and Kits (Molecular Probes) and a VICTOR™ X3 Multilabel Plate Reader (Perkin Elmer) per manufacturer's protocol. The GAG content of the pellets was normalized by dividing the DNA from the GAG contents.

### 6.2.7 Statistical analyses

All the statistical data analyses were performed using Statistical Package for Social Studies (SPSS) 17.0 for Windows (IBM), with the significance level set as $p < .05$ unless otherwise noted. Shapiro-Wilk and Levene's tests were used to test the assumptions of parametric data. The longitudinal IRAP transgene expression levels in conditioned media were analyzed using two-way mixed analysis of variance (ANOVA), with time as repeated measure and cytokine as independent variables (Fig. 1B). Pellet sizes and GAG contents were analyzed using two-way independent ANOVA with the AAV constructs and cytokine as independent variables (Figs. 2B, 3B, and 4B) and *post hoc* Tukey when there was a significant effect of AAV construct on the outcome variables (Figs. 3B and 4B). Student's *t*-test was used when the interaction effects were significant from the two-way ANOVAs to analyze the effect of cytokine stimulation.

## 6.3 RESULTS

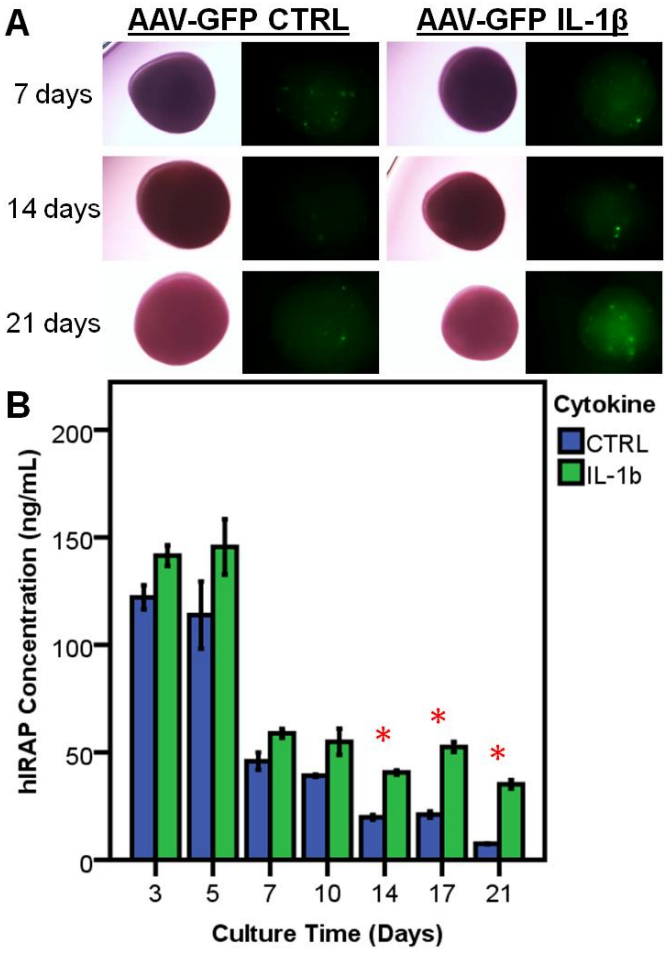


**Figure 6-1: Longitudinal transgene expression from AAV-transduced hMSC pellet culture**
**(A)** GFP-expression from AAV-GFP transduced hMSCs at 7, 14, and 21 days of chondrogenic culture, with and without IL-1β. **(B)** hIRAP concentration detected from conditioned culture media from AAV-hIRAP transduced hMSCs at various time points of chondrogenic culture with and without IL-1β. $n = 2 – 3$/group. *$p < .007$ between CTRL and IL-1β at each time points.

### 6.3.1 Longitudinal transgene expression

Robust GFP transgene expression was observed in AAV-GFP transduced hMSC chondrogenic pellets throughout the 21 day culture period (Fig. 6-1A). The IL-1β stimulated AAV-GFP group pellets, while smaller in size, showed brighter GFP signal than the control AAV-GFP group

pellets at all time points. No GFP-signal was observed from the untransduced control and AAV-hIRAP or AAV-TGF-$\beta_1$ transduced pellets (Data not shown). Detectable levels of hIRAP transgene product were seen in AAV-hIRAP transduced hMSC chondrogenic pellets throughout the 21 day culture period (Fig. 6-1B). There was a significant main effect of time on the hIRAP concentration ($p < .001$), with gradual decrease in the transgene expression over time. Although there was no significant effect of cytokine stimulation ($p = .276$), the interaction effect between the time and cytokine stimulation was significant ($p = .010$). Hence, the cytokine effect was further explored. There was a significant effect of cytokine stimulation at days 14, 17, and 21 on hIRAP production ($p$s $< .007$): hMSC pellets cultured in the presence of IL-1β produced more hIRAP than those cultured without IL-1β. No hIRAP was detected from the untransduced control and AAV-GFP or AAV-TGF-$\beta_1$ transduced pellets (Data not shown).

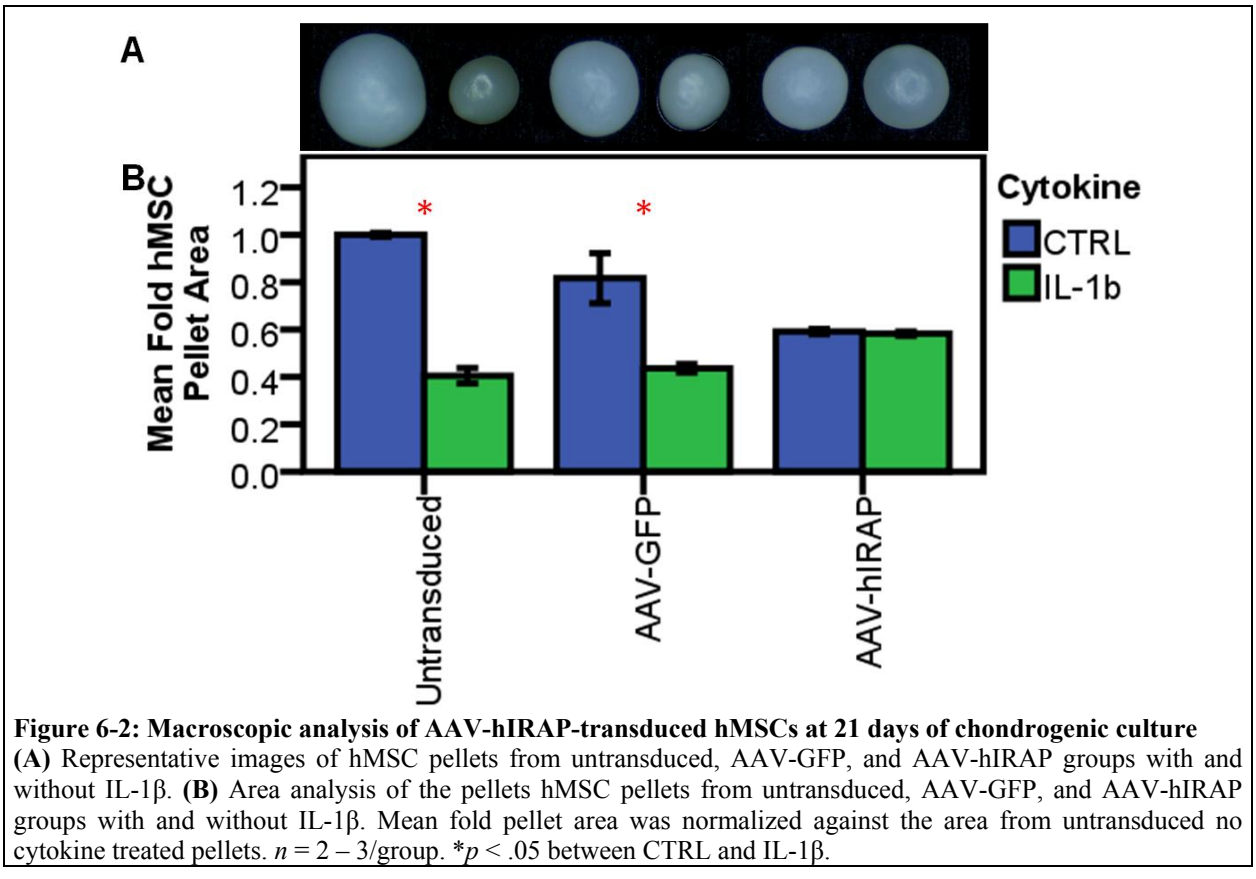


**Figure 6-2: Macroscopic analysis of AAV-hIRAP-transduced hMSCs at 21 days of chondrogenic culture** **(A)** Representative images of hMSC pellets from untransduced, AAV-GFP, and AAV-hIRAP groups with and without IL-1β. **(B)** Area analysis of the pellets hMSC pellets from untransduced, AAV-GFP, and AAV-hIRAP groups with and without IL-1β. Mean fold pellet area was normalized against the area from untransduced no cytokine treated pellets. $n = 2 – 3$/group. *$p < .05$ between CTRL and IL-1β.

### 6.3.2 hMSC pellet area evaluation

Macroscopic images of the hMSC pellets were taken at chondrogenic culture day 21 (Figs. 6-2 and -3). For the AAV-hIRAP pellet area analysis (Fig. 6-2B), there was a significant main effect of cytokine ($p < .001$). There was no significant effect of AAV constructs ($p = .158$); however, the interaction effect between the AAV construct and cytokine stimulation was significant ($p = .001$). When the cytokine effect on each of the AAV groups was further explored, the areas of hMSC chondrogenic pellets were significantly decreased by IL-1β stimulation for untransduced control and AAV-GFP groups ($p = .025$ and $p = .024$, respectively). On the other hand, the effect of cytokine stimulation for AAV-hIRAP group was not significant.

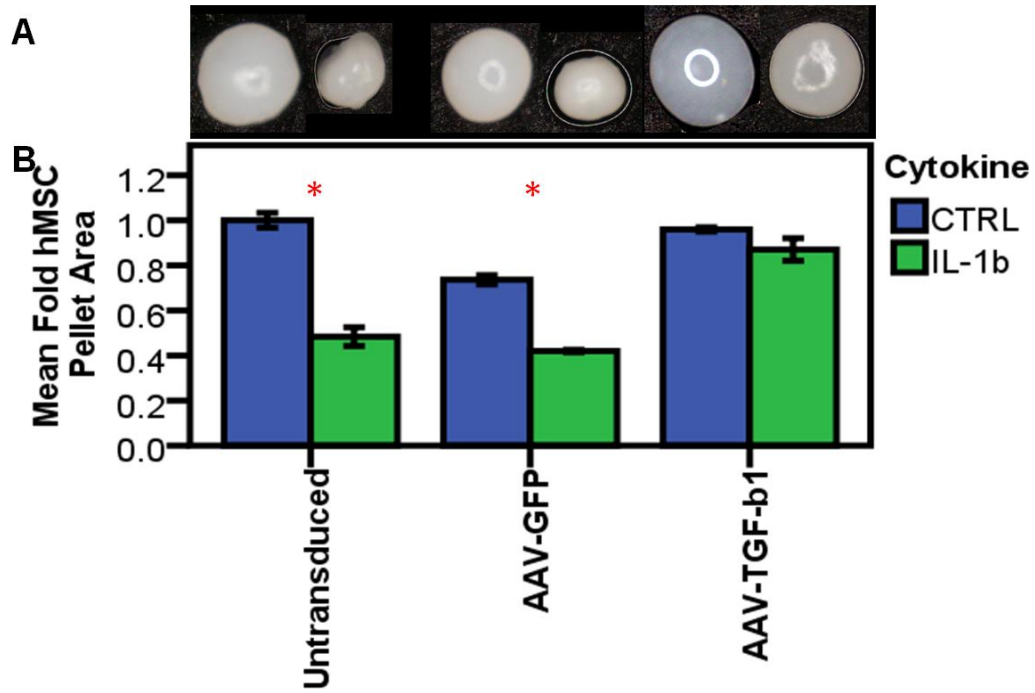


**Figure 6-3: Macroscopic analysis of AAV-TGF-$\beta_1$-transduced hMSCs at 21 days of chondrogenic culture**
**(A)** Representative images of hMSC pellets from untransduced, AAV-GFP, and AAV-hIRAP groups with and without IL-1β. **(B)** Area analysis of the pellets hMSC pellets from untransduced, AAV-GFP, and AAV-hIRAP groups with and without IL-1β. Mean fold pellet area was normalized against the area from untransduced no cytokine treated pellets. $n = 3 – 4$/group. *$p < .05$ between CTRL and IL-1β.

For the AAV-TGF-$\beta_1$ transduced hMSC pellets (Fig. 6-3B), their areas were significantly affected by both the AAV constructs and cytokine stimulation (*p*s < .001). As well, their interaction effect was significant ($p < .001$). *Post hoc* Tukey analysis showed that all three AAV construct groups were significantly different from one another (*p*s < .001 for all comparisons). The cytokine effect was further explored as well: the areas of hMSC chondrogenic pellets were significantly decreased by IL-1β stimulation for the untransduced control and AAV-GFP groups (*p*s < .001), but not for the AAV-TGF-$\beta_1$ transduced hMSC pellets.

### 6.3.3 hMSC glycosaminoglycan content

GAG contents of hMSC pellets were stained, measured and calculated after 21 days of chondrogenic culture (Fig. 6-4). Via Safranin-O Fast Green staining (Fig. 6-4A), the untransduced control hMSC pellets underwent the best chondrogenesis, while the untransduced IL-1β stimulated hMSC pellets performed the worst. Comparing the non-IL-1β stimulated control groups, the AAV-GFP and AAV-hIRAP transductions reduced the chondrogenic potential of hMSCs, with AAV-hIRAP having greater effect than the AAV-GFP. On the other hand, when the pellets were treated with IL-1β, AAV-hIRAP transduction rescued the IL-1β-mediated inhibition of hMSC chondrogenesis, while AAV-GFP had no effect.

When the GAG content was quantified via biochemical analyses (Fig. 6-4B), there were significant main effects of AAV constructs ($p = .031$) and cytokine stimulation ($p < .001$). As well, the interaction effect between the two main effects was significant ($p = .001$). *Post hoc* analysis of the three AAV constructs revealed that there was a significant difference between AAV-GFP and AAV-hIRAP pellets ($p = .009$), but no differences between any other pellets. When the cytokine effect for each AAV constructs was analyzed, the IL-1β stimulation

significantly decreased the GAG content for the untransduced control ($p$ = .014) and AAV-GFP groups ($p$ = .001), but not for the AAV-hIRAP groups.

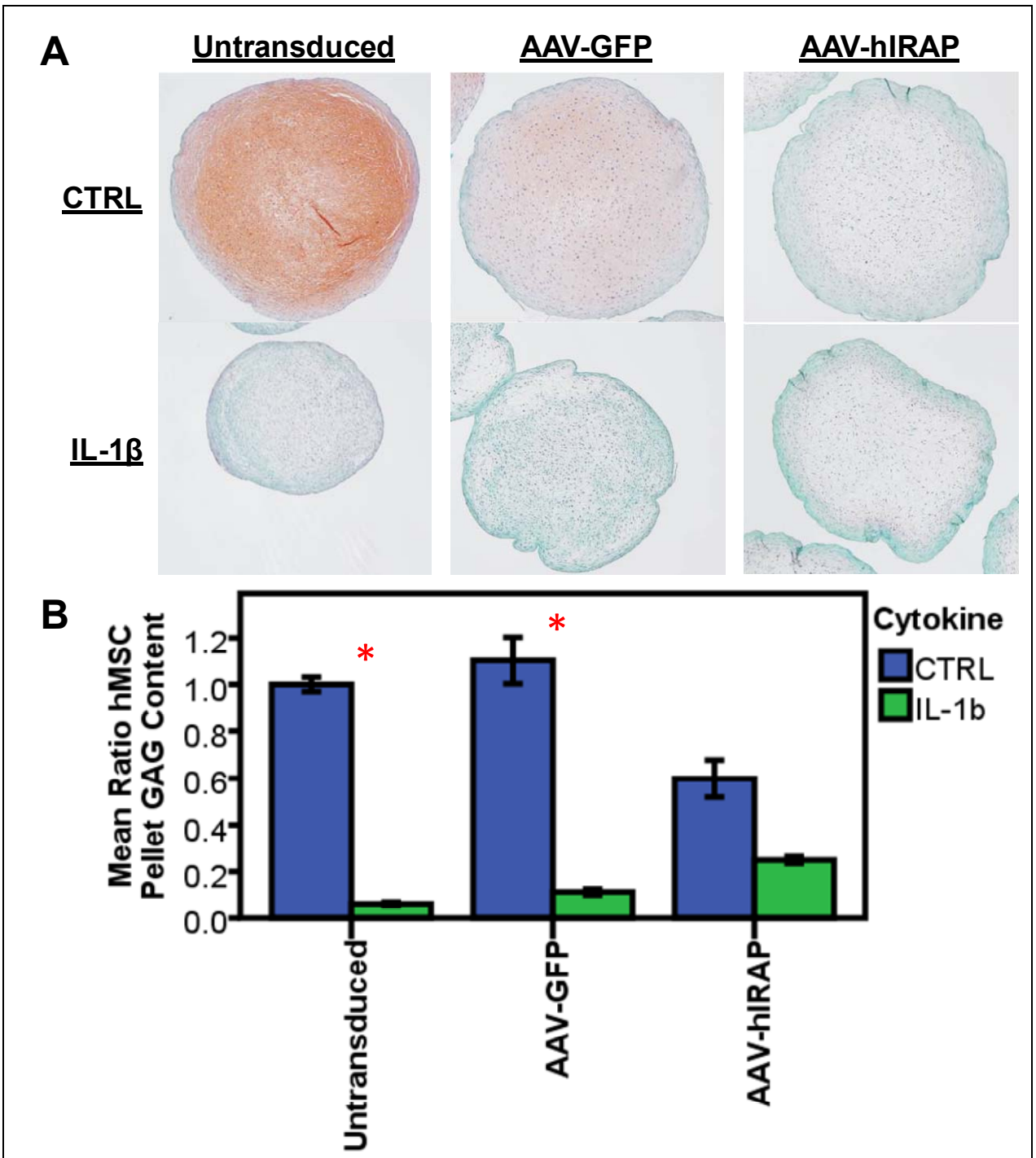


**Figure 6-4: GAG content of AAV-hIRAP transduced hMSC pellets at 21 days of chondrogenic culture**
**(A)** Representative Safranin O-Fast green images of hMSC pellets from untransduced, AAV-GFP, and AAV-hIRAP groups with and without IL-1β. **(B)** GAG content analysis of the pellets hMSC pellets from untransduced, AAV-GFP, and AAV-hIRAP groups with and without IL-1β. Mean ratio GAG content was normalized against that of the untransduced no cytokine treated pellets. $n$ = 2 – 3/group. *$p$ < .05 between CTRL and IL-1β.

## 6.4 DISCUSSION

Injuries to avascular articular cartilage, with its limited repair potential, frequently progress to debilitating osteoarthritis, which is a significant clinical problem with respect to its prevalence and cost in healthcare dollars (4, 5, 8). Numerous approaches are investigated to promote cartilage restoration; of which accessing of bone marrow derived MSCs via microfracture is a popular technique. These MSCs subsequently undergo chondrogenic differentiation; however, they often result in fibrocartilageneous phenotype with inferior matrix composition and biomechanical properties. It has been shown that inflammatory cytokines, generally present in the joint due to the disease/injury state or due to the surgical intervention, limit the chondrogenic differentiation potential of MSCs (71, 80). Therefore, the anti-catabolic side of the MSC chondrogenesis strategy is increasingly recognized to be important and warrants additional investigation.

IL-1 is the major inflammatory cytokine in injured joints and plays a pivotal role in osteoarthritis pathogenesis (172, 173). Numerous studies have investigated the inhibition of this cytokine as a treatment strategy against osteoarthritis progression (81). Of these approaches, interleukin-1 receptor antagonist (IRAP) that inhibits IL-1 at the cell receptor level has been a popular choice. A recombinant human IRAP is approved for human clinical use for subcutaneous injection treatment of rheumatoid arthritis (128). IRAP has been shown to have beneficial effect against symptoms and structural changes of articular cartilage degeneration of osteoarthritis models in a myriad of *in vitro* and *in vivo* studies (74, 172, 174, 175). As well, when IRAP was injected into the joint during a randomized controlled pilot trial, there was a reduction of knee pain and improvement of joint function in an acute injury setting (128). However, studies on using IRAP during MSC chondrogenesis or cartilage regeneration are limited (80, 176).

TGF-β is the most extensively examined anabolic growth factor for hMSC induction into the chondrogenic phenotype, especially the TGF-$\beta_1$ isoform (42, 57). In addition to its anabolic effect, TGF-$\beta_1$ has been shown to counteract the inflammatory cytokines during chondrogenesis to a certain extent (71). Hence, treatment of MSCs with IRAP and TGF-$\beta_1$ may enhance their chondrogenic differentiation in a disease/inflammatory state. However, appreciable and prolonged stimulation of these factors may be unachievable in a clinical setting with conventional protein applications due to their short half-lives, need for high repetitive dosing, and costly purification process. Therefore, AAVs were utilized to deliver genes encoding for these bioactive factors to MSCs for their production *in situ*.

The current study investigated *ex vivo* genetic manipulation of MSCs. We, however, recognize that this approach faces high regulatory barriers for clinical translation. Additionally, obtaining and expanding MSCs prolongs the time before treatment. Therefore, we have also explored other ways to apply AAV gene therapy, such as by direct intra-articular injection and by use of biodegradable scaffolds for release and delivery of bioactive AAVs to host MSCs within cartilage wounds for transduction *in situ* (47, 108, 140, 152-154). Hence, this *in vitro* study investigating the chondrogenesis of AAV-IRAP or AAV-TGF-$\beta_1$ transduced hMSCs would provide a basis for a future *in vivo* study using these alternative strategies.

In a three-dimensional chondrogenic pellet culture, AAV-transduced MSCs resulted in detectable levels of transgene expression throughout the 21 day culture period. Transgene expression from the IL-1β stimulated pellets was noted to be higher, with statistically significant increases on latter three 14, 17, and 21 day time points. This upregulation of AAV-transgene expression following cytokine treatment has also been noted by another study (46). The authors postulated its mechanism to be due to inflammation-induced cell proliferation or due to enhanced

activation of the CMV promoter via NF-κB signaling pathway. In the present study when the DNA content per pellet was quantified, it was significantly increased with IL-1β treatment in the AAV-GFP ($p$ = .002), but not for the AAV-hIRAP transduced hMSC pellets ($p$ = .829; Data not shown). Hence, IL-1β stimulated more cell proliferation in the AAV-GFP group, but this was blunted by IRAP treatment, making the latter IL-1β activation of promoter the more likely explanation. This IL-1β upregulation of its inhibitor is a highly advantageous mechanism to prevent IL-1β-mediated catabolic effects.

The area measurements of hMSC chondrogenic pellets showed that IL-1β has a negative effect on the pellet size. However, this negative effect was successfully blunted with the treatment of hMSCs with AAV-hIRAP or AAV-TGF-$\beta_1$. Of note, AAV-GFP transduction limited the chondrogenic potential of hMSCs compared to those of the untransduced control, suggesting AAV transduction itself limits hMSC chondrogenic potential to a certain extent. AAV-hIRAP transduction further inhibited hMSC chondrogenesis in a non-inflammatory environment. In fact, AAV-hIRAP transduction was only beneficial compared to other two groups in the presence of IL-1β. AAV-TGF-$\beta_1$ transduction, on the other hand, rescued the AAV inhibition of chondrogenesis to some extent in both non-inflammatory and inflammatory environments. Although a direct comparison between hIRAP and TGF-$\beta_1$ groups is not feasible since the two studies were done on separate trials, the mean fold value comparison suggests that the AAV-TGF-$\beta_1$ transduced hMSCs performed better than the AAV-hIRAP transduced hMSCs.

One of the limitations of pellet area measurement analysis is that area is a two-dimensional measure of a three-dimensional hMSC chondrogenic pellet. However, the area measurement is a convenient and widely used parameter to evaluate chondrogenesis outcome

(57). As well, a separate trial that compared pellet areas to pellet wet weights showed significant correlation between the two measures ($r = .955$, $p < .001$; Data not shown).

Histological and biochemical analysis of GAG contents of hMSC chondrogenic pellets further support the pellet area findings. Positive/red staining on Safranin O-Fast green stain indicate cartilageneous ECM development and hence an indicator of chondrogenesis (57). While all the hMSC pellets from the non-inflammatory cytokine stimulated environment showed positive Safrainin O-Fast green staining, the AAV-GFP and AAV-hIRAP transduced pellets had much less red staining than the untransduced control pellet. Among the pellets that were stimulated with IL-1β, AAV-hIRAP transduced pellet had the reddest staining. This general pattern was true for the GAG content quantification as well, with AAV-hIRAP pellets performing worst in non-inflammatory environment but best in the inflammatory environment. Of note, the inhibitory effect of AAV-GFP transduction on chondrogenesis compared to untransduced control was no longer appreciable in GAG content measurement.

The effect of hIRAP on hMSC chondrogenesis is unique in that it exerts inhibitory effects on chondrogenic differentiation in normal settings but protective effects in an inflammatory environment. A disease-regulated transgene expression system in this case would be beneficial with added measures of safety. A number of studies have investigated the development and characterization of the inflammation-inducible transgene promoters (177-179). These systems would allow expression of IRAP only when it is needed to exert protective effects while limiting its inhibitory effect on chondrogenesis.

## 6.5 CONCLUSIONS

In conclusion, this study supports the use of AAV-mediated gene therapy to enhance the chondrogenic potential of hMSCs, and shows that anti-inflammatory molecules like IRAP and TGF-$\beta_1$ blunts the cytokine-mediated inhibition of hMSC chondrogenesis. Use of this AAV gene therapy strategy to achieve localized and sustained expression of therapeutic factors from MSC pellets itself has a great promise for cartilage tissue engineering. The study also highlights the importance of adding the catabolic mediator inhibition in the strategy for MSC chondrogenesis. These results have implications for therapy design in terms of the choice of anti-inflammatory molecule, as well as the control of transgene expression. Overall, AAV is a promising gene transfer vehicle to deliver anti-catabolic bioactive molecules to hMSCs undergoing chondrogenic differentiation and its application to improve hMSC-mediated articular cartilage restoration should be further investigated.

# 7.0 OVERALL CONCLUSIONS

Osteoarthritis (OA) affects nearly 27 million people (5) and costs almost $128 billion per year in medical care and indirect expenses in the US alone (79). However, despite its prevalence and morbidity, effective disease modifying treatments are still lacking. Articular cartilage has poor regenerative potential. Therefore, strategies to improve cartilage regeneration have a strong potential to reduce the disease burden of OA. *In vitro* and *in vivo* studies support the use of mesenchymal stem cells (MSCs) to improve cartilage regeneration. A tissue engineering approach, with the use of mesenchymal stem cells, bioscaffolds, and growth factors, is a promising therapeutic strategy against articular joint pathologies. However, successful intra-articular delivery of therapeutic factors is limited due to their short half-lives, costly purification process, and need to administer supra-physiological doses and/or multiple delivery interventions. Adeno-associated viruses (AAVs) are a novel vector construct for gene therapy strategies that would allow the production of therapeutic proteins *in situ*. Here, we investigated various AAV-administration approaches and therapeutic genes to test the central hypothesis that modulation of various anabolic and catabolic factors involved in MSC chondrogenesis via AAV will enhance the outcomes of joint restoration.

In the first study presented in Chapter 2, AAV2 was delivered by a single intra-articular injection to an intact rat knee joint. This lead to persistent and stable transgene expression mainly in the intra-articular soft tissues, with limited expression in chondrocytes. Oral administration of

doxycycline following an intra-articular injection of an inducible AAV2 vector permitted external regulation of *in vivo* transgene expression. This regulation was possible not only immediately after AAV injection, but also a year later.

As intact joints are unlikely to require AAV intervention, characterization of AAV-mediated transgene expression in joint injury models was presented in a follow up study in Chapter 3. AAV transgene expression was again localized to the intra-articular soft tissues of the uninjured joints as well as the injured joints when AAV was injected pre-injury. On the other hand, AAV transduced few articular chondrocytes within the cartilage matrix when injected following injuries, as the cartilage matrix injury may have facilitated entry of more AAV into the cartilage. These data supports use of AAV therapy in injured joints for cartilage repair/protection. Different localization of transgene expression can further be used to tailor joint restoration strategies. The post-injury AAV injection method can be used for genes that need to directly target articular chondrocytes or cartilage repair cells. Alternatively, pre-injury AAV injection method can be beneficial for delivery of gene that to soft-tissues, from which the bioactive molecules would be secreted at high levels to act upon the articular cartilage.

For both studies in intact and injured joints, external control of intra-articular transgene expression was achieved using oral doxycycline. This greatly adds to the clinical utility of AAV as a treatment strategy for joint diseases. Doxycycline was further characterized for its effect on MSC chondrogenesis and cartilage repair in Chapter 4. There was a significant inhibition of MMP-13 expression in hMSC chondrogenic pellets cultured in the presence of doxycycline, leading to larger pellet size due to increased collagen-II retention. Oral administration of doxycycline in rats with osteochondral defects also lead to downregulation of MMP-13 expression and gross improvement of the cartilage repair tissues. Therefore, doxycycline can not

only be used as an inductive agent for external control of AAV-mediated transgene expression, it can also exert intrinsic beneficial effect on cartilage repair.

In the next part of the study in Chapter 5, we investigated and optimized fibrin glue (FG) as a potential AAV-releasing bioscaffold for *in situ* gene delivery. Diluted FG scaffolds had larger pores and thinner fibers, with enhanced release of AAV particles. More AAV was released from diluted FGs, which in turn transduced more target cells. With respect to cartilage tissue engineering applications, AAV-TGF-$\beta_1$ from diluted FG released and transduced more hMSCs, which produced more bioactive TGF-$\beta_1$, and resulted in higher upregulation of cartilage-specific genes than AAV-TGF-$\beta_1$ from undiluted FG. Hence, implantation of bioactive AAV-embedded dilute FG scaffolds has stronger potential to improve articular cartilage regeneration.

As the final part of the study, presented in Chapter 6, two bioactive therapeutic AAVs were explored for their potential to enhance hMSC chondrogenic differentiation in an environment that mimics the *in vivo* cartilage repair setting. AAV-IRAP transduction of hMSCs successfully blunted the inflammatory cytokine-mediated inhibition of hMSC chondrogenesis. However, AAV-TGF-$\beta_1$ transduction of hMSCs did not result in successful chondrogenesis. The study also highlighted that a therapeutic molecule may exert different effects depending on the inflammatory status of the chondrogenic environment. AAV-IRAP-transduced pellets performed the best in an inflammatory setting; however, they performed the worst in non-inflammatory control environment.

Instead of focusing on optimizing individual components of tissue engineering strategy, the fundamental focus of the current study was the potential for clinical translation. Therefore, we explored molecules, scaffolds, and cells that are already Food and Drug Administration (FDA)-approved, in clinical trials, or in clinical practice (54, 180). Thus, we hope our studies on

AAV serotype 2, doxycycline, FG, TGF-$\beta_1$ and IRAP, can accelerate the transition of basic science research into human clinical applications.

In conclusion, various aspects of AAV-mediated joint restoration approaches were investigated, from characterization of AAV delivery by direct injection or with the use of FG, to therapeutic applications with doxycycline, AAV-IRAP, and AAV-TGF-$\beta_1$. These results support continued investigations of therapeutic potential of AAV for safe, localized, and controlled delivery of bioactive substances to promote joint restoration, which may delay/prevent the onset of debilitating osteoarthritis.

# APPENDIX A

## CLINICAL AND BASIC SCIENCE OF CARTILAGE INJURY AND ARTHRITIS IN THE FOOTBALL (SOCCER) ATHLETE

Joint injuries are very common in the athletic population, especially professional soccer players, with an incidence of 10 to 35.5 injuries per 1,000 hours. Most soccer-related joint injuries occur in the lower extremities, with 16% to 46% occurring in the knee and 17% to 40% occurring in the ankle. Because of the limited healing capacity of cartilage and other intra-articular soft tissue structures, such as anterior cruciate ligament (ACL) and meniscus, joint injuries often lead to the development of early disabling osteoarthritis. Osteoarthritis in soccer players is 5 to 12 times more frequent than in the general population, and diagnosed 4 to 5 years earlier. It remains a major cause of disability from this sport. This review focuses on the epidemiology of soccer-related joint injuries and subsequent development of osteoarthritis in the hip, knee, and ankle joints. As well, two different pathways for pathogenesis are described: 1) primary osteoarthritis via direct trauma to the articular cartilage, and 2) secondary osteoarthritis that occurs indirectly through injury to the soft tissue structures that subsequently result in articular cartilage degeneration and loss.

## A.1 SOCCER AND JOINT INJURIES

Soccer is the most popular sport worldwide, with more than 240 million players overall, with 200,000 being professional/elite athletes (181, 182). However, as it is a high-speed contact sport with the highest intensity of joint impact and torsional loading, soccer is a sport that puts maximal demands on the joints (183). There is an incidence of 10 to 35.5 injuries per 1,000 training/playing hours (182, 184-186), with risk of injury during a match greater than that during training (187-190). This injury incidence is around 1,000 times higher than for high-risk industrial occupations (30, 190-193). Soccer, therefore, is estimated to be responsible for the majority of athletic injuries in Europe (185). Participation at a professional/elite level and/or more game hours can further increase the risk and severity of injuries (7, 29, 30, 181, 186, 187, 191, 194-199). Most soccer injuries occur in the lower extremities (52 – 95%), with the knee (16 – 46%) and the ankle (17 – 40%) being most prevalent (181, 185, 189, 195-198, 200-205). The subsequent risk of early development of osteoarthritis (OA) is also expected to be high, and OA has been reported to be the major chronic injury suffered by professional soccer players (206).

## A.2 EPIDEMIOLOGY OF SOCCER AND OSTEOARTHRITIS

The studies on OA and its relationship to soccer have been variable in terms of joint location, age groups, and outcome measures. Among former professional soccer players, 32% to 49% were medically diagnosed with OA (29, 193), with the knee being affected most frequently, followed by the ankle and hip (195). The prevalence of OA is greater in players who had retired due to

injury than those who had retired for other reasons (195). Soccer players had an increased odds ratio of 2.10 for hospital admissions, likely for total joint arthroplasty, for OA of the hip, knee, and ankle (29). Their mean age at first admission was also earlier at 56.2 years versus 61.2 years in controls. When the locations of the OA were separated, 8 incidences were for the hip, 5 for the knee, and 2 for the ankle. Hence, admissions for OA of the hip and knee were more common than for OA of the ankle.

### A.2.1 Ankle osteoarthritis in soccer

Ankle sprains are common soccer injuries and are generally thought to be benign. However, studies report persistent signs and symptoms for months to years in 59% to 100% of injured soccer athletes (207-209). Soccer was also the sport that most frequently gave rise to ankle injuries that caused post-traumatic ankle arthritis (210), with one study quoting 33% of injured ankles developing radiographic signs of arthritis after 25 years (194). This risk of developing arthritis was greater than that compared to the non-injured soccer players and age-matched general population controls. On the other hand, another study reported only 1 1.6% overall incidence of ankle osteoarthrosis in soccer players, when the definition of ankle OA was strictly narrowed to be a loss of joint space and formation of new bone at the articular surface via radiography (207).

### A.2.2 Knee osteoarthritis in soccer

Among former professional soccer players, the radiographic signs of knee OA in soccer players increased with age in a greater percentage than in the general public (211). Radiographic signs of

knee arthritis were present in 15.5% to 63% of injured knees (30, 194, 211, 212); however, the rate of clinical symptoms was significantly less. The prevalence of radiographic signs of knee OA was also greater among elite soccer players compared to controls and non-elite players (30). Thus, the authors concluded that soccer in associated with an increased risk of knee OA, especially at an elite level. Soccer players were also younger when they were diagnosed with knee OA. However, there was no difference in knee OA risk between the non-elite and controls when soccer players with known knee damage were excluded from the analysis.

Among patients with radiographic signs of knee OA, soccer was one of the sports that was significantly related to knee OA among men (213). This increased risk of knee OA with soccer remained after adjusting for body mass index (BMI), heredity, smoking, and occupation, but not after adjusting for previous knee injuries. Similarly, when patients undergoing total knee replacement were examined, there was an increased relative risk of severe knee OA among men aged between 55 and 65 years who were highly exposed to soccer (214).

On the other hand, some studies showed no difference in the frequency of radiograph-confirmed knee OA between former elite soccer players and controls (205, 215). Paradoxically, subjects having symptomatic knee OA were more frequent in the control group than in the former soccer player group, despite the more severe radiological structural damages in the latter (205).

### A.2.3 Hip osteoarthritis in soccer

In addition to the ankle and the knee, many studies report a higher incidence of hip OA in former soccer players compared to age-matched controls (191, 215, 216). The prevalence of hip OA between these two groups was significantly different, with an odds ratio of 10.2 (216). It was

also determined that hip OA in former elite soccer players was three times more common compared to non-elite players (191). Soccer players were diagnosed with hip OA at a younger age, similar to the knee OA findings. Among men who recently received a prosthesis due to severe idiopathic hip osteoarthrosis, there was an increased risk among men with medium and high exposure to soccer (11). Nonetheless, soccer was not one of the most hazardous sports, which included track and field sports and racket sports.

### A.2.4 Summary

Studies have variable findings, primarily due to different methodologies used; the outcome definition and criteria were rarely consistent across studies. Structural outcomes, such as radiographic changes, do not correlate well with patient-relevant aspects, such as pain and function (17). However, long-term soccer training/playing seems to increase the risk for early development of OA in the lower extremities, and this risk is higher in professional players.

## A.3 PATHOGENESIS OF SOCCER-RELATED OSTEOARTHRITIS

The most common soccer injuries are sprains and strains affecting mainly the ankle and knee joints. A single game of soccer has not been shown to directly result in increased cartilage breakdown products (217); however, soccer, may increase the risk for OA in two different ways: 1) directly by high loading on the articular cartilage that leads to primary OA and 2) indirectly by damaging the extra-cartilage soft tissue structures within the joint that will subsequently lead to

joint instability and secondary OA (206). The intensity and duration of a sporting activity increase the occurrence of arthritic impairment (205).

### A.3.1 Primary osteoarthritis

The articular cartilage surface can be damaged through sports participation via a single or repetitive impact or torsional loadings. The hip and the knee are the two main locations that many develop OA due to traumatic joint loading (206, 218). Direct acute trauma with an osteochondral impact may induce progressive cartilage damage and ultimately lead to OA (205). Some studies that reported an increased risk of former elite soccer players to develop hip OA also postulated that compression of the joint surface and sudden shock to the joints can cause cartilage degeneration (191, 216).

Potential mechanisms for the rapid progression of OA after such an injury are extensively studied in both *in vitro* and *in vivo* settings, and studies have shown that matrix degradation, chondrocyte death, and/or abolishment of anabolic functions occur after impact to articular cartilage. Chondrocyte death leads to biochemical changes of the extracellular matrix and weakening of its biomechanical properties. *In vitro* studies on human cartilage explants have also shown significantly increased glycosaminoglycan (GAG) breakdown and release from the injured versus unloaded intact cartilages during 0 to 3 days post-injury (219, 220). Since the mechanical properties of articular cartilage are largely defined by the GAG content, GAG loss is both a sign and stimulator of deterioration of load-bearing cartilage function. Chondrocyte apoptosis rate in the human explants study also correlated with the GAG findings, with significantly higher apoptosis in the loaded (34%) versus control explants at 96 hours post-injury (219).

### A.3.2 Secondary osteoarthritis

Indirect cartilage injury and subsequent arthritis development due to joint instability induced by damaging the extra-cartilage soft tissue structures that leads to chronic joint injury is a common soccer-related pathological process for the knee and ankle joints. Pathologic changes in all joint components, not just the cartilage, are an integral part of OA.

#### A.3.2.1 Ankle

When the mechanism of injury was investigated, 49.3% to 55% of all ankle sprains occurred during athletic activity, with soccer being one of the most common athletic activities (210). Most ankle sprains involve the lateral ligament complex of the ankle joint (194, 208). Post-traumatic OA of the ankle accounts for more than 70% of ankle arthritis (210). The overall mean latency time for the development of ligamentous post-traumatic ankle OA is 34.3 years, with a range of 6 to 57 years (210). There was a significant difference between the patients with a single severe ankle sprain and with recurrent ankle springs, with longer latency time with the latter group.

#### A.3.2.2 Knee

The knee anterior cruciate ligament (ACL) and menisci injuries are common in the general population and in soccer players. Studies report 24% to 40% and 21% to 31% of soccer injuries in the knee joint were ligamentous and meniscal injuries, respectively (29, 185, 192, 197, 200). Injuries to the ACL and menisci are believed to be the main reason for the increased risk of knee OA in soccer players (221). Both ACL and menisci injuries have been shown to be followed by arthritic changes of the knees (29). In addition to the initial high force that damages intra-articular structures involved in the trauma (30), the ACL and menisci disruptions initiate a

cascade of pathogenic processes in the acute phase that can lead to the development of OA in itself (17). There are also findings of greatly increased concentrations of markers of cartilage matrix metabolism in joint fluid in connection with trauma (222). In addition to acute effects, the lack of a functionally normal ACL or menisci leads to chronic changes in the static and dynamic loading of the knee and increases forces on the cartilage and other joint structures.

#### A.3.2.2.1 ACL injury and osteoarthritis in soccer players

The ACL is the most commonly disrupted knee ligament (17, 222). Nearly 40% of all soccer-related knee injuries are ACL injuries (222), and a risk increase has been estimated at 100 to 1,000 in professional soccer (195, 223). A complete ACL tear usually causes a long layoff from soccer and may even end the athletic career (224). Soccer athletes sustain more ACL injuries than basketball players when compared by sex (225). Nonetheless, isolated ACL ruptures are uncommon due to the high impact of the trauma, and it is often associated with injuries to other intra-articular structures. A meniscal injury most frequently accompanies an ACL injury: it is associated with 50% to 75% of all acute ACL cases (183).

The mechanism responsible for cartilage degeneration following ACL injury is unclear. Biomechanical instability of the joint does not appear to be the only factor, and additional biochemical factors, such as inflammatory cytokines from synovitis, are also important. Dogs that underwent surgical transection of the ACL had significant elevation of cartilage breakdown products, collagenase-generated cleavage epitope of type II collagen, and cross-linked peptides from the C-telopeptide domain of type II collagen in their joint fluid at 3 and 12 weeks post-operatively (226). The long-term clinical consequences of ACL rupture in soccer players have also been well studied: soccer players with an ACL tear are also more likely to develop knee OA than those players with intact ACL (183). At 12 to 14 years after an ACL tear, 75% of soccer

athletes had significant symptoms, and 41% to 77% had radiographic knee OA (221, 227). Additional meniscus injury requiring surgery was the most significant factor that may strongly influence the long-term symptoms and OA prevalence after ACL injury (227).

The effect of ACL reconstruction on the subsequent development of knee OA has been controversial. Most studies report that the increased risk of development of OA following ACL injury remains unchanged regardless of the surgical ACL repair status (17, 221). When the clinical and radiographic outcomes of surgical repair or non-surgical ACL treatments were compared, it was reported that an ACL reconstruction itself did not reduce the risk of OA (32). ACL repair also did not increase the subjective symptomatic scores; however, it did decrease instability problems. In conclusion, although ACL reconstruction may facilitate restoring the kinematics of the joint, it does not make the knee normal (17). There is a lack of evidence to support a protective role of ACL reconstruction surgery against OA, both in athletes and in the general population. Hence, the ACL-injured knee, whether it is repaired or not, will be subjected to abnormal loading over time, significantly increasing the risk of OA.

#### A.3.2.2.2 Meniscus injury and osteoarthritis in soccer players

Sports-related acute injuries to the menisci are common; however, the incidence of meniscus injuries in soccer is not as clearly described as the incidence of ACL injuries (206). ACL injuries, which are common in soccer, are associated with a meniscus tear in up to 75% of cases (183). As well, some investigators say that soccer is first and foremost a hazard to the menisci since a blow to the knee while weightbearing is more likely to cause damage to the menisci than to the ligaments (197). In a study on former elite soccer players compared to age-matched controls, 14% of the former players had meniscal injuries resulting in meniscectomy versus 2% in the control group (30). In another study, of the 33% of sports-related meniscal injuries resulting in

meniscectomy, 5% were soccer-related (228). Finally, in a study comparing meniscal tear patients to controls, meniscal tear and knee cartilage injuries were strongly associated with participation in sports, especially soccer, during the 12-months preceding the onset of symptoms (229).

One of the treatments available for meniscal injury is total meniscectomy. However, this results in increased load stresses on the underlying articular cartilage and development of knee OA. The degree of OA has also been shown to be directly proportional to the amount of meniscus removed (230). Hence, meniscal tears are a potent risk factor for the development of knee OA, regardless of the surgical status (192). However, as stressed above, meniscus lesion combined with ACL tear are associated with the greatest risk of OA development (194). In comparison to ACL patients, patients with isolated meniscus injury were about 10 years older when they had a comparable stage of OA (222).

About 50% of meniscal injury patients with a partial or total meniscectomy have both symptomatic and radiographic signs of OA of the knee 5 to 20 years after injury (222, 230-233). This represents an odds ratio of about 10 (17) and relative risk of 14.0 (233) for the presence of the more advanced radiographic changes compared with an age- and sex-matched control group without known knee injury. Among former soccer players, all players who had a meniscectomy presented radiographic signs of OA 10 to 20 years after surgery, compared to 40% in players who had not undergone meniscectomy (211).

## A.4 CONLUSIONS

Joint injuries, including ligament, meniscal, and cartilage injuries, are common in sports, especially in soccer. These soccer-related injuries are most common in the lower extremities, involving the knee, hip, and ankle. Subsequent cartilage damage of the affected joints is due to primary joint impact and/or secondary to the extra-cartilage soft tissue injuries that lead to joint instability and degeneration of articular cartilage. Although primary osteoarthritis from joint impact is frequently responsible for the development of osteoarthritis in the hip and knee, secondary arthritis associated with ligamentous injury occurs primarily in the ankle and knee. The anterior cruciate ligament and menisci are the two intra-articular soft tissues that most often get injured during soccer and also play a critical role in OA development. Unfortunately, currently available treatment strategies, surgical or conservative, are inadequate to prevent the development of OA. Hence, there is a strong need for the development of molecular, biological, and mechanical interventions to delay or prevent the onset of post-injury OA.

## BIBLIOGRAPHY


1. Imeokparia, R.L., Barrett, J.P., Arrieta, M.I., Leaverton, P.E., Wilson, A.A., Hall, B.J., et al., Physical activity as a risk factor for osteoarthritis of the knee. *Annals of Epidemiology*, 1994. **4**(3): p. 221-230.

2. Molloy, M.G. and Molloy, C.B., Contact sport and osteoarthritis. *British Journal of Sports Medicine*, 2011. **45**(4): p. 275-277.

3. Englund, M., Guermazi, A., Roemer, F.W., Aliabadi, P., Yang, M., Lewis, C.E., et al., Meniscal tear in knees without surgery and the development of radiographic osteoarthritis among middle-aged and elderly persons: The multicenter osteoarthritis study. *Arthritis & Rheumatism*, 2009. **60**(3): p. 831-839.

4. *Osteoarthritis Fact Sheet*, in *News from the Arthritis Foundation*. 2008, Arthritis Foundation.

5. Lawrence, R.C., Felson, D.T., Helmick, C.G., Arnold, L.M., Choi, H., Deyo, R.A., et al., Estimates of the Prevalence of Arthritis and Other Rheumatic Conditions in the United States: Part II. *Arthritis & Rheumatism*, 2008. **58**(1): p. 26-35.

6. Buckwalter, J.A., Sports, Joint Injury, and Posttraumatic Osteoarthritis. *Journal of Orthopaedic & Sports Physical Therapy*, 2003. **33**(10): p. 578-588.

7. Saxon, L., Finch, C., and Bass, S., Sports participation, sports injuries and osteoarthritis: Implications for prevention. *Sports Medicine*, 1999. **28**(2): p. 123-135.

8. Buckwalter, J.A., Saltzman, C., and Brown, T., The Impact of Osteoarthritis: Implications for Research. *Clinical Orthopaedics and Related Research*, 2004. **427S**: p. S6–S15.

9. Hootman, J.M. and Helmick, C.G., Projections of US Prevalence of Arthritis and Associated Activity Limitations. *Arthritis & Rheumatism*, 2006. **54**(1): p. 226-229.

10. Buckwalter, J.A. and Martin, J.A., Sports and osteoarthritis. *Current Opinion in Rheumatology*, 2004. **16**(5): p. 634-639.

11. Vingård, E., Alfredsson, L., Goldie, I., and Hogstedt, C., Sports and osteoarthrosis of the hip. *The American Journal of Sports Medicine*, 1993. **21**(2): p. 195-200.

12. Buckwalter, J.A. and Lane, N.E., Athletics and Osteoarthritis. *The American Journal of Sports Medicine*, 1997. **25**(6): p. 873-881.

13. Koelling, S., Kruegel, J., Irmer, M., Path, J.R., Sadowski, B., Miro, X., et al., Migratory Chondrogenic Progenitor Cells from Repair Tissue during the Later Stages of Human Osteoarthritis. *Cell Stem Cell*, 2009. **4**(4): p. 324-335.

14. Khan, I.M., Williams, R., and Archer, C.W., One Flew Over the Progenitor's Nest: Migratory Cells Find a Home in Osteoarthritic Cartilage. *Cell Stem Cell*, 2009. **4**(4): p. 282-284.

15. Vankemmelbeke, M.N., Holen, I., Wilson, A.G., Ilic, M.Z., Handley, C.J., Kelner, G.S., et al., Expression and Activity of ADAMTS-5 in Synovium. *European Journal of Biochemistry*, 2001. **268**(5): p. 1259-1268.

16. Cucchiarini, M., Ekici, M., Schetting, S., Kohn, D., and Madry, H., Metabolic activities and chondrogenic differentiation of human mesenchymal stem cells following recombinant adeno-associated virus-mediated gene transfer and overexpression of fibroblast growth factor 2. *Tissue Eng Part A*, 2011. **17**(15-16): p. 1921-33.

17. Lohmander, L.S., Englund, P.M., Dahl, L.L., and Roos, E.M., The long-term consequence of anterior cruciate ligament and meniscus injuries. *The American Journal of Sports Medicine*, 2007. **35**(10): p. 1756-1769.

18. Fan, H., Liu, H., Toh, S.L., and Goh, J.C.H., Anterior cruciate ligament regeneration using mesenchymal stem cells and silk scaffold in large animal model. *Biomaterials*, 2009. **30**(28): p. 4967-4977.

19. Danylchuk, K.D., Finlay, J.B., and Krcek, J.P., Microstructural organization of human and bovine cruciate ligaments. *Clin Orthop Relat Res*, 1978(131): p. 294-8.

20. Amiel, D., Frank, C., Harwood, F., Fronek, J., and Akeson, W., Tendons and ligaments: A morphological and biochemical comparison. *Journal of Orthopaedic Research*, 1983. **1**(3): p. 257-265.

21. Yasuda, K., van Eck, C.F., Hoshino, Y., Fu, F.H., and Tashman, S., Anatomic single- and double-bundle anterior cruciate ligament reconstruction, part 1: Basic science. *Am J Sports Med*, 2011. **39**(8): p. 1789-99.

22. Yates, E.W., Rupani, A., Foley, G.T., Khan, W.S., Cartmell, S., and Anand, S.J., Ligament tissue engineering and its potential role in anterior cruciate ligament reconstruction. *Stem Cells Int*, 2012. **2012**: p. 438125.

23. Messner, K. and Gao, J., The menisci of the knee joint. Anatomical and functional characteristics, and a rationale for clinical treatment. *Journal of Anatomy*, 1998. **193**(2): p. 161-178.

24. Hunter, D.J., Zhang, Y.Q., Niu, J.B., Tu, X., Amin, S., Clancy, M., et al., The association of meniscal pathologic changes with cartilage loss in symptomatic knee osteoarthritis. *Arthritis & Rheumatism*, 2006. **54**(3): p. 795-801.

25. Hellio Le Graverand, M.P., Vignon, E., Otterness, I.G., and Hart, D.A., Early changes in lapine menisci during osteoarthritis development Part II: Molecular alterations. *Osteoarthritis and Cartilage*, 2001. **9**(1): p. 65-72.

26. LaVallie, E.R., Chockalingam, P.S., Collins-Racie, L.A., Freeman, B.A., Keohan, C.C., Leitges, M., et al., Protein Kinase Czeta Is Up-regulated in Osteoarthritic Cartilage and Is Required for Activation of NF-kappaB by Tumor Necrosis Factor and Interleukin-1 in Articular Chondrocytes. *Journal of Biological Chemistry*, 2006. **281**(34): p. 24124-24137.

27. Price, J.S., Waters, J.G., Darrah, C., Pennington, C., Edwards, D.R., Donell, S.T., et al., The Role of Chondrocyte Senescence in Osteoarthritis. *Aging Cell*, 2002. **1**(1): p. 57-65.

28. Bayliss, M.T., Hutton, S., Hayward, J., and Maciewicz, R.A., Distribution of Aggrecanase (ADAMts 4/5) Cleavage Products in Normal and Osteoarthritic Human Articular Cartilage: The Influence of Age, Topography and Zone of Tissue. *Osteoarthritis and Cartilage*, 2001. **9**(6): p. 553-560.

29. Kujala, U.M., Kaprio, J., and Sarno, S., Osteoarthritis of weight bearing joints of lower limbs in former elite male athletes. *BMJ*, 1994. **308**(6923): p. 231-234.

30. Roos, H., Lindberg, H., Gärdsell, P., Lohmander, L.S., and Wingstrand, H., The prevalence of gonarthrosis and its relation to meniscectomy in former soccer players. *The American Journal of Sports Medicine*, 1994. **22**(2): p. 219-222.

31. Dunn, W.R., Lyman, S., Lincoln, A.E., Amoroso, P.J., Wickiewicz, T., and Marx, R.G., The effect of anterior cruciate ligament reconstruction on the risk of knee reinjury. *The American Journal of Sports Medicine*, 2004. **32**(8): p. 1906-1914.

32. Meunier, A., Odensten, M., and Good, L., Long-term results after primary repair or non-surgical treatment of anterior cruciate ligament rupture: a randomized study with a 15-year follow-up. *Scandinavian Journal of Medicine & Science in Sports*, 2007. **17**(3): p. 230-237.

33. Chu, C.R., Convery, F.R., Akeson, W.H., Meyers, M., and Amiel, D., Articular cartilage transplantation. Clinical results in the knee. *Clin Orthop Relat Res*, 1999(360): p. 159-68.

34. Kramer, J., Bohrnsen, F., Lindner, U., Behrens, P., Schlenke, P., and Rohwedel, J., In vivo matrix-guided human mesenchymal stem cells. *Cell Mol Life Sci*, 2006. **63**(5): p. 616-26.

35. Steadman, J.R., Briggs, K.K., Rodrigo, J.J., Kocher, M.S., Gill, T.J., and Rodkey, W.G., Outcomes of microfracture for traumatic chondral defects of the knee: average 11-year follow-up. *Arthroscopy*, 2003. **19**(5): p. 477-84.

36. Krishnan, S.P., Skinner, J.A., Carrington, R.W., Flanagan, A.M., Briggs, T.W., and Bentley, G., Collagen-covered autologous chondrocyte implantation for osteochondritis dissecans of the knee: two- to seven-year results. *J Bone Joint Surg Br*, 2006. **88**(2): p. 203-5.

37. Wakitani, S., Imoto, K., Yamamoto, T., Saito, M., Murata, N., and Yoneda, M., Human autologous culture expanded bone marrow mesenchymal cell transplantation for repair of cartilage defects in osteoarthritic knees. *Osteoarthritis Cartilage*, 2002. **10**(3): p. 199-206.

38. Jakobsen, R.B., Engebretsen, L., and Slauterbeck, J.R., An analysis of the quality of cartilage repair studies. *J Bone Joint Surg Am*, 2005. **87**(10): p. 2232-9.

39. Magnussen, R.A., Dunn, W.R., Carey, J.L., and Spindler, K.P., Treatment of focal articular cartilage defects in the knee: a systematic review. *Clin Orthop Relat Res*, 2008. **466**(4): p. 952-62.

40. Nishikawa, M. and Huang, L., Nonviral vectors in the new millennium: delivery barriers in gene transfer. *Hum Gene Ther*, 2001. **12**(8): p. 861-70.

41. Loser, P., Huser, A., Hillgenberg, M., Kumin, D., Both, G.W., and Hofmann, C., Advances in the development of non-human viral DNA-vectors for gene delivery. *Curr Gene Ther*, 2002. **2**(2): p. 161-71.

42. Pagnotto, M.R., Wang, Z., Karpie, J.C., Ferretti, M., Xiao, X., and Chu, C.R., Adeno-associated viral gene transfer of transforming growth factor-beta 1 to human mesenchymal stem cells improves cartilage repair. *Gene Therapy*, 2007. **14**(10): p. 804-813.

43. Caplan, A.I., Mesenchymal stem cells and gene therapy. *Clin Orthop Relat Res*, 2000(379 Suppl): p. S67-70.

44. Goater, J., Muller, R., Kollias, G., Firestein, G.S., Sanz, I., O'Keefe, R.J., et al., Empirical advantages of adeno associated viral vectors in vivo gene therapy for arthritis. *Journal of Rheumatology*, 2000. **27**(4): p. 983-9.

45. Pan, R.Y., Chen, S.L., Xiao, X., Liu, D.W., Peng, H.J., and Tsao, Y.P., Therapy and prevention of arthritis by recombinant adeno-associated virus vector with delivery of interleukin-1 receptor antagonist. *Arthritis and Rheumatism*, 2000. **43**(2): p. 289-97.

46. Pan, R.Y., Xiao, X., Chen, S.L., Li, J., Lin, L.C., Wang, H.J., et al., Disease-inducible transgene expression from a recombinant adeno-associated virus vector in a rat arthritis model. *J Virol*, 1999. **73**(4): p. 3410-7.

47. Payne, K.A., Lee, H.H., Haleem, A.M., Martins, C., Yuan, Z., Qiao, C., et al., Single intra-articular injection of adeno-associated virus results in stable and controllable in vivo transgene expression in normal rat knees. *Osteoarthritis Cartilage*, 2011. **19**(8): p. 1058-65.

48. Mueller, C. and Flotte, T.R., Clinical gene therapy using recombinant adeno-associated virus vectors. *Gene Ther*, 2008. **15**(11): p. 858-63.

49. Gelse, K., von der Mark, K., Aigner, T., Park, J., and Schneider, H., Articular cartilage repair by gene therapy using growth factor-producing mesenchymal cells. *Arthritis Rheum*, 2003. **48**(2): p. 430-41.

50. Madry, H., Kaul, G., Cucchiarini, M., Stein, U., Zurakowski, D., Remberger, K., et al., Enhanced repair of articular cartilage defects in vivo by transplanted chondrocytes overexpressing insulin-like growth factor I (IGF-I). *Gene Ther*, 2005. **12**(15): p. 1171-9.

51. Capito, R.M. and Spector, M., Collagen scaffolds for nonviral IGF-1 gene delivery in articular cartilage tissue engineering. *Gene Ther*, 2007. **14**(9): p. 721-32.

52. Guo, T., Zhao, J., Chang, J., Ding, Z., Hong, H., Chen, J., et al., Porous chitosan-gelatin scaffold containing plasmid DNA encoding transforming growth factor-beta1 for chondrocytes proliferation. *Biomaterials*, 2006. **27**(7): p. 1095-103.

53. Jang, J.H., Houchin, T.L., and Shea, L.D., Gene delivery from polymer scaffolds for tissue engineering. *Expert Rev Med Devices*, 2004. **1**(1): p. 127-38.

54. Spotnitz, W.D., Fibrin sealant: past, present, and future: a brief review. *World J Surg*, 2010. **34**(4): p. 632-4.

55. Breen, A., O'Brien, T., and Pandit, A., Fibrin as a delivery system for therapeutic drugs and biomolecules. *Tissue Eng Part B Rev*, 2009. **15**(2): p. 201-14.

56. Rubak, J.M., Reconstruction of articular cartilage defects with free periosteal grafts. An experimental study. *Acta Orthop Scand*, 1982. **53**(2): p. 175-80.

57. Payne, K.A., Didiano, D.M., and Chu, C.R., Donor sex and age influence the chondrogenic potential of human femoral bone marrow stem cells. *Osteoarthritis and Cartilage*, 2010. **18**(5): p. 705-713.

58. Estes, B.T., Diekman, B.O., Gimble, J.M., and Guilak, F., Isolation of adipose-derived stem cells and their induction to a chondrogenic phenotype. *Nat Protoc*, 2010. **5**(7): p. 1294-311.

59. Matsumoto, T., Cooper, G.M., Gharaibeh, B., Meszaros, L.B., Li, G., Usas, A., et al., Cartilage repair in a rat model of osteoarthritis through intraarticular transplantation of muscle-derived stem cells expressing bone morphogenetic protein 4 and soluble flt-1. *Arthritis & Rheumatism*, 2009. **60**(5): p. 1390-1405.

60. Piek, E., Heldin, C.-H., and Ten Dijke, P., Specificity, diversity, and regulation in TGF-ß superfamily signaling. *The FASEB Journal*, 1999. **13**(15): p. 2105-2124.

61. Fortier, L., Barker, J., Strauss, E., McCarrel, T., and Cole, B., The Role of Growth Factors in Cartilage Repair. *Clinical Orthopaedics and Related Research®*, 2011: p. 1-10.

62. Puetzer, J.L., Petitte, J.N., and Loboa, E.G., Comparative Review of Growth Factors for Induction of Three-Dimensional In Vitro Chondrogenesis in Human Mesenchymal Stem Cells Isolated from Bone Marrow and Adipose Tissue. *Tissue Engineering Part B: Reviews*, 2010. **16**(4): p. 435-444.

63. Danlin, X., Gechtman, Z.e., Hughes, A., Collins, A., Dodds, R., Xiaoling, C., et al., Potential involvement of BMP receptor type IB activation in a synergistic effect of chondrogenic promotion between rhTGFβ3 and rhGDF5 or rhBMP7 in human mesenchymal stem cells. *Growth Factors*, 2006. **24**(4): p. 268-278.

64. Blaney Davidson, E.N., van der Kraan, P.M., and van den Berg, W.B., TGF-[beta] and osteoarthritis. *Osteoarthritis and Cartilage*, 2007. **15**(6): p. 597-604.

65. Miyamoto, C., Matsumoto, T., Sakimura, K., and Shindo, H., Osteogenic protein-1 with transforming growth factor-β1: potent inducer of chondrogenesis of synovial mesenchymal stem cells in vitro. *Journal of Orthopaedic Science*, 2007. **12**(6): p. 555-561.

66. Mi, Z., Ghivizzani, S., Lechman, E., Glorioso, J., Evans, C., and Robbins, P., Adverse effects of adenovirus-mediated gene transfer of human transforming growth factor beta 1 into rabbit knees. *Arthritis Res Ther*, 2003. **5**(3): p. R132 - R139.

67. Watson, R.S., Gouze, E., Levings, P.P., Bush, M.L., Kay, J.D., Jorgensen, M.S., et al., Gene delivery of TGF-[beta]1 induces arthrofibrosis and chondrometaplasia of synovium in vivo. *Lab Invest*, 2010. **90**(11): p. 1615-1627.

68. Blaney Davidson, E., Vitters, E., van den Berg, W., and van der Kraan, P., TGF beta-induced cartilage repair is maintained but fibrosis is blocked in the presence of Smad7. *Arthritis Research & Therapy*, 2006. **8**(3): p. R65.

69. Scott, I., Midha, A., Rashid, U., Ball, S., Walding, A., Kerry, P., et al., Correlation of gene and mediator expression with clinical endpoints in an acute interleukin-1beta-driven model of joint pathology. *Osteoarthritis Cartilage*, 2009. **17**(6): p. 790-7.

70. Song, R.-H., Tortorella, M., D. , Malfait, A.-M., Alston, J., T. , Yang, Z., Arner, E., C. , et al., Aggrecan Degradation in Human Articular Cartilage Explants is Mediated by Both ADAMTS-4 and ADAMTS-5. *Arthritis & Rheumatism*, 2007. **56**(2): p. 575-585.

71. Wehling, N., Palmer, G.D., Pilapil, C., Liu, F., Wells, J.W., Müller, P.E., et al., Interleukin-1β and tumor necrosis factor α inhibit chondrogenesis by human mesenchymal stem cells through NF-κB–dependent pathways. *Arthritis & Rheumatism*, 2009. **60**(3): p. 801-812.

72. van de Loo, F.A.J. and van den Berg, W.B., Gene therapy for rheumatoid arthritis: Lessons from animal models, including studies on interleukin-4, interleukin-10, and interleukin-1 receptor antagonist as potential disease modulators. *Rheumatic Diseases Clinics of North America*, 2002. **28**(1): p. 127-149.

73. Kay, J.D., Gouze, E., Oligino, T.J., Gouze, J.N., Watson, R.S., Levings, P.P., et al., Intra-articular gene delivery and expression of interleukin-1Ra mediated by self-complementary adeno-associated virus. *Journal of Gene Medicine*, 2009. **11**(7): p. 605-14.

74. Arend, W.P., Malyak, M., Guthridge, C.J., and Gabay, C., Interleukin-1 receptor antagonist: role in biology. *Annu Rev Immunol*, 1998. **16**: p. 27-55.

75. Gafni, Y., Pelled, G., Zilberman, Y., Turgeman, G., Apparailly, F., Yotvat, H., et al., Gene therapy platform for bone regeneration using an exogenously regulated, AAV-2-based gene expression system. *Mol Ther*, 2004. **9**(4): p. 587-95.

76. Gossen, M. and Bujard, H., Tight control of gene expression in mammalian cells by tetracycline-responsive promoters. *Proc Natl Acad Sci U S A*, 1992. **89**(12): p. 5547-51.

77. Rivera, V.M., Gao, G.P., Grant, R.L., Schnell, M.A., Zoltick, P.W., Rozamus, L.W., et al., Long-term pharmacologically regulated expression of erythropoietin in primates following AAV-mediated gene transfer. *Blood*, 2005. **105**(4): p. 1424-30.

78. Roushan, M.R., Amiri, M.J., Janmohammadi, N., Hadad, M.S., Javanian, M., Baiani, M., et al., Comparison of the efficacy of gentamicin for 5 days plus doxycycline for 8 weeks versus streptomycin for 2 weeks plus doxycycline for 45 days in the treatment of human brucellosis: a randomized clinical trial. *J Antimicrob Chemother*, 2010. **65**(5): p. 1028-35.

79. Izal, I., Acosta, C.A., Ripalda, P., Zaratiegui, M., Ruiz, J., and Forriol, F., IGF-1 gene therapy to protect articular cartilage in a rat model of joint damage. *Arch Orthop Trauma Surg*, 2008. **128**(2): p. 239-47.

80. Heldens, G.T., Davidson, E.N., Vitters, E.L., Schreurs, B.W., Piek, E., Berg, W.B., et al., Catabolic factors and osteoarthritis-conditioned medium inhibit chondrogenesis of human mesenchymal stem cells. *Tissue Eng Part A*, 2012. **18**(1-2): p. 45-54.

81. Jotanovic, Z., Mihelic, R., Sestan, B., and Dembic, Z., Role of interleukin-1 inhibitors in osteoarthritis: an evidence-based review. *Drugs Aging*, 2012. **29**(5): p. 343-58.

82. Ye, X. and Yang, D., Recent advances in biological strategies for targeted drug delivery. *Cardiovasc Hematol Disord Drug Targets*, 2009. **9**(3): p. 206-21.

83. Coura, R. and Nardi, N., The state of the art of adeno-associated virus-based vectors in gene therapy. *Virology Journal*, 2007. **4**(1): p. 99.

84. Zincarelli, C., Soltys, S., Rengo, G., and Rabinowitz, J.E., Analysis of AAV Serotypes 1-9 Mediated Gene Expression and Tropism in Mice After Systemic Injection. *Mol Ther*, 2008. **16**(6): p. 1073-1080.

85. Adriaansen, J., Fallaux, F.J., de Cortie, C.J., Vervoordeldonk, M.J., and Tak, P.P., Local delivery of beta interferon using an adeno-associated virus type 5 effectively inhibits adjuvant arthritis in rats. *Journal of General Virology*, 2007. **88**(6): p. 1717-1721.

86. Adriaansen, J., Khoury, M., de Cortie, C.J., Fallaux, F.J., Bigey, P., Scherman, D., et al., Reduction of arthritis following intra-articular administration of an adeno-associated virus serotype 5 expressing a disease-inducible TNF-blocking agent. *Annals of the Rheumatic Diseases*, 2007. **66**(9): p. 1143-1150.

87. Khoury, M., Adriaansen, J., Vervoordeldonk, M.J.B.M., Gould, D., Chernajovsky, Y., Bigey, P., et al., Inflammation-inducible anti-TNF gene expression mediated by intra-articular injection of serotype 5 adeno-associated virus reduces arthritis. *Journal of Gene Medicine*, 2007. **9**(7): p. 596-604.

88. Mease, P.J., Wei, N., Fudman, E.J., Kivitz, A.J., Schechtman, J., Trapp, R.G., et al., Safety, Tolerability, and Clinical Outcomes after Intraarticular Injection of a Recombinant Adeno-associated Vector Containing a Tumor Necrosis Factor Antagonist Gene: Results of a Phase 1/2 Study. *Journal of Rheumatology*, 2010. **37**(4): p. 692-703.

89. Gelse, K., Muhle, C., Franke, O., Park, J., Jehle, M., Durst, K., et al., Cell-based resurfacing of large cartilage defects. *Arthritis and Rheumatism*, 2008. **58**(2): p. 475-488.

90. Hidaka, C., Goodrich, L.R., Chen, C.T., Warren, R.F., Crystal, R.G., and Nixon, A.J., Acceleration of cartilage repair by genetically modified chondrocytes over expressing bone morphogenetic protein-7. *Journal of Orthopaedic Research*, 2003. **21**(4): p. 573-583.

91. Kuroda, R., Usas, A., Kubo, S., Corsi, K., Peng, H.R., Rose, T., et al., Cartilage repair using bone morphogenetic protein 4 and muscle-derived stem cells. *Arthritis and Rheumatism*, 2006. **54**(2): p. 433-442.

92. Mason, J.M., Breitbart, A.S., Barcia, M., Porti, D., Pergolizzi, R.G., and Grande, D.A., Cartilage and bone regeneration using gene-enhanced tissue engineering. *Clinical Orthopaedics and Related Research*, 2000(379): p. S171-S178.

93. Bandara, G., Mueller, G.M., Galealauri, J., Tindal, M.H., Georgescu, H.I., Suchanek, M.K., et al., Intraarticular Expression of Biologically-Active Interleukin-1 Receptor-Antagonist Protein by Ex-Vivo Gene-Transfer. *Proceedings of the National Academy of Sciences of the United States of America*, 1993. **90**(22): p. 10764-10768.

94. Bandara, G., Robbins, P.D., Georgescu, H.I., Mueller, G.M., Glorioso, J.C., and Evans, C.H., Gene-Transfer to Synoviocytes - Prospects for Gene Treatment of Arthritis. *DNA and Cell Biology*, 1992. **11**(3): p. 227-231.

95. Hiraide, A., Yokoo, N., Xin, K.Q., Okuda, K., Mizukami, H., Ozawa, K., et al., Repair of articular cartilage defect by intraarticular administration of basic fibroblast growth factor gene, using adeno-associated virus vector. *Hum Gene Ther*, 2005. **16**(12): p. 1413-21.

96. Hung, G.L., Galea-Lauri, J., Mueller, G.M., Georgescu, H.I., Larkin, L.A., Suchanek, M.K., et al., Suppression of intra-articular responses to interleukin-1 by transfer of the interleukin-1 receptor antagonist gene to synovium. *Gene Therapy*, 1994. **1**(1): p. 64-9.

97. Santangelo, K.S., Baker, S.A., Nuovo, G., Dyce, J., Bartlett, J.S., and Bertone, A.L., Detectable reporter gene expression following transduction of adenovirus and adeno-associated virus serotype 2 vectors within full-thickness osteoarthritic and unaffected canine cartilage in vitro and unaffected guinea pig cartilage in vivo. *J Orthop Res*, 2010. **28**(2): p. 149-55.

98. Ulrich-Vinther, M., Stengaard, C., Schwarz, E.M., Goldring, M.B., and Soballe, K., Adeno-associated vector mediated gene transfer of transforming growth factor-beta1 to normal and osteoarthritic human chondrocytes stimulates cartilage anabolism. *Eur Cell Mater*, 2005. **10**: p. 40-50.

99. Watanabe, S., Imagawa, T., Boivin, G.P., Gao, G., Wilson, J.M., and Hirsch, R., Adeno-associated virus mediates long-term gene transfer and delivery of chondroprotective IL-4 to murine synovium. *Mol Ther*, 2000. **2**(2): p. 147-52.

100. Hadaczek, P., Eberling, J.L., Pivirotto, P., Bringas, J., Forsayeth, J., and Bankiewicz, K.S., Eight years of clinical improvement in MPTP-lesioned primates after gene therapy with AAV2-hAADC. *Mol Ther*, 2010. **18**(8): p. 1458-61.

101. Xiao, X., Li, J., and Samulski, R.J., Production of high-titer recombinant adeno-associated virus vectors in the absence of helper adenovirus. *J Virol*, 1998. **72**(3): p. 2224-32.

102. Goodrich, L.R., Choi, V.W., Carbone, B.A., McIlwraith, C.W., and Samulski, R.J., Ex vivo serotype-specific transduction of equine joint tissue by self-complementary adeno-associated viral vectors. *Hum Gene Ther*, 2009. **20**(12): p. 1697-702.

103. Takahashi, H., Kato, K., Miyake, K., Hirai, Y., Yoshino, S., and Shimada, T., Adeno-associated virus vector-mediated anti-angiogenic gene therapy for collagen-induced arthritis in mice. *Clin Exp Rheumatol*, 2005. **23**(4): p. 455-61.

104. Yokoo, N., Saito, T., Uesugi, M., Kobayashi, N., Xin, K.Q., Okuda, K., et al., Repair of articular cartilage defect by autologous transplantation of basic fibroblast growth factor gene-transduced chondrocytes with adeno-associated virus vector. *Arthritis and Rheumatism*, 2005. **52**(1): p. 164-70.

105. Chu, C.R., Coyle, C.H., Chu, C.T., Szczodry, M., Seshadri, V., Karpie, J.C., et al., In vivo effects of single intra-articular injection of 0.5% bupivacaine on articular cartilage. *J Bone Joint Surg Am*, 2010. **92**(3): p. 599-608.

106. Gouze, E., Gouze, J.N., Palmer, G.D., Pilapil, C., Evans, C.H., and Ghivizzani, S.C., Transgene persistence and cell turnover in the diarthrodial joint: implications for gene therapy of chronic joint diseases. *Mol Ther*, 2007. **15**(6): p. 1114-20.

107. Carlisle, R.C., Benjamin, R., Briggs, S.S., Sumner-Jones, S., McIntosh, J., Gill, D., et al., Coating of adeno-associated virus with reactive polymers can ablate virus tropism, enable

retargeting and provide resistance to neutralising antisera. *Journal of Gene Medicine*, 2008. **10**(4): p. 400-11.

108. Lee, H.H., Haleem, A.M., Yao, V., Li, J., Xiao, X., and Chu, C.R., Release of bioactive adeno-associated virus from fibrin scaffolds: effects of fibrin glue concentrations. *Tissue Eng Part A*, 2011. **17**(15-16): p. 1969-78.

109. Mease, P.J., Hobbs, K., Chalmers, A., El-Gabalawy, H., Bookman, A., Keystone, E., et al., Local delivery of a recombinant adenoassociated vector containing a tumour necrosis factor alpha antagonist gene in inflammatory arthritis: a phase 1 dose-escalation safety and tolerability study. *Annals of the Rheumatic Diseases*, 2009. **68**(8): p. 1247-54.

110. Boutin, S., Monteilhet, V., Veron, P., Leborgne, C., Benveniste, O., Montus, M.F., et al., Prevalence of serum IgG and neutralizing factors against adeno-associated virus (AAV) types 1, 2, 5, 6, 8, and 9 in the healthy population: implications for gene therapy using AAV vectors. *Hum Gene Ther*, 2010. **21**(6): p. 704-12.

111. Moutsatsos, I.K., Turgeman, G., Zhou, S., Kurkalli, B.G., Pelled, G., Tzur, L., et al., Exogenously regulated stem cell-mediated gene therapy for bone regeneration. *Mol Ther*, 2001. **3**(4): p. 449-61.

112. Peng, H., Usas, A., Gearhart, B., Young, B., Olshanski, A., and Huard, J., Development of a self-inactivating tet-on retroviral vector expressing bone morphogenetic protein 4 to achieve regulated bone formation. *Mol Ther*, 2004. **9**(6): p. 885-94.

113. Wubbenhorst, D., Dumler, K., Wagner, B., Wexel, G., Imhoff, A., Gansbacher, B., et al., Tetracycline-regulated bone morphogenetic protein 2 gene expression in lentivirally transduced primary rabbit chondrocytes for treatment of cartilage defects. *Arthritis and Rheumatism*, 2010. **62**(7): p. 2037-46.

114. Zhou, X., Vink, M., Klaver, B., Berkhout, B., and Das, A.T., Optimization of the Tet-On system for regulated gene expression through viral evolution. *Gene Therapy*, 2006. **13**(19): p. 1382-90.

115. Recommendations for the medical management of osteoarthritis of the hip and knee: 2000 update. American College of Rheumatology Subcommittee on Osteoarthritis Guidelines. *Arthritis Rheum*, 2000. **43**(9): p. 1905-15.

116. Evans, C.H., Gouze, J.N., Gouze, E., Robbins, P.D., and Ghivizzani, S.C., Osteoarthritis gene therapy. *Gene Ther*, 2004. **11**(4): p. 379-89.

117. Singh, G., Fort, J.G., Goldstein, J.L., Levy, R.A., Hanrahan, P.S., Bello, A.E., et al., Celecoxib versus naproxen and diclofenac in osteoarthritis patients: SUCCESS-I Study. *Am J Med*, 2006. **119**(3): p. 255-66.

118. Ulrich-Vinther, M., Maloney, M.D., Goater, J.J., Soballe, K., Goldring, M.B., O'Keefe, R.J., et al., Light-activated gene transduction enhances adeno-associated virus vector-mediated gene expression in human articular chondrocytes. *Arthritis Rheum*, 2002. **46**(8): p. 2095-104.

119. High, K.A. and Aubourg, P., rAAV human trial experience. *Methods Mol Biol*, 2011. **807**: p. 429-57.

120. Rehman, K.K., Wang, Z., Bottino, R., Balamurugan, A.N., Trucco, M., Li, J., et al., Efficient gene delivery to human and rodent islets with double-stranded (ds) AAV-based vectors. *Gene Ther*, 2005. **12**(17): p. 1313-23.

121. Lee, H.H., O'Malley, M.J., Friel, N.A., and Chu, C.R., Effects of doxycycline on mesenchymal stem cell chondrogenesis and cartilage repair. *Submitted*, 2012.

122. Williams, J.M., Felten, D.L., Peterson, R.G., and O'Connor, B.L., Effects of surgically induced instability on rat knee articular cartilage. *J Anat*, 1982. **134**(Pt 1): p. 103-9.

123. Ulrich-Vinther, M., Gene therapy methods in bone and joint disorders. *Acta Orthopaedica*, 2007. **78**(s325): p. 2-64.

124. Qiao, C., Yuan, Z., Li, J., He, B., Zheng, H., Mayer, C., et al., Liver-specific microRNA-122 target sequences incorporated in AAV vectors efficiently inhibits transgene expression in the liver. *Gene Ther*, 2011. **18**(4): p. 403-10.

125. Pasztoi, M., Nagy, G., Geher, P., Lakatos, T., Toth, K., Wellinger, K., et al., Gene expression and activity of cartilage degrading glycosidases in human rheumatoid arthritis and osteoarthritis synovial fibroblasts. *Arthritis Res Ther*, 2009. **11**(3): p. R68.

126. Yu, L.P., Smith, G.N., Brandt, K.D., Myers, S.L., O'Connor, B.L., and Brandt, D.A., Reduction of the severity of canine osteoarthritis by prophylactic treatment with oral doxycycline. *Arthritis & Rheumatism*, 1992. **35**(10): p. 1150-1159.

127. Zhou, Q., Guo, R., Wood, R., Boyce, B.F., Liang, Q., Wang, Y.J., et al., Vascular endothelial growth factor C attenuates joint damage in chronic inflammatory arthritis by accelerating local lymphatic drainage in mice. *Arthritis Rheum*, 2011. **63**(8): p. 2318-28.

128. Kraus, V.B., Birmingham, J., Stabler, T.V., Feng, S., Taylor, D.C., Moorman, C.T., 3rd, et al., Effects of intraarticular IL1-Ra for acute anterior cruciate ligament knee injury: a randomized controlled pilot trial (NCT00332254). *Osteoarthritis Cartilage*, 2012. **20**(4): p. 271-8.

129. Buckwalter, J.A. and Brown, T.D., Joint injury, repair, and remodeling: roles in post-traumatic osteoarthritis. *Clin Orthop Relat Res*, 2004(423): p. 7-16.

130. Nakajima, H., Goto, T., Horikawa, O., Kikuchi, T., and Shinmei, M., Characterization of the cells in the repair tissue of full-thickness articular cartilage defects. *Histochem Cell Biol*, 1998. **109**(4): p. 331-8.

131. Stieger, K., Belbellaa, B., Le Guiner, C., Moullier, P., and Rolling, F., In vivo gene regulation using tetracycline-regulatable systems. *Advanced Drug Delivery Reviews*, 2009. **61**(7–8): p. 527-541.

132. Beekman, B., Verzijl, N., de Roos, J.A.D.M., Koopman, J.L., and Tekoppele, J.M., Doxycycline Inhibits Collagen Synthesis by Bovine Chondrocytes Cultured in Alginate. *Biochemical and Biophysical Research Communications*, 1997. **237**(1): p. 107-110.

133. Brandt, K.D., Mazzuca, S.A., Katz, B.P., Lane, K.A., Buckwalter, K.A., Yocum, D.E., et al., Effects of doxycycline on progression of osteoarthritis: Results of a randomized, placebo-controlled, double-blind trial. *Arthritis & Rheumatism*, 2005. **52**(7): p. 2015-2025.

134. Fortier, L.A., Motta, T., Greenwald, R.A., Divers, T.J., and Mayr, K.G., Synoviocytes are more sensitive than cartilage to the effects of minocycline and doxycycline on IL-1α and MMP-13-induced catabolic gene responses. *Journal of Orthopaedic Research*, 2010. **28**(4): p. 522-528.

135. Golub, L.M., Ramamurthy, N.S., McNamara, T.F., Greenwald, R.A., and Rifkin, B.R., Tetracyclines Inhibit Connective Tissue Breakdown: New Therapeutic Implications for an Old Family of Drugs. *Critical Reviews in Oral Biology & Medicine*, 1991. **2**(3): p. 297-321.

136. Shlopov, B.V., Smith Jr, G.N., Cole, A.A., and Hasty, K.A., Differential patterns of response to doxycycline and transforming growth factor β1 in the down-regulation of collagenases in osteoarthritic and normal human chondrocytes. *Arthritis & Rheumatism*, 1999. **42**(4): p. 719-727.

137. Shlopov, B.V., Stuart, J.M., Gumanovskaya, M.L., and Hasty, K.A., Regulation of cartilage collagenase by doxycycline. *The Journal of Rheumatology*, 2001. **28**(4): p. 835-842.

138. Mehraban, F., Lark, M.W., Ahmed, F.N., Xu, F., and Moskowitz, R.W., Increased secretion and activity of matrix metalloproteinase-3 in synovial tissues and chondrocytes from experimental osteoarthritis. *Osteoarthritis and Cartilage*, 1998. **6**(4): p. 286-294.

139. Stevens, A.L., Wishnok, J.S., White, F.M., Grodzinsky, A.J., and Tannenbaum, S.R., Mechanical Injury and Cytokines Cause Loss of Cartilage Integrity and Upregulate Proteins Associated with Catabolism, Immunity, Inflammation, and Repair. *Molecular & Cellular Proteomics*, 2009. **8**(7): p. 1475-1489.

140. Ferretti, M., Marra, K.G., Kobayashi, K., Defail, A.J., and Chu, C.R., Controlled In Vivo Degradation of Genipin Crosslinked Polyethylene Glycol Hydrogels within Osteochondral Defects. *Tissue Engineering*, 2006. **12**(9): p. 2657-2663.

141. Bear, D.M., Szczodry, M., Kramer, S., Coyle, C.H., Smolinski, P., and Chu, C.R., Optical Coherence Tomography Detection of Subclinical Traumatic Cartilage Injury. *Journal of Orthopaedic Trauma*, 2010. **24**(9): p. 577-582 10.1097/BOT.0b013e3181f17a3b.

142. *ICRS Cartilage Evaluation Package 2000*. December 1, 2011]; Available from: http://www.cartilage.org/_files/contentmanagement/ICRS_evaluation.pdf.

143. Bertram, H., Boeuf, S., Wachters, J., Boehmer, S., Heisel, C., Hofmann, M.W., et al., Matrix Metalloprotease Inhibitors Suppress Initiation and Progression of Chondrogenic Differentiation of Mesenchymal Stromal Cells In Vitro. *Stem Cells and Development*, 2009. **18**(6): p. 881-892.

144. Borzí, R.M., Olivotto, E., Pagani, S., Vitellozzi, R., Neri, S., Battistelli, M., et al., Matrix metalloproteinase 13 loss associated with impaired extracellular matrix remodeling disrupts chondrocyte differentiation by concerted effects on multiple regulatory factors. *Arthritis & Rheumatism*, 2010. **62**(8): p. 2370-2381.

145. Wei, F., Zhou, J., Wei, X., Zhang, J., Fleming, B.C., Terek, R., et al., Activation of Indian Hedgehog Promotes Chondrocyte Hypertrophy and Upregulation of MMP-13 in Human Osteoarthritic Cartilage. *Osteoarthritis and Cartilage*, 2012(0).

146. Yelin, E., Murphy, L., Cisternas, M.G., Foreman, A.J., Pasta, D.J., and Helmick, C.G., Medical care expenditures and earnings losses among persons with arthritis and other rheumatic conditions in 2003, and comparisons with 1997. *Arthritis & Rheumatism*, 2007. **56**(5): p. 1397-1407.

147. Steinmeyer, J., Daufeldt, S., and Taiwo, Y.O., Pharmacological effect of tetracyclines on proteoglycanases from interleukin-1 -treated articular cartilage. *Biochemical Pharmacology*, 1998. **55**(1): p. 93-100.

148. Smith, G.N., Yu, L.P., Brandt, K.D., and Capello, W.N., Oral administration of doxycycline reduces collagenase and gelatinase activities in extracts of human osteoarthritic cartilage. 1998. **25**(3): p. 532-5.

149. Bedi, A., Fox, A.J., Kovacevic, D., Deng, X.H., Warren, R.F., and Rodeo, S.A., Doxycycline-mediated inhibition of matrix metalloproteinases improves healing after rotator cuff repair. *Am J Sports Med*, 2010. **38**(2): p. 308-17.

150. Greenwald, R.A., Treatment of Destructive Arthritic Disorders with MMP Inhibitors. *Annals of the New York Academy of Sciences*, 1994. **732**(1): p. 181-198.

151. de Bri, E., Lei, W., Svensson, O., Chowdhury, M., Moak, S.A., and Greenwald, R.A., Effect of an Inhibitor of Matrix Metalloproteinases on Spontaneous Osteoarthritis in Guinea Pigs. *Advances in Dental Research*, 1998. **12**(1): p. 82-85.

152. Haleem, A.M., El Singergy, A.A., Sabry, D., Atta, H., Rashed, L.A., Chu, C.R., et al., The clinical use of human culture-expanded autologous bone marrow mesenchymal stem cells transplanted on platelet-rich fibrin glue in the treatment of articular cartilage defects – A Pilot Study and Preliminary Results. *Cartilage*, 2010. **Epub Ahead of Print**.

153. Tan, H., Chu, C.R., Payne, K.A., and Marra, K.G., Injectable in situ forming biodegradable chitosan-hyaluronic acid based hydrogels for cartilage tissue engineering. *Biomaterials*, 2009. **30**(13): p. 2499-2506.

154. Tan, H., DeFail, A.J., Rubin, J.P., Chu, C.R., and Marra, K.G., Novel multiarm PEG-based hydrogels for tissue engineering. *Journal of Biomedical Materials Research Part A*, 2010. **92A**(3): p. 979-987.

155. Ho, W., Tawil, B., Dunn, J.C., and Wu, B.M., The behavior of human mesenchymal stem cells in 3D fibrin clots: dependence on fibrinogen concentration and clot structure. *Tissue Eng*, 2006. **12**(6): p. 1587-95.

156. Breen, A., Dockery, P., O'Brien, T., and Pandit, A., Fibrin scaffold promotes adenoviral gene transfer and controlled vector delivery. *J Biomed Mater Res A*, 2009. **89**(4): p. 876-84.

157. Schillinger, U., Wexel, G., Hacker, C., Kullmer, M., Koch, C., Gerg, M., et al., A fibrin glue composition as carrier for nucleic acid vectors. *Pharm Res*, 2008. **25**(12): p. 2946-62.

158. Wan, L., Li, D., and Wu, Q., Perivenous Application of Fibrin Glue as External Support Enhanced Adventitial Adenovirus Transfection in Rabbit Model. *Journal of Surgical Research*, 2006. **135**(2): p. 312-316.

159. Zhao, H., Ma, L., Gong, Y., Gao, C., and Shen, J., A polylactide/fibrin gel composite scaffold for cartilage tissue engineering: fabrication and an in vitro evaluation. *J Mater Sci Mater Med*, 2009. **20**(1): p. 135-43.

160. Schugar, R.C., Chirieleison, S.M., Wescoe, K.E., Schmidt, B.T., Askew, Y., Nance, J.J., et al., High Harvest Yield, High Expansion, and Phenotype Stability of CD146 Mesenchymal Stromal Cells from Whole Primitive Human Umbilical Cord Tissue. *Journal of Biomedicine and Biotechnology*, 2009. **2009**: p. 11.

161. DeFail, A.J., Chu, C.R., Izzo, N., and Marra, K.G., Controlled release of bioactive TGF-[beta]1 from microspheres embedded within biodegradable hydrogels. *Biomaterials*, 2006. **27**(8): p. 1579-1585.

162. Wang, X., Chen, Y., Lv, L., and Chen, J., Silencing CD36 gene expression results in the inhibition of latent-TGF-beta1 activation and suppression of silica-induced lung fibrosis in the rat. *Respiratory Research*, 2009. **10**(1): p. 36.

163. De Laporte, L. and Shea, L.D., Matrices and scaffolds for DNA delivery in tissue engineering. *Advanced Drug Delivery Reviews*, 2007. **59**(4-5): p. 292-307.

164. Pannier, A.K. and Shea, L.D., Controlled Release Systems for DNA Delivery. *Mol Ther*, 2004. **10**(1): p. 19-26.

165. Mithoefer, K., McAdams, T., Williams, R.J., Kreuz, P.C., and Mandelbaum, B.R., Clinical efficacy of the microfracture technique for articular cartilage repair in the knee: an evidence-based systematic analysis. *Am J Sports Med*, 2009. **37**(10): p. 2053-63.

166. Breen, A., Strappe, P., Kumar, A., O'Brien, T., and Pandit, A., Optimization of a fibrin scaffold for sustained release of an adenoviral gene vector. *Journal of Biomedical Materials Research Part A*, 2006. **78A**(4): p. 702-708.

167. Kawamura, K., Chu, C.R., Sobajima, S., Robbins, P.D., Fu, F.H., Izzo, N.J., et al., Adenoviral-mediated transfer of TGF-[beta]1 but not IGF-1 induces chondrogenic differentiation of human mesenchymal stem cells in pellet cultures. *Experimental Hematology*, 2005. **33**(8): p. 865-872.

168. Fortier, L.A., Cole, B.J., and McIlwraith, C.W., Science and Animal Models of Marrow Stimulation for Cartilage Repair. *J Knee Surg*, 2012. **25**(01): p. 003,008.

169. Buckwalter, J.A. and Mankin, H.J., Articular cartilage repair and transplantation. *Arthritis Rheum*, 1998. **41**(8): p. 1331-42.

170. Francioli, S., Cavallo, C., Grigolo, B., Martin, I., and Barbero, A., Engineered cartilage maturation regulates cytokine production and interleukin-1beta response. *Clin Orthop Relat Res*, 2011. **469**(10): p. 2773-84.

171. Goldring, M.B. and Otero, M., Inflammation in osteoarthritis. *Curr Opin Rheumatol*, 2011. **23**(5): p. 471-8.

172. Baragi, V.M., Renkiewicz, R.R., Jordan, H., Bonadio, J., Hartman, J.W., and Roessler, B.J., Transplantation of transduced chondrocytes protects articular cartilage from interleukin 1-induced extracellular matrix degradation. *J Clin Invest*, 1995. **96**(5): p. 2454-60.

173. Pelletier, J.P., Martel-Pelletier, J., and Raynauld, J.P., Most recent developments in strategies to reduce the progression of structural changes in osteoarthritis: today and tomorrow. *Arthritis Res Ther*, 2006. **8**(2): p. 206.

174. Caron, J.P., Fernandes, J.C., Martel-Pelletier, J., Tardif, G., Mineau, F., Geng, C., et al., Chondroprotective effect of intraarticular injections of interleukin-1 receptor antagonist in experimental osteoarthritis. Suppression of collagenase-1 expression. *Arthritis Rheum*, 1996. **39**(9): p. 1535-44.

175. Pelletier, J.P., Caron, J.P., Evans, C., Robbins, P.D., Georgescu, H.I., Jovanovic, D., et al., In vivo suppression of early experimental osteoarthritis by interleukin-1 receptor antagonist using gene therapy. *Arthritis Rheum*, 1997. **40**(6): p. 1012-9.

176. Morisset, S., Frisbie, D.D., Robbins, P.D., Nixon, A.J., and McIlwraith, C.W., IL-1ra/IGF-1 gene therapy modulates repair of microfractured chondral defects. *Clin Orthop Relat Res*, 2007. **462**: p. 221-8.

177. Geurts, J., Joosten, L.A., Takahashi, N., Arntz, O.J., Gluck, A., Bennink, M.B., et al., Computational design and application of endogenous promoters for transcriptionally targeted gene therapy for rheumatoid arthritis. *Mol Ther*, 2009. **17**(11): p. 1877-87.

178. Cai, G., Nie, X., Guo, P., Guan, Z., Zhang, J., and Shen, Q., A new inducible adenoviral expression system that responds to inflammatory stimuli in vivo. *J Gene Med*, 2006. **8**(12): p. 1369-78.

179. van de Loo, F.A., de Hooge, A.S., Smeets, R.L., Bakker, A.C., Bennink, M.B., Arntz, O.J., et al., An inflammation-inducible adenoviral expression system for local treatment of the arthritic joint. *Gene Ther*, 2004. **11**(7): p. 581-90.

180. Evans, C.H., Ghivizzani, S.C., and Robbins, P.D., Getting arthritis gene therapy into the clinic. *Nat Rev Rheumatol*, 2011. **7**(4): p. 244-9.

181. Engström, B., Johansson, C., and Tornkvist, H., Soccer injuries among elite female players. *The American Journal of Sports Medicine*, 1991. **19**(4): p. 372-375.

182. Junge, A. and Dvorak, J., Soccer injuries: A review on incidence and prevention. *Sports Medicine*, 2004. **34**(13): p. 929-938.

183. Neyret, P., Donell, S.T., Dejour, D., and Dejour, H., Partial meniscectomy and anterior cruciate ligament rupture in soccer players. *The American Journal of Sports Medicine*, 1993. **21**(3): p. 455-460.

184. Dvorak, J. and Junge, A., Football injuries and physical symptoms. *The American Journal of Sports Medicine*, 2000. **28**(suppl 5): p. S-3-S-9.

185. Nielsen, A.B. and Yde, J., Epidemiology and traumatology of injuries in soccer. *The American Journal of Sports Medicine*, 1989. **17**(6): p. 803-807.

186. Keller, C.S., Noyes, F.R., and Buncher, C.R., The medical aspects of soccer injury epidemiology. *The American Journal of Sports Medicine*, 1987. **15**(3): p. 230-237.

187. Ekstrand, J., Waldén, M., and Hägglund, M., Risk for injury when playing in a national football team. *Scandinavian Journal of Medicine & Science in Sports*, 2004. **14**(1): p. 34-38.

188. Waldén, M., Hägglund, M., and Ekstrand, J., Injuries in Swedish elite football—a prospective study on injury definitions, risk for injury and injury pattern during 2001. *Scandinavian Journal of Medicine & Science in Sports*, 2005. **15**(2): p. 118-125.

189. Morgan, B.E. and Oberlander, M.A., An examination of injuries in major league soccer. *The American Journal of Sports Medicine*, 2001. **29**(4): p. 426-430.

190. Hawkins, R.D., Hulse, M.A., Wilkinson, C., Hodson, A., and Gibson, M., The association football medical research programme: an audit of injuries in professional football. *British Journal of Sports Medicine*, 2001. **35**(1): p. 43-47.

191. Lindberg, H., Roos, H., and Gärdsell, P., Prevalence of coxarthrosis in former soccer players: 286 players compared with matched controls. *Acta Orthopaedica*, 1993. **64**(2): p. 165-167.

192. Turner, A.P., Barlow, J.H., and Heathcote-Elliott, C., Long term health impact of playing professional football in the United Kingdom. *British Journal of Sports Medicine*, 2000. **34**(5): p. 332-336.

193. Krajnc, Z., Vogrin, M., Rečnik, G., Crnjac, A., Drobnič, M., and Antolič, V., Increased risk of knee injuries and osteoarthritis in the non-dominant leg of former professional football players. *Wiener Klinische Wochenschrift*, 2010. **122**(0): p. 40-43.

194. Larsen, E., Jensen, P.K., and Jensen, P.R., Long-term outcome of knee and ankle injuries in elite football. *Scandinavian Journal of Medicine & Science in Sports*, 1999. **9**(5): p. 285-289.

195. Drawer, S. and Fuller, C.W., Propensity for osteoarthritis and lower limb joint pain in retired professional soccer players. *British Journal of Sports Medicine*, 2001. **35**(6): p. 402-408.

196. Poulsen, T.D., Freund, K.G., Madsen, F., and Sandvej, K., Injuries in high-skilled and low-skilled soccer: a prospective study. *British Journal of Sports Medicine*, 1991. **25**(3): p. 151-153.

197. Sandelin, J., Santavirta, S., and Kiviluoto, O., Acute soccer injuries in Finland in 1980. *British Journal of Sports Medicine*, 1985. **19**(1): p. 30-33.

198. Roaas, A. and Nilsson, S., Major injuries in Norwegian football. *British Journal of Sports Medicine*, 1979. **13**(1): p. 3-5.

199. Peterson, L., Junge, A., Chomiak, J., Graf-Baumann, T., and Dvorak, J., Incidence of football injuries and complaints in different age groups and skill-level groups. *The American Journal of Sports Medicine*, 2000. **28**(suppl 5): p. S-51-S-57.

200. Chomiak, J., Junge, A., Peterson, L., and Dvorak, J., Severe injuries in football players. *The American Journal of Sports Medicine*, 2000. **28**(suppl 5): p. S-58-S-68.

201. Maehlum, S. and Daljord, O.A., Football injuries in Oslo: a one-year study. *British Journal of Sports Medicine*, 1984. **18**(3): p. 186-190.

202. McMaster, W.C. and Walter, M., Injuries in soccer. *The American Journal of Sports Medicine*, 1978. **6**(6): p. 354-357.

203. Giza, E., Mithöfer, K., Farrell, L., Zarins, B., and Gill, T., Injuries in women's professional soccer. *British Journal of Sports Medicine*, 2005. **39**(4): p. 212-216.

204. Ekstrand, J. and Gillquist, J., The avoidability of soccer injuries. *Int J Sports Med*, 1983. **04**(02): p. 124,128.

205. Elleuch, M.H., Guermazi, M., Mezghanni, M., Ghroubi, S., Fki, H., Mefteh, S., et al., Knee osteoarthritis in 50 former top-level footballers: A comparative (control group) study. *Annales de Réadaptation et de Médecine Physique*, 2008. **51**(3): p. 174-178.

206. Roos, H., Are there long-term sequelae from soccer? *Clinics in sports medicine*, 1998. **17**(4): p. 819-831.

207. Adams, I.D., Osteoarthrosis and sport. *Journal of Royal Society of Medicine*, 1979. **72**(3): p. 185-187.

208. Anandacoomarasamy, A. and Barnsley, L., Long term outcomes of inversion ankle injuries. *British Journal of Sports Medicine*, 2005. **39**(3): p. e14.

209. Yeung, M.S., Chan, K.M., So, C.H., and Yuan, W.Y., An epidemiological survey on ankle sprain. *British Journal of Sports Medicine*, 1994. **28**(2): p. 112-116.

210. Valderrabano, V., Hintermann, B., Horisberger, M., and Fung, T.S., Ligamentous post-traumatic ankle osteoarthritis. *The American Journal of Sports Medicine*, 2006. **34**(4): p. 612-620.

211. Chantraine, A., Knee joint in soccer players: osteoarthritis and axis deviation. *Medicine & Science in Sports & Exercise*, 1985. **17**(4): p. 434-439.

212. Kujala, U.M., Kettunen, J., Paananen, H., Aalto, T., Battié, M.C., Impivaara, O., et al., Knee osteoarthritis in former runners, soccer players, weight lifters, and shooters. *Arthritis & Rheumatism*, 1995. **38**(4): p. 539-546.

213. Thelin, N., Holmberg, S., and Thelin, A., Knee injuries account for the sports-related increased risk of knee osteoarthritis. *Scandinavian Journal of Medicine & Science in Sports*, 2006. **16**(5): p. 329-333.

214. Sandmark, H. and Vingård, E., Sports and risk for severe osteoarthrosis of the knee. *Scandinavian Journal of Medicine & Science in Sports*, 1999. **9**(5): p. 279-284.

215. Klünder, K.B., Rud, B., and Hansen, J., Osteoarthritis of the hip and knee joint in retired football players. *Acta Orthopaedica*, 1980. **51**(1-6): p. 925-927.

216. Shepard, G.J., Banks, A.J., and Ryan, W.G., Ex-professional association footballers have an increased prevalence of osteoarthritis of the hip compared with age matched controls despite not having sustained notable hip injuries. *British Journal of Sports Medicine*, 2003. **37**(1): p. 80-81.

217. Roos, H., Dahlberg, L., Hoerrner, L.A., Lark, M.W., Thonar, E.J.M.A., Shinmei, M., et al., Markers of cartilage matrix metabolism in human joint fluid and serum: the effect of exercise. *Osteoarthritis and Cartilage*, 1995. **3**(1): p. 7-14.

218. Kettunen, J.A., Kujala, U.M., Räty, H., Videman, T., Sarna, S., Impivaara, O., et al., Factors associated with hip joint rotation in former elite athletes. *British Journal of Sports Medicine*, 2000. **34**(1): p. 44-48.

219. D'Lima, D.D., Hashimoto, S., Chen, P.C., Colwell, C.W., and Lotz, M.K., Human chondrocyte apoptosis in response to mechanical injury. *Osteoarthritis and Cartilage*, 2001. **9**(8): p. 712-719.

220. D'Lima, D.D., Hashimoto, S., Chen, P.C., Colwell, C.W., and Lotz, M.K., Impact of mechanical trauma on matrix and cells. *Clinical Orthopaedics & Related Research*, 2001. **391**(Supplement): p. S90-S99.

221. von Porat, A., Roos, E.M., and Roos, H., High prevalence of osteoarthritis 14 years after an anterior cruciate ligament tear in male soccer players: a study of radiographic and patient relevant outcomes. *Annals of the Rheumatic Diseases*, 2004. **63**(3): p. 269-273.

222. Roos, H., Adalberth, T., Dahlberg, L., and Lohmander, L.S., Osteoarthritis of the knee after injury to the anterior cruciate ligament or meniscus: the influence of time and age. *Osteoarthritis and Cartilage*, 1995. **3**(4): p. 261-267.

223. Hawkins, R.D. and Fuller, C.W., A prospective epidemiological study of injuries in four English professional football clubs. *British Journal of Sports Medicine*, 1999. **33**(3): p. 196-203.

224. Waldén, M., Hägglund, M., Magnusson, H., and Ekstrand, J., Anterior cruciate ligament injury in elite football: a prospective three-cohort study. *Knee Surgery, Sports Traumatology, Arthroscopy*, 2011. **19**(1): p. 11-19.

225. Agel, J., Arendt, E.A., and Bershadsky, B., Anterior cruciate ligament injury in national collegiate athletic association basketball and soccer. *The American Journal of Sports Medicine*, 2005. **33**(4): p. 524-531.

226. Matyas, J.R., Atley, L., Ionescu, M., Eyre, D.R., and Poole, A.R., Analysis of cartilage biomarkers in the early phases of canine experimental osteoarthritis. *Arthritis & Rheumatism*, 2004. **50**(2): p. 543-552.

227. Lohmander, L.S., Östenberg, A., Englund, M., and Roos, H., High prevalence of knee osteoarthritis, pain, and functional limitations in female soccer players twelve years after anterior cruciate ligament injury. *Arthritis & Rheumatism*, 2004. **50**(10): p. 3145-3152.

228. Baker, B.E., Peckham, A.C., Pupparo, F., and Sanborn, J.C., Review of meniscal injury and associated sports. *The American Journal of Sports Medicine*, 1985. **13**(1): p. 1-4.

229. Baker, P., Coggon, D., Reading, I., Barrett, D., McLaren, M., and Cooper, C., Sports injury, occupational physical activity, joint laxity, and meniscal damage. *The Journal of Rheumatology*, 2002. **29**(3): p. 557-563.

230. Englund, M., Roos, E.M., Roos, H.P., and Lohmander, L.S., Patient-relevant outcomes fourteen years after meniscectomy: influence of type of meniscal tear and size of resection. *Rheumatology*, 2001. **40**(6): p. 631-639.

231. Englund, M. and Lohmander, L.S., Risk factors for symptomatic knee osteoarthritis fifteen to twenty-two years after meniscectomy. *Arthritis & Rheumatism*, 2004. **50**(9): p. 2811-2819.

232. Englund, M., Roos, E.M., and Lohmander, L.S., Impact of type of meniscal tear on radiographic and symptomatic knee osteoarthritis: A sixteen-year followup of meniscectomy with matched controls. *Arthritis & Rheumatism*, 2003. **48**(8): p. 2178-2187.

233. Roos, H., Laurén, M., Adalberth, T., Roos, E.M., Jonsson, K., and Lohmander, L.S., Knee osteoarthritis after meniscectomy: Prevalence of radiographic changes after twenty-one years, compared with matched controls. *Arthritis & Rheumatism*, 1998. **41**(4): p. 687-693.